Alterations in Autophagy Marker Distribution in Different Genetic Subtypes of Frontotemporal Lobar Degeneration

Richard Heale

For the consideration of the award of PhD

School of Science, Engineering and Environment

Supervisor: Dr Gemma Lace

Co-Supervisor: Dr Lucy Smyth

2023

Alzheimer's Research UK The Power to Defeat Dementia

University of Salford MANCHESTER

Table of Contents

Table of Figures

Tables

Acknowledgements

I would like to especially thank my supervisor Dr Gemma Lace for supporting me over the last few years providing emotional and academic support whenever needed. I would also like to thank my friends and family for being with me throughout this journey, especially my parents, Stuart and Joy as well as Autumn Browne, Natasha Hadgraft and Chloe Jones for reminding me I probably need to eat or drink.

This project would not have been possible without the funding from Alzheimer's Research UK, to whom I am very grateful as well as everyone who has made a donation to them. I would also like to thank those who have donated their brains to Brains for Dementia Research as well as their families for supporting their decisions I would also like to thank David Mann and Andrew Robinson of the Manchester Brain bank for working tirelessly to provide the tissue. I would also like to thank Kirk Siddals of the University of Manchester for allowing us to use his facilitates for the protein extraction, and also Sarah Withers for providing the contact.

I would also like to thank my lab colleagues Diana-Madalina Stan, Neha Tomar and Toby Aarons for providing a collaborative, supportive and enjoyable place to work. Finally, I'd like to thank the staff at the university of Salford especially my co-supervisor Dr Lucy Smyth for providing her antibody expertise and the postgraduate support services who have been nothing but kind and helpful.

I would also like to thank my colleagues at Lush who have provided support over the last few years, a break when thesis writing got too much and plenty of bath bombs.

Abbreviations

ABC – Avidin-biotin complex

AD – Alzheimer's disease

AGD – Argyrophilic Grain Disease

ALS – Amyotrophic Lateral Sclerosis

Aβ – Amyloid β

bvFTD – Behavioural Variant Frontotemporal Dementia

CBD – Corticobasal degeneration

CMA – Chaperone Mediated Autophagy

CTF – C-Terminal Fragment

DAB – 3,3'-Diaminobenzidine

DLB- Dementia with Lewy Bodies

DN – Dystrophic Neurites

DNA – Deoxyribonucleic acid

ECL – Enhanced Chemiluminscence

FTD –Frontotemporal Dementia

FTLD – Frontal Temporal Lobar Degeneration

HD – Huntingtons Disease

HRP – Horseradish peroxidase

hsc70 – Heat Shock Cognate 70kDa

Hsp70 – Heat Shock Protein 70kDa

IQR – Interquartile Range

IBMPFD – Inclusion Body Myopathy with Paget's disease of bone and Frontotemporal Dementia

LAMP2A- Lysosome associated membrane protein type 2A

MAP – Microtubule Associated Protein

Mdn - Median

MND – Motor Neuron Disease

MSA – Multiple System Atrophy

mTOR – mammalian Target of Rapamycin

NCI – Neuronal Cytoplasmic Inclusion

NFT – Neurofibrillary Tangles

NII – Neuronal Intracellular Inclusion

NT – Neuropil Threads

NTF- N-Terminal Fragment

PiD – Picks' Disease

PNFA – Progressive Non-Fluent Aphasia

PSP – Progressive Supranuclear Palsy

RNA – Ribonucleic Acid

SD – Semantic Dementia

TAR – Trans-Activation Response

TBS-T – Tris-buffered saline with Tween 20

TDP-43 – TAR DNA-binding Protein 43

Abstract

Frontotemporal dementia (FTD) is the second most common type of early-onset dementia and is characterised by impairments in language and behavioural changes whilst memory is normally well preserved; it can be clinically subdivided into behavioural variant FTD, progressive non-fluent aphasia and semantic dementia. Underlying these dementia subtypes is a group of diseases that are referred to as frontotemporal lobar degeneration (FTLD). Macroscopically these diseases show cell loss in the frontal and temporal lobes which is accompanied by intracellular protein aggregation, which is used to pathologically differentiate FTLD into subtypes; FTLD-Tau, FTLD-TDP43 and FTLD-FUS. Abnormal accumulation of protein in some neurodegenerative disease has been linked to an impairment in autophagy, a cellular waste disposal process, however, this has not been well studied in FTLD. This study used markers associated with two subtypes of autophagy, macroautophagy (MA) (LC3 and Beclin-1) and chaperone-mediated autophagy (CMA) (Hsc70 and LAMP2a) in order to explore variation in autophagy associated protein distribution in the three most common genetic causes of FTLD: *C9orf72*, *MAPT* and *GRN*. Human tissue from the frontal, temporal and occipital cortex from the Manchester Brain Bank was used to immunohistochemically assess a total of 24 FTLD cases which demonstrated genetic mutations in *GRN* (7 cases), *C9orf72* (8 cases) and *MAPT* (9 cases), in addition to 8 cases with Alzheimer's Disease (AD) and 9 no-disease aged controls. Results showed that there was a regional decrease ($P < 0.05$) in the amount of LC3 and Beclin-1 detected in the hippocampus of FTLD-*GRN* cases. In addition, this decrease in MA marker detection was observed in all FTLD mutation groups and controls in Layer VI of the frontal grey matter. Moreover, Beclin-1 was also decreased in temporal grey matter of FTLD-*GRN* cases. No significant differences

were found between controls and the individual mutation groups for either of the CMA markers, LAMP2a and Hsc70.

The findings suggest a potential regional impairment in the formation of autophagosomes in addition to general impairment in MA initiation in FTLD, whilst the more selective CMA pathway were largely unaffected. Therapies restoring autophagsome formation and maturation therefore may have a therapeutic benefit in FTLD.

1 Introduction

1.1 Neurodegenerative diseases

Neurodegenerative diseases are a group of disorders defined by a progressive loss of neurons in specific brain regions and include diseases such as Alzheimer's disease, Parkinson's disease, frontotemporal dementia, Dementia with Lewy Bodies, Cortical Basal Degeneration and Progressive supranuclear palsy (Matej et al., 2019). This broad group of diseases have a significant socioeconomic impact across the globe and have consequently been the focus of many research programmes.

One subgroup of neurodegenerative disease are the diseases that give rise to dementia. According to the World Health Organization (WHO, 2021b), dementia is an umbrella term used to describe the diseases that cause a loss of cognitive functioning at a higher rate that is usually expected due to normal ageing. Dementia manifests in a clinically heterogenous way, depending on the underlying disease process driving it, with symptoms including memory loss, confusion, personality changes, communication deficits, sleep disturbances, behavioural changes and depression.

Dementia impacts 56 million people worldwide (WHO, 2021a; WHO, 2021b) and an estimated 885,000 people in the UK, with 426,301 currently recorded diagnoses of dementia in England alone as of November 2021; this has been reported to cost the UK economy £34.7 billion with this figure expected to rise to £94.1 billion by 2040 (Wittenberg et al., 2019). There is currently no disease modifying therapy available for this group of diseases and so it is vital that we understand the pathogenic processes underlying dementia and strive to identify new targets for therapeutic intervention.

Dementia is caused by numerous diseases, in order of prevalence these include: Alzheimer's Disease (AD), accounting for two-thirds of all cases, followed by vascular dementia (VD), which accounts for up to a 20% of cases, then Dementia with Lewy Bodies (DLB), which drives approximately 15% of dementia cases, then finally frontotemporal dementia (FTD) which accounts for less than 5% of dementia cases (ARUK, 2018b).

Whilst FTD accounts for less than 5% overall dementia cases, it is the second most common cause of early onset dementia. The earlier clinical manifestation of early onset dementias (i.e, below the age of 65 years) brings an additional range of personal, family and societal challenges given patients may still have substantive work and family commitments. Whilst research into FTD has flourished over the last few decades, this heterogeneous group of disorders are still not fully understood with respect to variation in the pathogenic drivers of disease and how these may contribute the variation in clinical and pathological manifestation.

The next section of the thesis will explore what is already known about FTD with respect to its clinical, pathological and genetic background along with an exploration of the autophagy pathways which are hypothesised to function differentially in relation to the different genetic subtypes of disease.

1.1.1 Frontotemporal dementia

Frontotemporal dementia (FTD) is more common in the under 65 age group, and is thus described as an early-onset dementia, and affects between 4 and 15 per 100,000 people within this age category (Coyle-Gilchrist et al., 2016; Rabinovici & Miller, 2010) making FTD

the second most common form of early-onset dementia (Mulders et al., 2016; Ting et al., 2016).

FTD is a pathologically and genetically heterogeneous group of disorders that presents with variable clinical manifestations, depending on the subtype of disease. The main clinical variants are behavioural variant FTD (bvFTD), progressive non-fluent aphasia (PNFA) and Semantic Dementia (SD) though progressive supranuclear palsy syndrome (PSPS), corticobasal syndrome (CBS) and FTD with motor neuron disease (FTD-MND) are all considered to also fall within the complex spectrum of FTD (Ferrari et al., 2011; Snowden et al., 2007; Warren et al., 2013; Woollacott & Rohrer, 2016). The FTD disorders can be categorised based on their clinical manifestations, their pathological presentation and/or the presence of genetic mutation or disease-causing variation, with clear overlaps being evident which underlies the tendency to consider these diseases on a spectrum.

1.1.1.1 Clinical manifestations of FTD

FTD can be divided into a number of clinically distinct disorders including bvFTD, PNFA and SD, with CBS, PSPS and FTD-MND also forming part of the FTD disease spectrum as shown in Figure 1.1 (Fernández-Matarrubia et al., 2015). The most common form of FTD is bvFTD which has been shown to account for approximately 70% of all FTD cases (Snowden et al., 2002,Snowden et al., 2002) whereas PSPS is much more rare, with an estimated prevalence of 0.3-1.39 per 100,000 (Vanacore et al., 2001). Within these FTD subgroups, there have been additional phenotypic variations reported (Woollacott & Rohrer, 2016) but for simplicity, the typical disease manifestations as demonstrated in figure 1.1 (Fernández-Matarrubia et al., 2015).

As mentioned previously, bvFTD is the most common clinical subtype of FTD, often presenting with apathy, selfishness and poor hygiene, along with disinhibition of behaviour (leading to a decline in socially appropriate behaviour), changes in diet (in particular, an increased consumption and a preference for sweet food) and an increase in wandering and hoarding behaviours (Kirshner, 2014; Seelaar et al., 2011). In contrast to bvFTD, both PNFA and SD demonstrate a characteristic and specific deficit in language. Patients with PNFA present with language that is hesitant and effortful, usually combined with a lack of grammatical flow, with phonetic or articulatory errors. As the disease progresses apraxia associated symptoms develop, such as impaired yawning and swallowing (Kirshner, 2014; Warren et al., 2013). In SD however, patient language remains grammatically correct and fluid , but instead the comprehension of single words is lost or confused, and semantic memory is impaired (Kirshner, 2014; Seelaar et al., 2011).

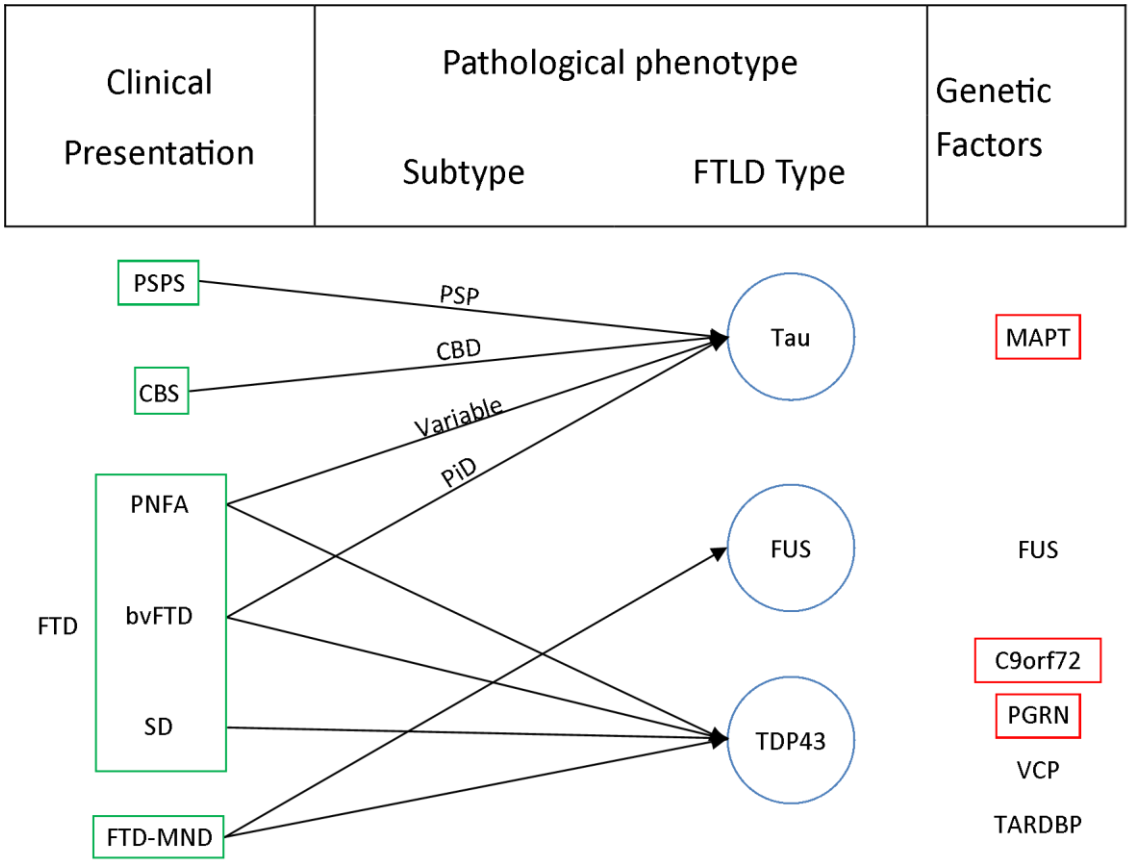

Figure 1.1: Clinical presentations of FTLD and the genetic associations. Arrows indicate association's clinical and pathological associations. Image adapted from Fernández-Matarrubia et al. (2015). PSPS, Progressive Supranuclear Palsy Syndrome; PSP, Progressive Supranuclear Palsy; CBS, Corticobasal Syndrome; CBD, Corticobasal Degeneration; PNFA, Progressive Non-Fluent Aphasia; PiD, Pick's Disease; bvFTD, behavioural variant FTD; SD, Semantic Dementia; FTD-MND, Frontotemporal Dementia with Motor Neuron Disease.

Due to the nature of the aggregate proteins, FTD is associated with a wider spectrum of clinical presentations including the pure FTDs (bvFTD, PNFA, SD), CBS, PSPS and FTD-MND, as described previously (see section 1.1.1.1, as shown in Figure 1.1).

Corticobasal Syndrome (CBS) and Progressive Supranuclear Palsy Syndrome (PSPS) are both defined by a myriad of motor symptoms, most often including Parkinsonism (Attems & Jellinger, 2013). Symptoms of CBS include limb apraxia and rigidity, cortical sensory loss, myoclonus, bradykinesia, tremor and dystonia (Boeve, 2011), whereas PSP presents with postural instability resulting in frequent falls, supranuclear gaze deficits, dysarthia and cognitive impairment (Litvan et al., 1996).Litvan et al., 1996,Litvan et al., 1996). CBS typically presents with an asymmetrical phenotype in contrast to PSPS being symmetrical in motor symptom manifestation (Seltman & Matthews, 2012).

MND is another neurodegenerative disease, characterised by a progressive loss of motor functioning leading to total paralysis and death, with an expected survival rate of up to five years following diagnosis (Turner et al., 2003; Williams et al., 2014,Turner et al., 2003; Williams et al., 2014), depending on the subtype such as Amyotrophic Lateral Sclerosis (ALS). In a subgroup of patients with FTD, MND may occur and present with muscle weakness and atrophy which is initially more prominent in the upper extremities and/or the tongue. This form of disease is particularly rapidly progressing with a mean survival of approximately 3 years (Coon et al., 2011,Coon et al., 2011), though since FTD-MND itself is considered to be a spectrum disorder, the clinical manifestations are expectedly variable (Couratier et al., 2017,Couratier et al., 2017).

One thing that sets FTD aside from other more common forms of dementia such as Alzheimer's Disease (AD), is the fact that episodic memory is generally well preserved (Silveri, 2007,Silveri, 2007). However, there is some pathological overlap between FTD and AD, as well as overlap between FTD and other tauopathies such as CBD, PSP and argyrophilic

grain disease (AgD). How clinical variations in disease are supplemented by genetic and pathological heterogeneity will be discussed in the subsequent sections.

1.1.1.2 Pathological and genetic heterogeneity of FTD

Pathologically, FTD is associated with variable pathological protein aggregation alongside significant cell loss and subsequent atrophy in the frontal and temporal lobes of the cerebrum, this feature often being referred to as Frontotemporal Lobar Degeneration (FTLD) (Ferrari et al., 2011,Ferrari et al., 2011). Rather than being a single entity, FTLD is a group of diseases that can be distinguished by the composition of the protein aggregates characteristic of each subtype of disease; FTLD-Tau, FTLD-FUS and FTLD-TDP-43. There are also reports of atypical cases of Multiple System Atrophy (MSA), a disease associated with α-synuclein aggregation, that presents with FTD and has cell loss concurrent with FTLD (Aoki et al., 2015; Rohan et al., 2015,Aoki et al., 2015; Rohan et al., 2015) and AgD is often seen as a comorbidity alongside FTD (Gil et al., 2018)(Gil et al., 2018)). The term FTLD therefore is often used to describe the atrophy and associated brain pathology, whereas the term FTD is more commonly used when referring to the clinical phenotype.

It has been reported that approximately 25-30% of FTD cases are familial, having a known causative genetic link, with many previously reported sporadic cases having also later being demonstrated to have a genetic risk association (Turner et al., 2017,Turner et al., 2017) The most common of these genetic associations impact *C9orf72, MAPT* and *GRN* (Lashley et al., 2015; Woollacott & Rohrer, 2016)(Lashley et al., 2015; Woollacott & Rohrer, 2016).

Figure 1.1 (from Fernández-Matarrubia et al. (2015) demonstrates the relationships between the pathology describing FTLD groups in relation to the clinical FTD subtypes, whilst also highlighting the main genetic links. The characteristic pathology of each of these FTLD groups will now be explored along with evidence for genetic influence on protein aggregate formation, since this thesis aims to explore the relationship between genetic mutation/variation, abnormal protein accumulation and levels of detectable autophagic markers.

1.1.2 FTLD-Tau

Figure removed due to copyright.

Figure 1.2: Splicing of the MAPT gene and the six isoforms of tau protein. N1 and N2 denote amino acid chain in the amino-terminal half of the protein whilst R2 demonstrates the inclusion or exclusion of exon 10 given 4R and 3R tau respectively. Image adapted from Wang and Mandelkow (2016).

FTLD-tau is a subtype of FTLD that is defined by aggregation of abnormal tau protein associated with cell loss, and includes Pick's Disease (PiD), CBD, PSP and FTLD-tau associated with *MAPT* mutations (Seelaar et al., 2011). Tau is a microtubule associated protein (MAPT)

and is implicated in the formation and stabilisation of microtubules (Goedert, 2004; Williams, 2006), which, in neurons, are found mainly in the axons and form part of the cytoskeleton (Letourneau, 1996). Tau's role in microtubule maintenance is important in supporting the axonal transport of cellular cargo such as neurotransmitters (Sheetz et al., 1987) and autophagosomes (Ravikumar et al., 2005), which are involved in synaptic transmission and macroautophagy respectively. Tau exists in a total of six isoforms, the function of which are explored in a review by Wang and Mandelkow (2016) (see figure 1.2). Briefly, the six isoforms can be divided into two groups, those of which have three microtubule binding domains (3R-Tau) and those with four microtubule binding domains (4R-Tau), with 4R-tau having greater stabilization effect on the microtubule than 3R-tau (Barbier et al., 2019). Those with three isoforms have an exclusion of a 31 amino acid repeat in the carboxyl terminal half of the protein (leading to the three microtubule binding repeats) whilst an inclusion leads to four repeats seen in 4R-Tau. Further variations in the isoforms are due to the inclusions or exclusion of a 29 or 58 amino acid chain in the amino terminal half of the protein (Goedert, 2004). Mutations in introns 10 and 16 of the *MAPT* gene are associated with an altered production of the different tau isoforms in disease, and this has been shown to be linked to disease pathogenesis (Kopach et al., 2021; Sposito et al., 2015; Strang et al., 2019). These mutations will be discussed later in this section.

As demonstrated in figure 1.1, FTLD-Tau most often associates with PNFA and bvFTD, however there are some reports of an association with SD. These stronger FTLD-Tau associations are related to specific subtypes with bvFTD, associating most often with PiD, whilst PNFA appears most commonly with CBD and PSP as previously discussed (Fernández-Matarrubia et al., 2015; Kertesz et al., 2007). Whilst PiD, CBD and PSP are clinically distinct diseases, referred to collectively as tauopathies, they each have their own pathological

presentation in the brain and epidemiology (Dickson et al., 2011) which will now be discussed.

According to Barker et al. (2002) PiD is a rare cause of dementia, accounting for less than 5% of dementias. The characteristic lesion of this disease are the Pick Bodies, which are spherical intraneuronal inclusions consisting of 3R-Tau tau (Figure 1.3a-c). Pick bodies are most commonly found in the granular layer of the dentate gyrus, CA1 (Cornu ammonis) of the hippocampus and the cortical grey matter, and they are less commonly reported in the brainstem, cerebellum and hippocampal areas CA2-4 and the subiculum (Attems & Jellinger, 2013; Dickson et al., 2011). In some patients, 4R-Tau positive astrocytic tau inclusions known as ramified astrocytes have been reported (Figure 1.3f, Dickson et al. (2011)), in addition to small, round oligodendroglial inclusions in the white matter (Figure 1.3e).

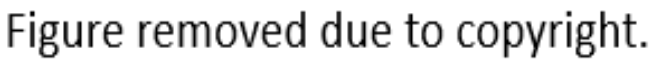

Figure 1.3: Pathology of Pick's Disease showing pick bodies, (a, b and c), Ballooned neurons (d); Oligendroglial inclusions (e) and ramified astrocytes (f). Image from Dickson et al. (2011).

In contrast to the 3R predominant lesions that characterise PiD, PSP and CBD are similar diseases characterised by asymmetrical atrophy and pathological protein burden of aggregated and hyperphosphorylated 4R tau in the frontal and temporal gyri (Dickson et al., 2011; Sha

et al., 2006,Dickson et al., 2011; Sha et al., 2006). They can be distinguished by their characteristic astrocytic lesions, the tufted astrocytes in PSP (Figure 1.4a) and the astrocytic plaque in CBD (Figure 1.4b) (Komori et al., 1998). Tufted astrocytes show AT8 immunoreactivity in their processes and cell membrane with sparing of the cell soma, whilst astrocytic plaques resemble neuritic plaques (when immunostained for tau) with denser globular aggregations spaced out from the cell body (Dickson, 1999; Dickson et al., 2007,Dickson, 1999; Dickson et al., 2007). Moreover, CBD has a higher number of granular ballooned or achromatic neurons (figure 1.4c) whilst the neuronal inclusions in PSP are more often flame-like or globus neurons (figure 1.4d). Additionally, the morphology of the white matter lesions in PSP and CBD are different (figure 1.4f) with those in PSP taking a more classical coiled body shape (figure 1.4f) whilst in CBD the white matter lesions are prevalent and more threadlike (figure 1.4e) (Dickson et al., 2011).

The clinical manifestations of CBS and PSPS are associated with aggregation of tau and their most common pathological classifications are Corticobasal Degeneration (CBD) and Progressive Supranuclear Palsy (PSP) respectively (Fernández-Matarrubia et al., 2015). Patients affected with either of these syndromes often meet the criteria for a diagnosis of bvFTD or PNFA (Armstrong et al., 2013; Kertesz et al., 2007) linked a pathological diagnosis of CBD with the clinical presentation and identified four distinct clinical presentations within the cohort, CBS, bvFTD, PNFA and PSPS, highlighting the need for a distinction between the clinical and pathological terms.

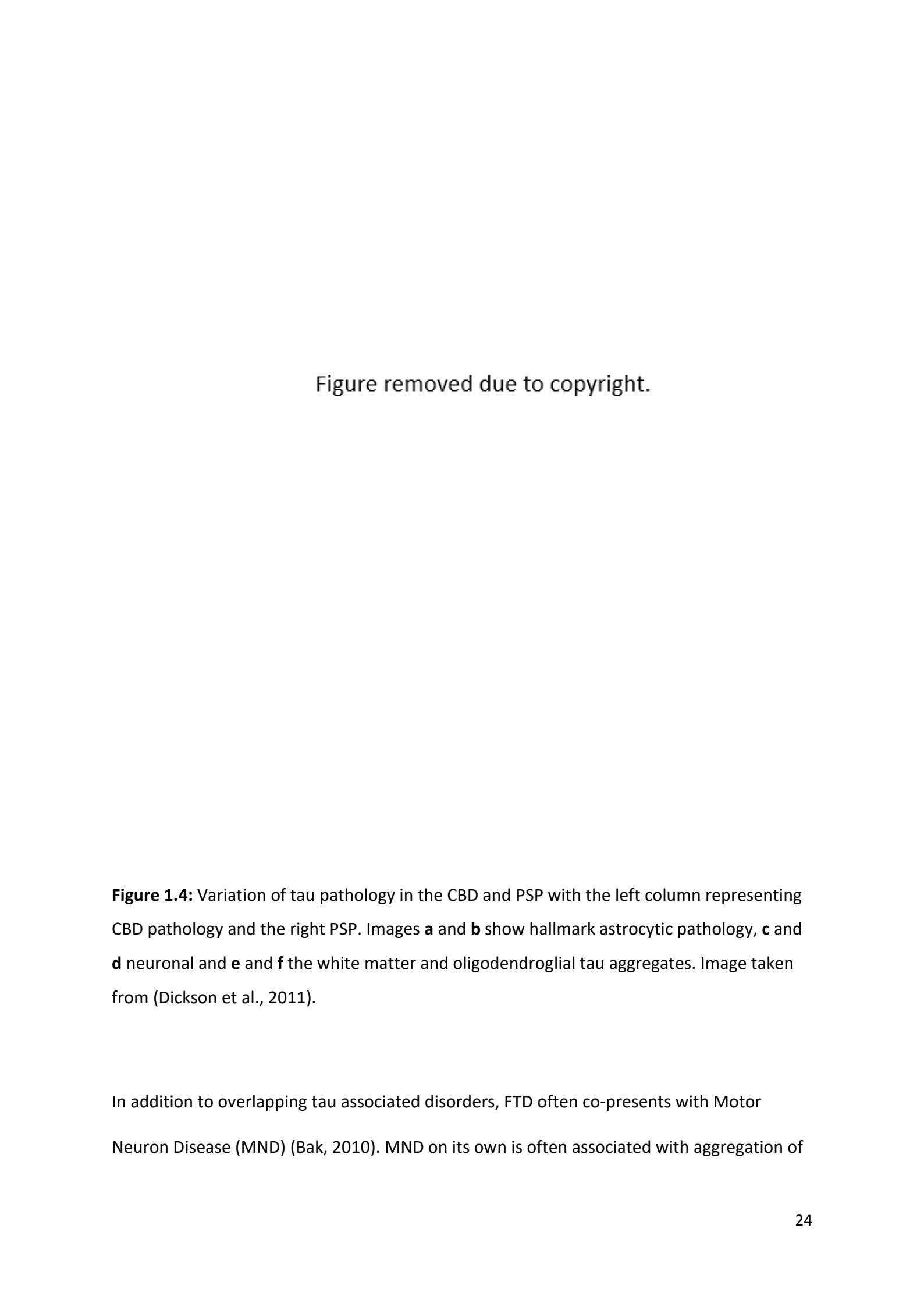

Figure 1.4: Variation of tau pathology in the CBD and PSP with the left column representing CBD pathology and the right PSP. Images **a** and **b** show hallmark astrocytic pathology, **c** and **d** neuronal and **e** and **f** the white matter and oligodendroglial tau aggregates. Image taken from (Dickson et al., 2011).

In addition to overlapping tau associated disorders, FTD often co-presents with Motor Neuron Disease (MND) (Bak, 2010). MND on its own is often associated with aggregation of

Superoxide Dismutase 1 (SOD1), however MND can co-present with FTD when the protein aggregate is mostly composed of FUS or TDP-43 (Tiryaki & Horak, 2014). This further supports the notion that FTD and MND exists on a spectrum as previously described (see section 1.1.1.1), with co-presentations existing in the centre and FTD-only and MND-only diseases existing at either end.

FTLD-Tau has a genetic association which presents in approximately 30% of familial FTLD cases (van Swieten & Spillantini, 2007). The genetic mutations have been found in the gene that codes for the MAP-tau protein, *MAPT*, with three groups first reporting mutations in 1998 (Hutton et al., 1998; Poorkaj et al., 1998; Spillantini et al., 1998; Farlow, Klug & Ghetti, 1998). From these initial mutations, the number of familial FTLD types with *MAPT* cases has grown to up to 63 reported mutations.

MAPT mutations have been reported in numerous neurodegenerative disorders and can be found in exons 9-13 or an intronic mutation following on from exon 10, with the leading theory behind the pathogenesis of these mutations is that mutation leads to the disruption of 3R-Tau and 4R-Tau ratio, leading to the subsequent formation of tau aggregates (Bodea et al., 2016; Hutton et al., 1998; Spillantini et al., 1998). The mutations specifically linked to FTLD-MAPT include the K257T missense mutation and the IVS10+16 intronic mutation (Forrest et al., 2019). Disruption of 3R:4R-Tau ratio is significant, given these different tau forms have different physiological functions. For example, 4R-Tau has been shown to assembly more quickly than 3R-Tau (Goedert & Jakes, 1990) whilst Adams et al. (2010), showed that 3R-Tau can inhibit the assembly of 4R filaments which leads to increased formation tau aggregates. However, the exact mechanism by which overexpression of 4R-Tau leads to aggregation is not understood. Additionally, the 3R and 4R isoforms of tau are

differentially distributed in pathological lesions in disease, with the Pick Bodies of PiD consisting of 3R-Tau whereas the astrocytic lesions associated with CBD and PSP containing predominantly 4R-Tau (Fyfe, 2018; Tolnay & Probst, 1999).

Whilst it is known that the pathological accumulation of tau in FTD is associated with neurotoxicity and enhanced cognitive impairment (Theofilas et al., 2018) and mutations in *MAPT* are sufficient to give rise to FTLD, this is still a developing area of research. Not only have the insoluble tau aggregates been linked to neurotoxicity, but soluble and oligomeric forms of tau have been shown to induce cellular damage (Niewiadomska et al., 2021; Sebastian-Serrano et al., 2018; Silva & Haggarty, 2020) and so the role of tau homeostasis in brain function is complex, with still much to learn.

1.1.3 FTLD-TDP43

TDP43 (TAR DNA-binding protein 43) is found in the nucleus and is a transactive response protein involved in the regulation of gene transcription, alternative splicing and RNA stability (Buratti & Baralle, 2008). It is proposed that it does this by binding to both DNA and RNA (Kuo et al., 2009 Shen and Yuan, 2009), with numerous RNA-binding sites in particular being discovered (Buratti & Baralle, 2001; Sephton et al., 2011); Sephton et al. (2011) showed that TDP43 binds to RNAs encoding other proteins associated with neurodegeneration such as Tau, Fused in Sarcoma (FUS) and progranulin and thus is implicated in regulating the expression of these proteins. More recent research has shown TDP43 is also involved in the tethering of the endoplasmic reticulum and mitochondria, a function which allows Ca^{2+} uptake by the mitochrondria after release from the endoplasmic

reticulum (Peggion et al., 2021). Additionally, TDP-43 has been linked to the regulation of autophagy and lysosomal function (Bose et al., 2011; Leibiger et al., 2018).

Under pathological conditions, TDP-43 is found translocated from the nucleus to the cytoplasm and is both hyperphosphorylated and hyperacetylated. Physiologically, these modifications and altered cellular localisation results in an impaired ability to bind RNA and promotes the formation of cytosolic aggregates (Cohen et al., 2015).

Mackenzie et al. (2011) proposed criteria that pathologically characterised FTLD-TDP43 into four groups, which combined both previously proposed pathological categorisation techniques from Sampathu et al. (2006) and Mackenzie et al. (2006). The first group, Type A (figure 1.5a-e), is characterised by a prevalence of short dystrophic neurites (DN) and neuronal cytoplasmic inclusions in layer II of the isocortex (figure 1.5a) and is clinically associated with bvFTD and PNFA and is commonly linked to a *GRN* mutations and *C9orf72* expansions which codes for a protein called progranulin. Type B (figure 1.5f-i) often presents as bvFTD or MND with FTD linked to *C9orf72* expansions (DeJesus-Hernandez et al., 2011; MacKenzie & Neumann, 2020; Renton et al., 2011) and is histopathological categorised by a moderate amount of NCI in all of the cortical layers, but with a distinctive lack of DN, whilst Type C has few NCI (figure 1.5k) and elongated DN (figure 1.5j,l,m) in the upper isocortical layers, often presenting as SD or bvFTD. Finally, Type D (figure 1.5 n-q) is often comorbid with Inclusion Body Myopathy with Paget's disease of bone and Frontotemporal Dementia (IBMPFD), a variant where muscle weakness presents during adulthood followed by clinical presentation of FTD (Bayraktar et al., 2016). Pathologically, this type this has many short DN (figure 1.5p) and often has lentiform Neuronal Intracellular Inclusions (NII) (figure 1.5q) and is associated with Valosin Contain Protein (*VCP*) mutations. An additional subtype, Type E,

was added by Lee et al. (2017), which was associated with a rapid onset of symptoms and an average time to death of approximately three years, most of these cases were of the bvFTD variant and one had comorbid MND, however there were no consistent patterns of genetic mutations elucidated. Pathologically there were widespread phosphorylated TDP-43 granulofilamentous neuronal inclusions (GFNI) inclusions and grains whilst NCI were rare. Protein aggregations were detected in grey matter of the frontal, temporal and parietal cortices, as well as the deep grey matter areas of the hippocampus, amygdala, striatum and thalamus; these deeper areas also demonstrated oligodendroglial coiled bodies, which were further present in the white matter of the subcortical white matter, corpus callosum and descending corticospinal tracts (figure 1.6). Recently, distinct patterns of TDP43 pathology have also been described in Alzheimer's disease (Tome et al., 2020) and due to the increasing prevalence of TDP43 pathology in neurodegenerative disease, this protein has received increasing research focus (Chen & Mitchell, 2021; Mol et al., 2021).

Figure removed due to copyright.

Figure 1.5: Image from Lashley, Rohrer, Mead and Revesz (2015) demonstrating the different TDP-43 lesions when using anti-TDP43 antibody. Arrows show pathological aggregates, whilst diffusely stained cells show normal TDP-43 distribution. **a, f, j** and **n** show the frontal cortex whilst **b, g, k** and **o**, show the hippocampus with the scale bar referencing 40µm. **c**, **d**, **e, h, I, l, m, p** and **q** are scaled to 10µm

Figure removed due to copyright.

Figure 1.6: Image from Lee et al. (2017) demonstrating the TDP43 positive inclusions found in FTLD-TDP43 Type E. The frontal, hippocampal and striatum demonstrate grey matter pathology, whilst the corpus callosum is indicative of white matter pathology and the occipital neocortex shows sparing of this region.

Whilst some cases of FTLD-TDP43 are due to mutations in the *TARDBP* gene that codes for TDP43, this actually represents a minority of cases in both FTLD and MND, and is more likely to be associated with ALS than FTD (Mackenzie, Rademakers & Neumann, 2010). The *TARDBP* mutations associated with FTLD include the P112H (Moreno et al., 2015) and, p.A382T TARDBP missense mutation (Floris et al., 2015). The *TARDBP* mutations predominantly increase the truncation of the TDP-43 protein (Gendron et al., 2013) resulting in C-terminal (CTF) and N-terminal fragments (NTF). Research into the aggregation of the TDP-43 has demonstrated that CTFs are more involved in TDP-43 aggregation (Yang et al., 2010) and it is the CTFs that are more toxic to the cell. The leading theory behind TDP-43 induced cell death is that within the cell there is an accumulation of toxic CTFs which are

unable to be cleared from the cell which results in increased cellular stress, particularly, within the endoplasmic reticulum (Wang, Ma, et al., 2015).

A hexanucleotide repeat expansion in *C9orf72* is now known to be the most common genetic cause of FTD and MND (DeJesus-Hernandez et al., 2011; Renton et al., 2011) with this genetic variation being associated with the underlying FTLD-TDP43 pathology. The *C9orf72* gene is found on the short arm of chromosome 9 and the hexanucleotide repeat expansion of GGGGCC has been found in both familial and sporadic forms of the disease (DeJesus-Hernandez et al., 2011; Renton et al., 2011). Up until recently, the role of C9orf72 protein was unknown, but recent research has identified a role in cellular homeostasis pathways including membrane trafficking and macroautophagy (Webster et al., 2016) and for review, see Nassif et al. (2017)). However, how the hexanucleotide repeat expansion gives rise to FTLD-TDP-43 pathogenesis is poorly understood.

The second most common group of genetic mutations associated with FTLD-TDP43 proteinopathy are mutations in the *GRN* gene which codes for progranulin. Proganulin is a protein which is considered to be involved in the promotion of cell proliferation, cell survival and angiogenesis, from investigations into cancer and embryo biology (Arechavaleta-Velasco et al., 2017; Desmarais et al., 2008; He et al., 2002), whilst immunological research supports an anti-inflammatory role, as well as enhancing bacterial clearance and organ survival (Tian et al., 2020). Within neurodevelopment progranulin is implicated in the synaptic pruning processing, with Uesaka and Kano (2018) finding that retrograde signalling of progranulin from the Purkinje cells of the cerebellum to climbing fibers inhibited the pruning of these synapses. Progranulin is expressed in the CNS, epithelial cells and immune system (Daniel et al., 2000; Townley et al., 2018) and within the CNS progranulin is

predominately expressed in astrocytes, neocortical neurons neurons, purkinje cells, motor neurons, activated mciroglia and within the pyramidal and granule cells of the hippocampus (Townley et al., 2018).

GRN mutations are found in up to 26% of familial FTLD cases and in both of the original papers identifying *GRN* mutations (Baker et al., 2006; Cruts et al., 2006), the mutations were hypothesised to produce null alleles, suggesting that its link to FTLD-TDP43 is due to a loss of function, rather than progranulin accumulation. This loss of progranulin function was shown by (Tanaka et al., 2014) to be associated with lysosomal dysfunction and TDP43 accumulation and more recent studies have also shown that progranulin deficiency causes an impairment of macroautophagy and subsequent accumulation of pathogenic TDP43 forms (Chang et al., 2017). The newly emerging research linking progranulin to the regulation of the autophagy-lysosome pathway provides evidence that disturbances to the autophagy systems can lead to abnormal protein accumulation and cell damage (Elia et al., 2019) and suggests a major role for autophagy disturbances in the pathogenesis of FTD. This will be explored further in chapter 1.3.

The final gene often attributed to FTLD-TDP43 is the *VCP* gene which encodes the protein VCP (valosin-containing protein). A group of six missense mutations in a cohort of 13 families with inclusion body myopathy with early-onset Paget disease and frontotemporal dementia (IBMPFD) were discovered by (Watts et al., 2004), then further research has expanded this to ten *VCP* missense mutations in other families (Kimonis et al., 2008 2008). VCP has been attributed to a number of functions including membrane fusion and chromatin organisation, and has additionally been linked to the protein degradation

pathways, including the Ubiquitin-proteasome system (UPS) and autophagy (Yamanaka et al., 2012). Initial findings by Weihl et al. (2006) demonstrated that *VCP* mutations associated with IBMPFD impaired endoplasmic reticulum-associated protein degradation which was elicited by a failure of VCP to deliver proteins to the proteasome in the UPS. More recent findings by Ju et al. (2009) and Vesa et al. (2009) demonstrate a role of the regulation of autophagy where VCP has been shown to regulate autophagosome biogenesis and thus in the initiation of autophagy (Hill et al., 2021).

Whilst it is clear that many of these FTLD-TDP43 mutations share a role in regulating protein degradation, it remains unclear why and how this gives rise to such clinical and pathological heterogeneity. One hypothesis associated with this work is that subtle variations in autophagy pathway deficit may underlie FLTD variation and the role of autophagy in disease will be explored in Chapter 1.2.

1.1.4 FTLD-FUS

Fused in Sarcoma (FUS) is a protein that is involved in the regulation of gene transcription, similar to TDP43. Most commonly, FUS binds to both single stranded DNA (Tan et al., 2012 Bussemaker and Manley, 2012) and RNA, but has also been show to bind to double stranded DNA (Wang, Schwartz, et al., 2015). FUS has been shown to share RNA targets with TDP43 (Honda et al., 2013) and along with TDP43, has been shown to be involved in mRNA stability, mRNA transport, mitochondrial function, cellular stress response and the regulation of autophagy by influencing the transcription of genes associated with autophagosome formation (Arenas et al., 2021; Birsa et al., 2020).

FTLD-FUS was first described by Neumann et al. (2009), and was previously characterised by the presence of ubiquitin-positive inclusions lacking p62 immunoreactivity. The pathological hallmarks of FTLD-FUS are demonstrated in figure 1.6. Briefly, FTLD-FUS is characterised by neuronal cytoplasmic inclusions (NCI), neuronal intranuclear inclusions (NII) and dystrophic neurites (DN) (figure 1.6B-H). Pathological glial inclusions were also reported (figure 1.6I) and both neuronal and glial inclusions were shown to be distinct from those associated with normal ageing (figure 1.6A). Regional analysis identified the dentate gyrus of the hippocampus, the frontal and temporal lobes and striatum as the most often affected regions (Neumann et al., 2009) with later research confirming these findings and highlighting caudate nucleus atrophy as a key feature (Snowden et al., 2011)

Figure removed due to copyright.

Figure 1.7: Demonstrating the range of pathologies seen in FTLD-FUS. Morphology is shown in normal control brain tissue (**A**) and FTLD-FUS (**B-I**), arrows indicate abnormal FUS deposition. **B** shows an example of neuronal inclusion (arrow) in an FTLD-FUS case with **C-E** demonstrate the NCI in the middle and deep grey matter **F** and **G** show oval inclusions within the granule cells of the dentate gyrus whilst **E** provides example of a crescentic inclusion type. **H** is a globular NCI in a lower motor neuron. **I** is glial inclusions in the white matter. Taken from (Neumann et al., 2009).

FUS additionally appears to be involved in ALS, and forms aggregates within the lower motor neurons ((Neumann et al., 2009), see figure 1.6H). Due to this association both (Kwiatkowski et al., 2009)) and (Vance et al., 2009) decided to investigate the genetic associations in relation to disease, and both groups found missense mutations in the gene that codes for FUS located on chromosome 16. They suggested this was due to a loss of function of regulated RNA transcription and neuronal inclusions, drawing parallels to the mechanisms of disease associated with TDP43 mutations. However most *FUS* mutations

results in ALS (Ishigaki & Sobue, 2018), whilst only novel mutations so far being linked to cases of FTLD (Langenhove, et al., 2010; Snowden, et al., 2011).

1.1.5 Other tauopathies

There are a number of so called tauopathies (neurodegenerative disorders characterised by neuronal or glial tau pathology) that align with FTD and/or FTLD due to either their similar clinical presentation or overlapping pathological features. These can be defined as primary or secondary tauopathies (Kovacs, 2018). As described previously in section 1.1.2, primary tauopathies can be defined as those disorders where tau pathology forms the predominant histopathological feature, and include diseases such as PSP, PiD, CBD, frontotemporal dementia linked to chromosome 17 (FTDP-17), AgD and globular glial taopathy. Secondary tauopathies however have other significant pathological characteristics, such as the accumulation of beta-amyloid containing lesions, and consequently AD and Down's syndrome are considered to be secondary tauopathies. Given the likely variation in pathogenic drivers between primary and secondary tauopathies, this study also incorporated an inclusion of AD cases, given AD is arguably the most well studied of the neurodegenerative disorders and the most common cause of dementia (Castellani et al., 2010). For completion, the next section will briefly summarise AD and the parallels and differences in disease process, in comparison to FTLD.

1.1.6 Alzheimer's disease

Alzheimer's disease (AD) is the most common form of dementia, accounting for approximately 70% of overall dementia cases (Castellani et al., 2010; Garre-Olmo, 2018; WHO, 2021a). Clinically it presents as memory impairment and a dysfunction of at least one other cognitive area such as speech or personality. The significant memory impairment

associated with AD is one of the major differences in clinical manifestation in comparison to FTD, though it should be noted that this symptom can present in FTD though with lower prevalence. Pathologically, AD is characterised by proteinaceous aggregations in the form of neuritic plaques (NP), neurofibrillary tangles (NFT) and neuropil threads (NT). NP are composed of a core containing mainly aggregated amyloid-β (Aβ), with fibrils of tau surrounding the densely packed core, referred to as the neuritic corona (Lace et al., 2007). NFT and NT are comprised of hyperphosphorylated tau, occurring mostly in layer III and V of the cortical grey matter (Charles Duyckaerts et al., 2009). According to Braak and Braak (19951991) tau pathology starts in the entorhinal cortex and spreads through the hippocampus to the isocortex; whereas amyloid pathology starts in the isocortex and spreads through the medial brain structures to the cerebellum (Braak et al., 2006; Braak & Braak, 1997; Thal et al., 2002). Other notable pathological features include cerebral amyloid angiopathy (CAA) which is an accumulation of Aβ within the walls of blood vessels (Biffi & Greenberg, 2011), glial pathology and the presence of AgD. Like FTD, AD is macroscopically characterised by significant and irreversible synaptic and neuronal loss and numerous research studies have evidenced a relationship between increased abnormal protein accumulation and cellular damage.

1.1.7 Current Treatments for AD and FTD

Current treatments for both FTD and AD focus on symptom management rather than altering disease progression and there are currently no preventative or curative therapies available for these diseases. Given the substantial socioeconomic impact of AD and FTD, it is

essential that disease modifying therapies are developed to halt the disease process and/or interfere with disease onset.

In a review by Boxer and Boeve (2007) the most often prescribed class of drugs for FTD were selective serotonin reuptake inhibitors (SSRIs), normally used to treat depression and anxiety, but these also have effects on the digestive system, such as nausea. The SSRIs are used to manage mood and behavioural disturbances in patients with FTD (Devenney et al., 2015).

The antidepressant trazodone has also been shown to help control behavioural problems associated with bvFTD (Trieu et al., 2020) and anti-psychotics and anti-epileptics are also sometimes prescribed specifically to target the disease associated behavioural symptoms, however the efficacy of these treatments is questionable and there is minimal substantive research evidence to back up their utility (Tsai & Boxer, 2016). Additionally, antipsychotics often cause adverse effects such as rigidity and immobility and as mentioned previously, have no impact on slowing disease progression.

While like FTD, there are no disease modifying therapies of AD, there are however four licensed drugs available for the treatment of AD which include donezepil, galantamine, memantine and rivastigmine (ARUK, 2018a). Donezepil, galantamine and rivastigmine are acetylcholinesterase inhibitors that function to enhance cholinergic transmission in patients and induce positive cognitive effects with AD patients (Courtney et al., 2004; Polinsky, 1998; Wilcock et al., 2000). Memantine however is an uncompetitive N-methyl-D-aspartate (NMDA) receptor antagonist those mechanism of action is still not fully understood, but clinical trial evidence has demonstrated that this drug can be used to evoke cognitive benefits in AD patients (Thomas & Grossberg, 2009).

These four approved AD drugs are often used in combination with other drugs to help treat some of the specific psychiatric symptoms of AD (ARUK, 2018a) however, they do not interfere with disease progression and so the need for disease modifying therapies is urgent.

When specifically considering the lack of disease modifying therapies for FTD, given the complexity and clinical and pathological heterogeneity of the disease, it is no wonder that there is no single drug available that can prevent or disrupt the disease process. The current treatments available only manage the psychological symptoms associated with FTD and they have little to no effect on the underlying protein aggregation; as a result, the person affected will continue to decline (Boxer & Boeve, 2007). This highlights a need for novel approaches in the treatment of FTD, that take into consideration the pathological heterogeneity of the group of disorders, that either enhances the clearance of protein aggregations to prevent neurotoxicity or work to prevent the initial aggregation or build-up of abnormal protein aggregates, which are known to have toxic effects on neurons. As discussed previously, it is known that the accumulation of these aggregates is linked to advancing cellular toxicity and subsequent cell death (Ferrari et al., 2011; Ghemrawi & Khair, 2020; Nelson et al., 2012; Seelaar et al., 2011; Wilson et al., 2013) and so interfering with this process has clear potential therapeutic benefits.

There exists in healthy individuals a group of pathways that aim to clear abnormal proteins and defunct cellular components, and these are the autophagy pathways. Given that some of the genetic risk factors for FTD have roles associated with this group of protein clearance pathways, it could be hypothesised that the different genetic forms of FTD (ie those harbouring *MAPT* or *GRN* mutations, or C9orf72 repeat expansions) might demonstrate

different types of autophagy deficit and this might be what drives some of the variation in clinical manifestation and may contribute to the heterogeneity of the pathology. Understanding why abnormal proteins aren't detected and cleared via autophagy in FTD, and precisely where in these complex pathways the deficits lie, could help identify new therapeutic targets for the different forms of FTD. The following section will explore the autophagy processes in detail, along with how they relate to the abnormal accumulation of protein in FTD.

1.2 Autophagy

Autophagy is a complex biological mechanism that functions to remove misfolded and damaged proteins and organelles and consequently has a significant role in cellular homeostasis (Dikic & Elazar, 2018). There are three main types of autophagy; Macroautophagy (often referred to as simply autophagy), chaperone-mediated autophagy and microautophagy (Yin et al., 2016). Each of these forms of autophagy will be explored in the following section, with particular focus on macroautophagy and microautophagy, given their association with the clearance of proteins associated with neurodegenerative disease (see chapter 1.3).

1.2.1 Macroautophagy

Macroautophagy (MA) is the main autophagy pathway, responsible for processing both aggregated proteins and damaged cellular organelles (see figure 1.7). The function to remove organelles that are damaged or in overabundance is particularly important in neurons given the need to maintain mitostasis and general cellular homeostasis to ensure longevity of health (Graef, 2020; Misgeld & Schwarz, 2017).

MA is initiated physiologically under cellular stress conditions such as nutrient starvation, which results in inhibition of mTOR (mammalian target of Rapamycin) or activation of AMPK (AMP-activated protein kinase) (Kim et al., 2011) , Russell et al. (2013). This results in activation of ULK1, then phosphorylation of Beclin-1 which subsequently interacts with VPS34 to allow the recruitment of membranes into immature precursor vesicles, called phagophores. These phagophores then flatten and join to form a structure called an

autophagosome, which engulfs the damaged organelles and proteins (see figure 1.7). To guide this assembly an ATG5-ATG12-ATG16 L (Menzies et al., 2015; Romanov et al., 2012) complex mediates the fusion of phagophores whilst, in mammalian cells, LC3B-II guides the closure of the mature functional vesicle, the autophagosome, around the autophagic cargo (Menzies et al., 2017; Menzies et al., 2015). In order to target only damaged components for clearance, LC3B-II uses receptor proteins as a guide to mark the damaged proteins and organelles for degradation. These receptor proteins include proteins such as p62/Sequestosome1 (hereafter referred to as p62), optineurin (Korac et al., 2013) and huntingtin (HTT) (Menzies et al., 2015; Pankiv et al., 2007); in some cases this can also act as a positive feedback loop, for example optineurin both activates autophagy via ULK1 translocation and is further recruited by ATG8-homologues such as LC3 (Padman et al., 2019). Following the assembly of the autophagosome, it is transported to the cytosolic area surrounding the cell nucleus for degradation via the influx of catabolic enzymes delivered by lysosomes, which fuse with the formed autophagosome. The autophagic cargo is then degraded along with LC3B-II and the receptor proteins, releasing recyclable constituents such as amino acids into the cytosol (Menzies et al., 2015).

Figure removed due to copyright.

Figure 1.8: A diagram showing the overall process of macroautophagy, showing the key proteins and their involvement in neurodegeneration. Taken from Menzies et al. (2015).

It is important to note that the membrane bound LC3B-II is the 15KDa cleaved isoform of the cytosolic protein LC3B-I, which is a 17kDa protein, whereby LC3B-I is cleaved to form LC3B-II during the process of autophagosome formation. LC 3B-II then attaches to the autophagosomal membrane by a subsequent conjugation to phosphatidylethanolamine (Kabeya et al., 2004 Oshitani-Okamoto, Ohsumi and Yoshimori, 2004; Sou et al., 2006 Ueno and Kominami, 2006). For this reason the ratio of LC3B-I and LC3B-II can be used as a marker of MA, specifically to indicate the formation of autophagosome (Ghosh & Pattison, 2018; Sharifi et al., 2015).

Another useful marker in the assessment of MA is p62, since this binds to most ubiquitinated proteins tagged for macroautophagic clearance, and is often used in neuropathology to visualise numerous protein aggregates (Kuusisto et al. (2001). P62 can be used to visualise pathologically relevant lesions containing α-synuclein or tau, and other studies have shown that p62 can be used as a marker of some types of TDP43 lesions but not FUS aggregates (Kuusisto et al., 2008; Neumann et al., 2009). This suggests that TDP43,

Tau and α-synuclein are MA substrates and this has been further demonstrated in a series of other studies (Caballero et al., 2018) though some mutant forms of pathogenic protein (eg tau) do not get readily degraded via this process (Lee et al., 2013). Since p62 binds with LC3-II and becomes degraded within the lysosome, changes in p62 can be indicative of altered autophagic flux but since p62 can also be degraded by the ubiquitin protease system (UPS), then this measure can only be used as a corroborative measure alongside assessment of other markers, such as LC3 (Ghosh & Pattison, 2018). Considering this evidence, p62 can be used as an indirect indicator of alterations in MA as well as a marker of damaged, aggregated protein accumulation.

Beclin-1 is another common marker used to study MA, due to its role in regulating the autophagic activity of Vps34 and thus the recruitment of membranes to the process of autophagosome formation (Pickford et al., 2008). Used together, LC3, P62 and Beclin-1 are markers that can shed light on different parts of the MA pathway, from initiation, autophagosome formation, recruitment of cargo and autophagic flux. Failure of MA could occur at each of these different stages and consequently contribute to the abnormal accumulation of proteins in FTD as well as other neurodegenerative disorders. Assessment of LC3, P62 and Beclin-1 across different subtypes of FTD could therefore allow a deeper understanding of MA associated deficits in normal protein degradation.

1.2.2 Chaperone-Mediated Autophagy

Chaperone-mediated autophagy (CMA) is a more selective protein degradation pathway (figure 1.8) and degrades single proteins as opposed to aggregates or organelles (Xilouri & Stefanis, 2015). Physiologically, CMA therefore functions to control cellular protein quality and is able to degrade damaged proteins before aggregation occurs (Kaushik & Cuervo, 2018).

As the name suggests, the CMA process utilises a chaperone, which takes the form of a protein such as heat shock cognate 70 (hsc70) (Chiang et al., 1989) which functions to guide the dysfunctional protein through the protein degradation process. In order for a protein to be removed by CMA, it needs to possess a specific pentapeptide KFERQ motif, which becomes exposed upon damage (Bejarano & Cuervo, 2010; Ciechanover & Kwon, 2015; Kiffin et al., 2004). Hsc70 then binds to this motif along with co-chaperone proteins (see figure 1.8), such as hsp90 and hsc70-interacting protein (Bejarano & Cuervo, 2010). This chaperone complex then transports the single protein to a lysosome where it binds to a receptor called lysosome-associated membrane protein type 2A (LAMP2A), which exists as a monomer and this triggers assembly with other LAMP2A monomers to form a pore in the lysosomal membrane (Bandyopadhyay et al., 2008). Once bound to the receptor, a lysosolic-hsc70 binds to the KFERQ-like motif, initiating further unfolding of the protein so it can pass through the newly assembled LAMP2A receptor (Salvador et al., 2000) and into the lysosome where is it degraded. Meanwhile the hsc70/cochaperone complex detaches from the outside of the lysosome and the LAMP2A complex dissembles (Bandyopadhyay et al., 2008).

Figure removed due to copyright.

Figure 1.9: Diagram of chaperone mediated autophagy, showing the unfolding location of the KFERQ-like motif, being targeted by chaperone proteins and transported to the lysosome for degradation. Figure from Bejarano and Cuervo (2010).

The KFERQ-like motif is an important part of the suitability of a protein to be degraded by CMA, it refers to an amino-acid chain on the protein and was identified by Dice et al. (1990). In order to have a KFERQ-like motif the protein must have a sequence that follows a set of rules: chiefly a Q (Glutamine) should be the flanking amino acid, either at the beginning of the end of the motif, next there can be a maximum of two hydrophobic amino acids (I – Isoleucine, F- Phenylalanine, L- Leucine or V – Valine) or two positive residues (R - Arginine or K – Lysine) however there can be only one negative charge (E – Glutamic Acid or D – Aspartic acid) (Cuervo, 2010). Many of the proteins associated with neurodegeneration are known to be potential substrates of CMA, for example, tau contains two of these regions QVEVK and KDRVQ meaning it has high suitability for degradation in a hsc70 dependent system (Wang et al., 2009). TDP43 however only contains one such motif (QVKKD) which is

required for its degradation by CMA and this could be inhibited in mutants that affect the required pentapeptide motif (Huang et al., 2014).

LAMP2A is most often used as a marker to monitor CMA due to its formation of the lysosomal membrane receptor during activity pathway recruitment and low cytosolic availability in comparison to hsc70 (Bandyopadhyay et al., 2008). There is an abundance of hsc70 in the cytosol since it is required for chaperoning damaged proteins to the lysosome and so changes in detection of hcs70 could indicate an inability to target damaged proteins to the lysosome and a subsequent accumulation of damaged protein. Analysing both LAMP2a and hsc70 simultaneously therefore allows the study of the machinery required for correct detection and transport of damaged proteins to the lysosome, along with insight into the formation of the transmembrane pore. It is currently unclear if these key elements of the CMA pathway function differentially within the different types of FTD and so understanding in the first instance if there is variable detection between disease subgroups is an essential starting point in exploring CMA functioning in FTD.

1.2.3 Microautophagy

Microautophagy was reviewed by Li et al. (2012) and is a non-selective process by which proteins are degraded. It involves lysosomes directly engulfing proteins via specific invaginations called autophagic tubes, this tubes close engulfing the cargo inside the tube, along with a portion of the lysosolic membrane. Mijaljica et al. (2011) stated on of the most commonly used techniques to observe microautophagy was using electron microscopy to

observe the formation of the autophagic tubes, however this technique is expensive, and they state the role of microautophagy in the degradation of neurodegeneration specific proteins is unclear. An alternative method of study is demonstrated by Kawamura et al. (2012) and involves using LAMP2A to track the lysosome and a confocal microscope; however this requires the use of live cells and therefore cannot be applied to post-mortem tissue making it difficult to study with respect to neurodegenerative disease. This study will therefore focus on the potential role of MA and CMA in FTD given the nature of the tissue available for study and the evidence linking both these processes to the process of FTD associated protein degradation.

1.3 Autophagy in Neurodegeneration

Due to protein aggregation being associated with cell loss in neurodegenerative diseases, research has turned to autophagy as a potential therapeutic target which could be used to eliminate abnormal proteins using the cells own innate biological mechanisms (Liu & Li, 2019). Given the complexity of these protein degradation pathways it is imperative to understand if specific autophagy pathway deficits are associated with different subtypes of the disease and how this relates to protein aggregation and accumulation. It is also vital to understand if there are specific failures are within these complex pathways so that targeted functionally restorative medicines can be developed, which would reduce the likelihood of off target impacts.

Over the last few decades there has accumulated increasing evidence that autophagy is impaired in a number of neurodegenerative disease and that autophagy failure directly contributes to the abnormal protein build up that pathologically characterises a number of disorders the drive the development of dementia (Liu & Li, 2019). Whilst the investigation of the role of autophagy with FTD is still in its infancy, there is a more substantial body of research exploring the role of protein degradation pathway failure in the most commonly researched neurodegenerative disorders, namely AD and PD (Liu & Li, 2019).

1.3.1 Autophagy impairments in PD

Research into autophagy in Parkinson's disease (PD) particularly has given insight into some of the mechanisms behind the familial forms of the disease, with many of the genes associated with PD being known to have key roles within the autophagy systems. *SNCA, LRRK2, PARK7* and *VPS35* are known to be involved in both MA and CMA, whereas *PINK1,*

PRKN, SNCA, LRRK2, FBX07, VPS35 and *VPS13C* have also been implicated in mitophagy (for review see Hou et al. (2020)).

For example, one of the most common pathogenic mutations in PD is leucine-rich repeat kinase (LRRK2) G2019S (Bouhouche et al., 2017) which has been associated with impaired α-synuclein protein degradation via the CMA pathway. Orenstein et al. (2013) showed that this was due to improper translocation of the protein following binding to the LAMP2A receptor, preventing the degradation of α-synuclein. This has demonstrated that a "jamming" of the autophagy pathway can lead to neurodegeneration where clearance of misfolded or damaged proteins is impaired.

Other research has shown that the PD associated pathological mutations in the *SNCA* gene (which codes for the protein α-synuclein), often affect the KFERQ-like motif of the protein, meaning that the chaperone proteins associated with CMA cannot bind to α-synuclein. This means α-synuclein cannot be efficiently targeted to the lysosome for degradation where *SNCA* mutations disrupt the pentapeptide recognition sequence, and this seems to lead to protein aggregation and cell death (Cuervo et al., 2004).

Autophagy changes have also been detected in post-mortem human brain tissue derived from PD patients. LC3, which as described previously is responsible for autophagosome formation in MA, has been found in Lewy neurites and in the halo of LB within dopaminergic neurones, where it also co-localised with α-synuclein (Dehay et al., 2010). In this same study, LC3-II was found to be elevated in the PD samples, compared to the controls. Whereas HSC70 were found to be significantly decreased in samples derived from the substantia nigra of PD cases, in comparison to controls (Alvarez-Erviti et al., 2010). This

evidences a variation in protein degradation across multiple autophagy pathways, yet it is unclear if this variation is also evidence across FTD brains.

1.3.2 Autophagy impairments in AD

Impairments in CMA are not specific to PD, with research into the fragmentation of tau across other diseases, including AD, has shown that whilst the procedure starts in the cytosol, it is completed on the surface of the lysosomal membrane, suggestive of incomplete translocation into the lysosome and subsequent failure of degradation (Wang et al., 2009). Furthermore, (Caballero et al., 2021 found that whilst tau is normally degraded by CMA, acetylated tau inhibits the process in their mouse model. This group also reported elevated levels of acetylated tau in association with lysosomes in the brains of AD patients. Other research has confirmed CMA as a potential viable therapeutic target in AD by demonstrating that upregulating this pathway can reduce the formation of Aß oligomers in iPSC models (Dou et al., 2020) and plaques in mouse models (Xu et al., 2021).

Moreover, the autophagy deficit in AD has not just been shown in CMA. Research by Pickford et al. (2008) has shown that in both post mortem human brain tissue and mouse models there is an impairment in the MA recruitment mediated by Beclin-1, evidenced by a reduced expression of this key MA associated protein with increasing Braak Stage. Another later study (Esteves & Cardoso, 2020) showed differences in the regional expression of autophagy markers, with reduced beclin-1 levels in the cortex and an increase in p62 and LC3-II in the cortex and hippocampus, which could be indicative of incomplete macroautophagy within some brain regions. This study also highlighted the need for

regional assessment of these key markers in relation to abnormal protein accumulation, something that has not yet been done in relation to FTD.

1.3.3 Autophagy impairment in FTD - evidence so far

Within FTD, most autophagy research has focused upon cell culture and mouse models which has allowed some consideration of the impact of specific FTD associated genetic factors, but leaves gaps in understanding with respect to FTD in humans, given the clinical, pathological and genetic heterogeneity of the group of diseases.

Given the evidence described previously (see Chapter 1.1) in relation to the key FTD genes such as *C9orf72* and *GRN* having roles in autophagy and lysosomal function, and the reduced accessibility to FTD brain tissue due to its decreased societal prevalence, it makes sense that much of the FTD based protein degradation pathway research has been done in animal and cellular based models of disease.

In a mouse model of FTLD-TDP43, rapamycin was used by Wang et al. (2013) as potential treatment to reduce proteinaceous accumulations and subsequent cell death. Findings showed that when rapamycin was administered from 2-months of age (when the mice start to show impairments in motor and memory function) impairment is rescued and sustained up to for four months. If a combination of mTOR dependent and mTOR-independent drugs were given at six months of age, improvement was sustained for one month and the survival of neurons was increased. While these findings suggested that a there was a rescuable deficit in autophagy in FTLD-TDP43, it did not identify the exact nature of the deficit and where abouts in the complex pathways the system was failing.

Valproate is another drug with autophagy enhancing properties and this particular drug has been trailed unsuccessfully (Piepers et al., 2009) in the treatment of TDP43 proteinopathy in humans. However, this may have been due to a limitation of the dosage used before adverse effects presented and overshadowed and potential benefits of protein clearance. To further explore this, subsequent research has attempted to see how valproate attenuates the toxic effects of TDP43. By using plasmids for full length TDP43 and shorter fragments (TDP-5 and TDP25) on SH-SY5Y cells, Wang, Ma, et al. (2015) showed that whilst the shorter TDP43 C-terminal fragments enhanced toxicity, all TDP43 fragments also enhanced MA, demonstrated by an increase in LC3-I to II conversion and an upregulation of Beclin-1. This was in conjunction with an increase in endoplasmic reticulum stress. However, with the administration of valproate, endoplasmic reticulum stress was decreased and autophagy further increased, thus suggesting that autophagy upregulation could be a cellular defence mechanism in TDP43 proteinopathy which when combined with ER stress could lead to cell death. The authors proposed that valproate not only increased the autophagic activity but it also decreased the ER stress, though the exact mechanism was not elucidated.

Other studies have also explored the relationship between FTD and autophagy. Ju et al. (2009) demonstrated with respect to macroautophagy using U-2 OS cells and found that silencing the *VCP* gene resulted in an accumulation of autophagos and when autophagogy was induced using rapamycin the autophagosomes failed to mature. An accumulation of TDP43 was also noted. Furthermore, other research by Webster et al. (2016) discovered a possible autophagy associated function of C9orf72 protein and discussed how its role implicates autophagy disruption in FTLD-TDP43. Using cell culture methods, they found that C9orf72 is a protein that is involved in the initiation of autophagy by controlling the

phosphorylation of the ULK1 complex as previously described (see 1.2.1), however a loss did not prevent activation of the ULK1 complex, but it did prevent the translation of the ULK1 complex to RAB1a. Moreover, their study showed that haploinsufficiency of C9orf72 with the hexanucleotide repeated expansion, as found in patients with FTLD and ALS, resulted in an increase in p62 accumulation suggesting a defect in early autophagy, as opposed to late autophagy. Specifically, it implies that C9orf72 expansions appear to inhibit the ability of cells to degrade abnormally protein that has been marked by p62. Unfortunately, it does not fully explain at which stage as the downstream effects on other MA initiation proteins or if the accumulation in p62 is due to a lack of engulfment by the autophagosome meaning it is not catabolised following fusion to the lysosome.

A mouse knockout study by Wooten et al. (2008) supports p62's role in the protein clearance, finding that mice lacking p62 developed tau pathology with neurofibrillary tangles which was associated with cell death. This also implies that neurons lack an appropriate alternative to mark these aggregated proteins for degradation by MA. P62 therefore is not just a useful marker of abnormal proteins marked for clearance, but in relation to proteins such as tau, it could also shed light on MA given its crucial role in the process.

Many studies have also shifted focus towards the lysosome given their key involvement in the degradation of damaged proteins (for review see (Darios & Stevanin, 2020)). There is conflicting evidence for C9orf72's impact on overall lysosomal counts, with several cell culture models suggesting an increase in lysosomes in these models of neurodegeneration, whilst the opposite has been reported in patient-derived motor neuron models (Casterton et al., 2020). This raises the question as to whether there is a more global variation in

autophagy associated deficit across the different forms of FTD, given the different genetic mutations and pathological proteins seem to have been differentially implicated across the subtypes of disease.

Whilst the research outlined above investigates the role of autophagy in FTLD related protein aggregation, it heavily relies upon cellular or animal models of the disease. Likewise, it does not often consider the individual subtypes of the FTLD proteinopathy observed in humans or how that relates to the clinical phenotype or genetic background. It is now known that many of the different genetic risk factors associated with FTD are differentially associated with the autophagy pathways, yet it is unclear if variations in autophagy associated proteins and machineries exist in the brain as manifestations of the FTD associated mutation. Due to this, valuable insight can be gained by looking at post mortem human brain tissue to see if pathological protein aggregation relates to autophagy marker distribution, and if this varies in relation to FTD genetic background. Furthermore, by looking at markers of specific stages of the autophagy pathway this will narrow down the autophagy impairment which will give targets for more selective drugs that could address the issues associated with more generic prescriptions such as valproate and rapamycin.

Due to the nature of the *in vitro* model studies, where pathology is induced, they don't explain the process by which some cells avoid becoming burdened with protein aggregates. This is particularly of interest in relation to the genetic mutations, as despite universal expression there is still specificity of the pathology in terms of the affected brain regions. Looking at post mortem tissue could resolve this as the areas of high protein burden can be compared alongside those that appear to age normally, without the accumulation of abnormal protein, and this will allow an exploration further down the line to see if there

seems to be any compensatory mechanism initiated in the ‘healthy’ cells of the disease brains and this could shed light on key neuroprotective mechanisms.

2. Project Aims

The overall goal of this project is to investigate alterations in autophagy pathway marker distribution in human FTLD brain tissue, in relation to genetic background, with AD and normal-aged brain tissue also being investigated providing both disease and no-disease group comparisons. To achieve this, markers of different stages of MA (p62, Beclin-1, LC3) and CMA (LAMP2a and hsc70) were investigated using immunohistological methods in brain regions differentially impacted by FTLD in different forms of FTD (including those with *MAPT* or *GRN* mutations, or *C9orf72* variation). To date there have been no studies that have compared MA and CMA marker distribution across different genetic forms of FTD and so this study has the potential to give a novel insight to the potential variation in autophagic pathway disturbances in relation to abnormal protein accumulation, in FTD.

Moreover, to assess variations in relationships between autophagic machinery and pathological protein burden in regions that are differentially impacted by disease pathogenesis in FTD, sections from the frontal and the temporal lobes will be compared, due to their varying subregional involvement in disease with respect to abnormal protein accumulation. In addition, the temporal sections will include the hippocampus, an area of the brain associated with memory formation and retrieval (Fell et al., 2001) which has subregions that are affected differently by each of the disease subtypes, as described previously.

The techniques involved in this study will allow for the visualisation of the relationship between the autophagy pathways. Immunohistochemical study will give valuable information related to the regional distribution of autophagy markers, whilst shedding light

on the utility of further western blotting type analysis which would give more quantifiable information changes in markers of autophagic flux in a given area, will also be explored. Some pilot data will be presented on western blot analysis of autophagic flux and a consideration of this method will be presented. An exploration of the utility of other approaches such as immunofluorescent double labelling will also be offered, as this approach has the potential to show both the pathological protein and the autophagy marker distribution at a cellular level which could give further insights into relationship between autophagy impairment and protein aggregation. Given the precious nature of human brain tissue and the limited amount of tissue available for the project, this exploration part of the future experiments that could add value to the immunohistochemistry data is important given the scarcity of post-mortem human brain tissue studies.

3 Methods

3.1 Cohort

The cohort being studied is summarised in table 3.1 and includes 24 cases of FTLD, comprised of genetic mutations in *GRN* (7 cases), *C9orf72* (7 cases) and *MAPT* (7 cases). Human brain tissue from patients with AD (8 cases) and no-disease, aged controls (9 cases) were also taken from a previous project exploring the changes in autophagy markers in AD. The no-disease aged controls were used for optimisation of immunohistochemistry runs.

Disease group	Count (N)	Mean Age at death *(SD)*	Min age	Max Age	% Female
No-disease	9	86 *(4.74)*	76	94	66.6
GRN	7	68 *(3.93)*	61	73	57.1
C9orf72	7	67 *(7.81)*	58	73	42.9
MAPT	7	61 *(4.71)*	55	70	71.4
AD	8	76 *(4.39)*	70	82	50.0

Table 3.1: Summary of the basic demographic data from the cohort used in this study.

Human brain tissue was sourced from the Manchester Brain Bank, part of the Brains for Dementia Research project. Brains were collected from donors at autopsy and sent to the Manchester Brain Bank for processing and storage. Tissue is stored in paraffin wax blocks following fixation in formalin or fresh-frozen and stored at -80°C. Data on the relevant genetic info including FTLD associated mutation (*MAPT, GRN* or *C9orf72*) and APOE status, age at time of death, gender and clinical and pathological diagnosis has been provided to experimenters though the PI, who held this data to ensure experimental blinding. Each case has a unique anonymous code which is used to identify sections and to achieve blinding

when regions are scored, and it was agreed that clinical data would not be used unless to address a specific hypothesis arising after preliminary investigation.

3.2 Ethics

Local ethical approval for this project was granted by the University of Salford and ethical approval for the tissue collection, storage and distribution of human brain tissue was granted to the Manchester Brain Bank. Human brain tissue used by the University of Salford in accordance with their guidance and requisition was granted under REC 09/H0906/52.

3.3 Immunohistochemistry

Five micrometre thick sections of formalin fixed-wax embedded sections of human brain tissue from the Manchester Brain Bank were used in the current study, sections were provided from the frontal lobe and temporal lobe, with the latter including the hippocampus; these were chosen as these areas include a variety of anatomically distinct sub-regions which are known to be differentially impacted by the accumulation of pathogenic protein aggregates in AD and the FTD subtypes and at different stages of the disease process (Barnes et al., 2006; Braak et al., 2006; Braak & Braak, 1997; Mackenzie & Neumann, 2016). All experiments were conducted using a previously stained positive control (from a case previously identified by either the Manchester Brain Bank or previous study into autophagy markers and AD (Stan, 2018) to harbour the antigens of interest and a primary antibody devoid negative control.

For all immunohistochemistry experiments sections were dewaxed in Histoclear (National Diagnostics) via two five-minute incubations then rehydrated through five-minute incubations in descending alcohols (100%, 100%, 95% and 75% to distilled water). Antigen

retrieval for hsc70 facilitated then by a four-hour incubation in >99% formic acid before blocking endogenous peroxidase.

Endogenous peroxidase was blocked using 3% H_2O_2 in methanol, with a 20-minute incubation for primary antibodies including, AT8 (Mouse, Pierce) antibody and whilst a one-hour incubation for anti-P62 (Mouse, Abcam), anti-LC3 (Rabbit, Santa Cruz), anti-LAMP2a (Rabbit, Abcam), anti-Beclin1 (Mouse, Abcam) and anti-Hsc70 (Mouse, Abcam) antibodies was required to adequately prevent non-specific reactivity. Heat Induced Epitope Retrieval (HIER) was employed by microwaving the sections in boiling 0.01M tri-sodium citrate buffer pH 6.5 for 10 minutes for anti-p62 however this resulted in significant loss of sections and subregions so whilst a LabVision^{TM} PT module (Thermofisher) was used for all other antibody experiments, except for anti-Hsc70 as this required boiling in a at 126^{o}C for 10 minutes in a pressure cooker to unmask the antigen for detection. The automated system heats the slides up to 98^{o}C for 20 minutes then cools the buffer to a temperature of 85^{o}C, in all cases sections were cooled in running tap water. For anti-TDP-43 (Rabbit, ProteinTech) immunohistochemistry, HEIR was conducted before the endogenous peroxidase block, achieved via a 30-minute incubation in 3% H_2O_2 in methanol.

Non-specific binding sites were blocked prior to primary antibody incubation using the relevant 1.5% normal serum from the appropriate Vectorstain ELITE kit (Vector Laboratories) and incubated at room temperature for 30 minutes for AT8, anti-LC3 and one hour for anti-P62, anti-LAMP2a, anti-Beclin-1, anti-Hsc70 whilst anti-TDP43 was incubated in blocking serum for 16 hours at 4^{o}C, times were adjusted for each antibody to prevent on-specific staining.

Primary antibodies where incubated for one hour at room temperature and used at a dilution of 1:750 for AT8, 1:200 for P62, 1:500 for anti-LAMP2a, 1:5000 for anti-LC3 and 1:1000 for anti-TDP43 antibodies; Meanwhile anti-Beclin-1 and anti-hsc70 antibodies were incubated for 16 hours overnight at 4^{o}C using a dilution of 1:2000 and 1:4000 respectively, before washing with tris-buffered saline (TBS, 50mM Tris Base, 150mM NaCl , pH 7.5) with 0.1% Tween 20. TDP43 immunohistochemistry washing protocols were an exception where Phosphate Buffered Saline (PBS, Sigma-Alrich) was used as an alternative to TBS. This was succeeded by a 30-minute incubation in animal specific anti-IgG secondary antibody (1:200, Vectorstain ELITE). Sections were then washed with TBST or PBS (anti-TDP43 only) and incubated for another 30 minutes in avidin-biotin complex (ABC, 1:25, Vectorstain ELITE), made up 30 minutes prior as per manufacturer's instructions before a final wash in TBST/PBS.

Antibody	**Host species**	**Dilution**	**Antigen retrieval**	**Manufacturer**
AT8	Mouse	1:750	HEIR @ 98°C 20 mins	Pierce
P62	Mouse	1:200	HEIR @ 98°C 20 mins	Abcam
LAMP2a	Rabbit	1:500	HEIR @ 98°C 20 mins	Abcam
LC3	Rabbit	1:5000	HEIR @ 98°C 20 mins	Santa-Cruz
TDP43	Rabbit	1:1000	HEIR @ 98°C 20 mins	ProteinTech
Hsc70	Mouse	1:4000	4 hours Formic acid HEIR @ 128°C 20 mins	Abcam
Beclin-1	Mouse	1:1000	HEIR @ 98°C 20 mins	Abcam

Table 3.2: A summary of the antibodies used in immunohistochemistry, blocking serums and secondary antibodies where from the appropriate VectaStain Elite kit.

Immunopositivity was visualised using 3, 3’ Di-aminobenzidine (DAB) using DAB tablets (Sigma-Aldrich) (anti-P62, AT8, anti-TDP43, anti-LC3 and anti-LAMP2a), or DAB powder (ThermoFisher Scientific) made up to 1:100 in PBS 0.096% H_2O_2 (anti-Beclin-1 and anti-hsc70). The difference in DAB protocols was due to consulting with the team at Queen Square brain bank due to inconsistent visualisation of the anti- Beclin-1 and hsc70 markers, where more favourable results were achieved with the latter protocol. Visualisation of the antigen was conducted with reference to the positive control for a maximum of ten minutes and the same positive control was used to ensure consistency between experimental runs. Development of peroxidase activity was stopped by washing in tap water thoroughly. Sections were counterstained in haematoxylin, washed in tap water and dehydrated by 5 minute incubations through ascending alcohols (75%, 95% and 100%, 100%) and cleared in fresh Histoclear, then mounted and cover slipped using Dibutyl Phthalate with Xylene (DPX). A summary of the antibodies used and the antigen retrieval methods used can be found in table 3.1.

3.4 Assessment

3.4.1 *Hippocampal assessment*

Figure removed due to copyright.

Figure 3.1: Anatomy of the hippocampus, showing the dentate gyrus, CA4-1, the subiculum and parahippocampal gyrus, which contains the entorhinal cortex with transitions into the temporal cortex at the collateral sulcus (not shown). Image from *Hippocampus* 2011).

Immunoreactivity for p62, Beclin-1, hsc70, LAMP2a and LC3 were scored in the temporal lobe of a cohort made up of 7 cases with *C9orf72* expansions, 7 *GRN* mutations, 7 *MAPT* mutations, 8 AD and 9 normal-aged. The sections of the temporal lobe were taken at the level of the hippocampus and so given the anatomical complexity of this region, a number of different subregions were independently assessed for the markers of interest, given these regions are known to differentially demonstration pathological load in relation to the stage and type of neurodegenerative disease. The subregions scored included the dentate gyrus, CA4, CA1, the subiculum and hippocampal white matter. The grey matter areas included in

the assessment can be seen in figure 3.1. Additionally, temporal grey and white matter was scored in inferior temporal gyrus.

The proportion of cells stained was scored on a semi-quantitative scale from 0- (0% positively stained cells), 1 – mild (>20% positively stained cells), 2-moderate (20-70% positively stained cells or 3- severe (>70% positively stained cells). Since there was a notable variation in the intensity of the staining documented (even when the positive control remained consistent), this too was noted on a semi-quantitative and this scale is demonstrated in figure 3.2 and ranged from 0-absent, + -pale, ++ -mild, +++ - intense).

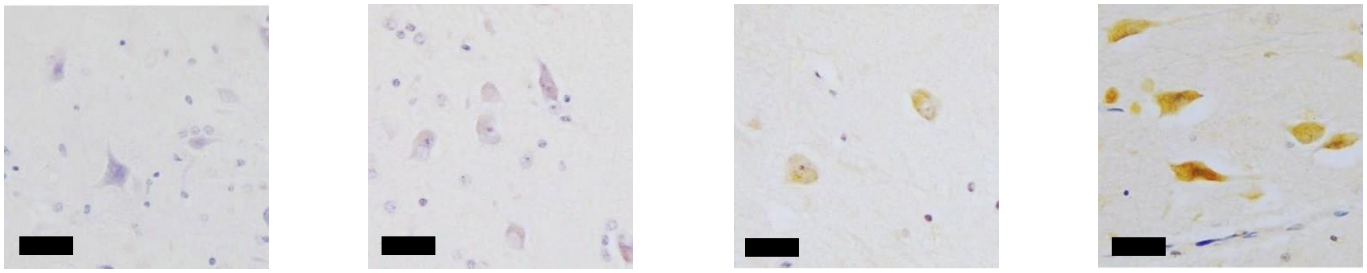

Absent 0 Pale + Moderate ++ Intense +++

Figure 3.2: images showing severity of scoring using anti-LC3 immunohistochemistry an example, showing 0 to intense staining from left to right. Bar indicates 50µm

The scores were combined by adding them together for analysis to give a final value between 0 and 6 for each subregion (Dentate gyrus (DG), CA4, CA1, Subiculum, Temporal Grey Matter, and Temporal and Hippocampal white matter.

This semi-quantitative scoring approach which considered both number of cells impacted and intensity of staining was a scoring methodology in use at the Manchester Brain Bank and was also was similar to Pickford et al. (2008) and Ma et al. (2010) in their assessment of Beclin-1 and LC3 immunohistochemistry in human brain studies.

Scoring was conducted with the assessor blind to the pathological subtypes of FTLD and Braak-stage. Specifically, when assessing neuronal inclusions, threads, grains and oligodendroglial coiled bodies were scored according using the above semi-quantitative scale. There was also an additional category for comments about the nature of the lesions or if there was any other pathology of note, such as unspecified WM pathology or significant spongiosis in the tissue, which could allow for further investigation at a later time.

3.4.2 *Frontal lobe assessment*

For the frontal lobe scoring criteria was the same for as for the temporal lobe and has been completed and analysis for anti-LC3, anti-LAMP2a, anti-Beclin-1 and anti-Hsc70 immunohistochemistry. The regions of interest in the frontal lobe were the six layers of the grey matter (noted as Layers I, II, III, IV, V and VI) which are numbered from the most superficial layer (Layer I) to the deepest grey matter layer (Layer VI) (figure 3.3). These cell layers are known to be differentially impacted by pathogenic protein load in different types and stages of neurodegenerative disease (Charles Duyckaerts et al., 2009; Mackenzie & Neumann, 2016). Each layer was scored 0 to 3 for both number of cells stained and the intensity of the staining and combined to give a final score of 0 to 6, in the same fashion as the temporal cortex. The frontal white matter immediately below Layer VI was also scored, with this particular region of white matter being used to ensure the same type of white matter was scored in each case.

For AT8 and TDP-43 immunohistochemistry, only rudimentary information on the ability of these methods to detect the proteins target and lesion types has been collected due to the mitigating circumstances that interrupted part of this project.

Figure removed due to copyright.

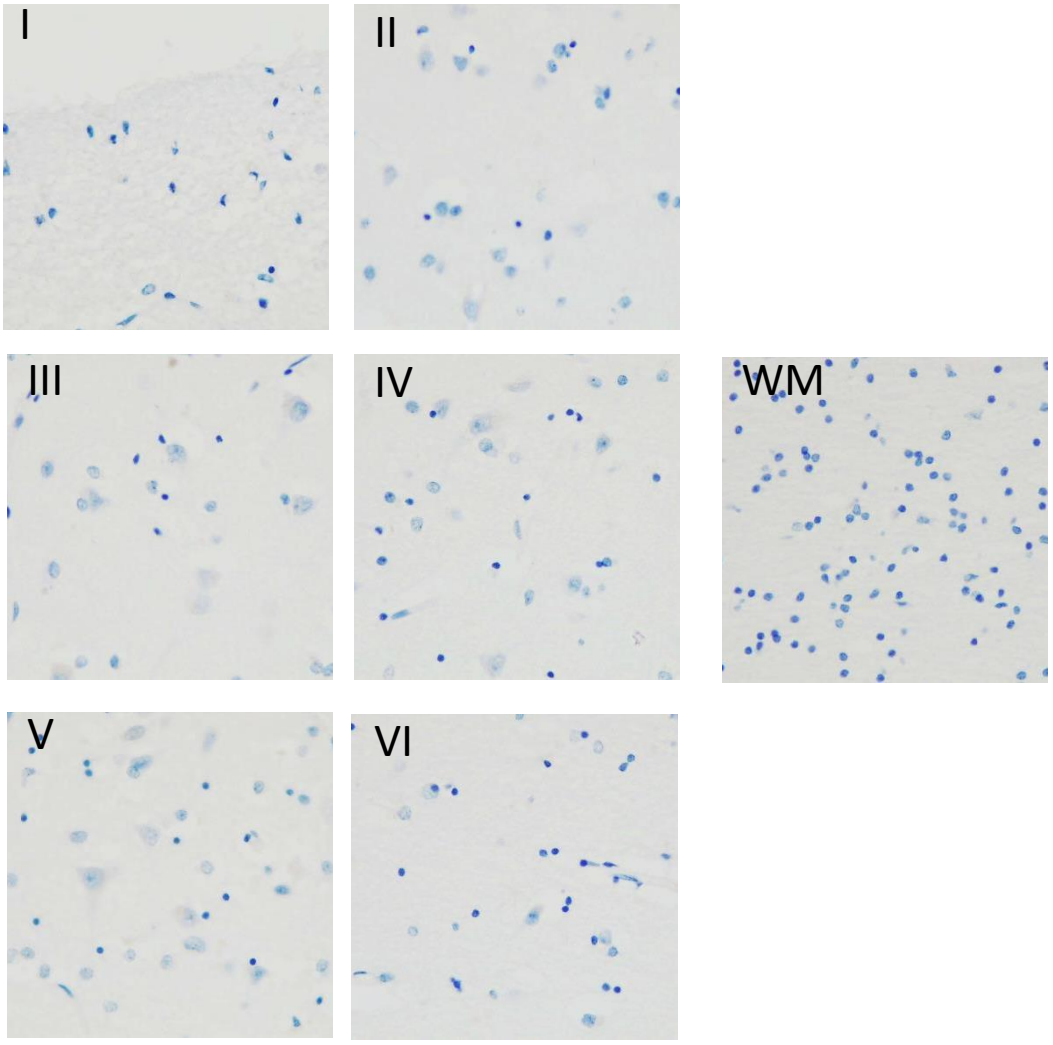

Figure 3.3: Micrograph demonstrating the layers in the GM seen in the frontal lobe (image from Orehek AJ, Iglesias-Rozas JR and Garrosa M, 2018). Inset regions show x400 magnification micrographs of these layers as stained in this project.

3.5 Statistical Analysis and Software

To visualise the prevalence of P62 positive lesions in different regions and disease groups, scores were dichotomised so that scores of 0 and 1 were grouped into 'no significant pathology' and score of 2 and 3 were grouped into a 'significant pathology' group. These

groups were encoded as a binary variable of 0 and 1 respectively. Regional variation in pathology and the lesions types were then analysed with respect to the disease types (FTLD-*MAPT*, FTLD-*C9orf72*, FTLD-*GRN*, AD and no-disease controls). This method was employed as the aim was to assess if there was variation in the ability for p62 to mark the proteins for degradation rather than to rely on p62 to assess pathological protein burden; however due to mitigating circumstances associated with the project, the pathological protein markers scoring has not been complete for this comparison.

For each of the autophagy markers, scores (LAMP2A, LC3, Beclin-1 and Hsc70) were combined into a single score by addition giving a final value between 0 and 6 as described previously, to allow consideration of both number of cells demonstrating positive staining along with the intensity of staining. Analysis was conducted using IBM SPSS statistics version 22 using Kruskal-Wallis test to observe differences between the mutation groups (FTLD-*MAPT*, FTLD-*C9orf72*, FTLD-*GRN*, AD and no-disease). For *post hoc* assessment Dunn-Bonferroni test was utilised, due to the small sample size and, to assess the significant differences between two disease groups. Significance was set at $p \leq 0.05$ without exception, exact p-values are reported unless otherwise stated.

3.6 Protein extraction and Western Blotting

Some preliminary work initiated as part of this project aimed to begin the optimisation of western Blotting studies and assess the utility of this method in exploring alterations in autophagic flux.

3.6.1 *Human-derived fibroblasts*

In order to minimise the use of fresh-frozen human brain tissue, skin-derived fibroblasts from a healthy individual used for another project were used in the optimisation of the

western blotting. Cells had been stored in liquid nitrogen and were thawed in a 37°C and centrifuge for four minutes at x400g, the pellet was resuspended in cell culturing media and incubated for 24-48hrs in a culturing flask at 37°C, 5% CO_2. For all fibroblast culturing MEM media enriched with 15% Fetal-Bovine Serum, 1% non-essential amino-acids, 1% MEM non-Vitamins, 2mM Glutamine and 100µg/ml penicillin-streptomycin was used. After 24- and 48-hours cells where checked for adhesion, once cells had adhered culturing media was changed every two days until they reached approximately 80% confluency.

Once cells had grown to cover 80% of the flask they were subcultured, frozen or underwent protein extraction. In all cases, cells were washed twice in sterile PBS and incubated with 5mls of Trypsin/EDTA at 37°C for up to 3 minutes, culturing media was added to the flask to neutralise the trypsin and then centrifuged at x400g for 4 minutes.

For subculturing, supernatant was discarded, pellet resuspended into 6ml of media, and one third of this resuspension was added to each T75 flask with culturing media added to a make a final volume of 17ml. To freeze cells, the cell pellet was resuspended in 1ml of freezing media containing DMSO, placed in a Mr Frosty™ (Thermo Scientific) and left in a -80°C freezer for at least 24 hours before transferring back to liquid nitrogen.

For protein extraction, the pellet was washed via resuspension in PBS and centrifuges at x400g three times, before the final pellet was resuspended in 150µl RIPA buffer containing 1x protease and 1x phosphatase inhibitor cocktails. The resuspension was lysed on ice whilst agitating for five minutes and then transferred to storage at -80°C.

3.6.2 *Human Brain Protein Extraction*

Protein was extracted from fresh-frozen human brain tissue in accordance with the method used by Murphy et al. (2014), which was an adaption of the methodology used by Zhou et al. (2011). In brief, 300mg of brain tissue from the frontal lobe was homogenised using a motor driven homogeniser in 3ml of homogenisation buffer (0.32m sucrose, 1mM EDTA, 10mM Tris-Hcl pH 7.4, 1 x protease inhibitor cocktail [Roche] and 1 x phosphatase inhibitor cocktail [Roche]). This homogenate was centrifuged for 10 minutes at 1000g 4^{o}C and the pellet washed twice by resuspending in buffer and repeating the centrifugation. The pellet from this step contained mostly unbroken cells and the resulting supernatant was harvested and then centrifuged at 17,000g for 15 minutes at 4^{o}C to produce a lysosomal enriched pellet, which was then resuspended in the homogenisation buffer. Finally, this supernatant was centrifuged at 100,000g 4^{o}C for 30 minutes producing a supernatant containing the cytosolic compounds and a pellet of the microsomal extract. All fractions were stored at -80°C until use.

3.6.3 *Sample Preparation*

All samples were prepared for SDS-PAGE by adding equal volumes of the homogenate sample with to an activated sample buffer, composed of 2x sample buffer (100mM TrisHcl, pH6.8, 4% SDS, 0.02% Bromophenol blue) and 200 mM Dithiothreitol (DTT) in a 4:1 mixing ratio. Samples were boiled in a dry bath at 99.9^{o}C for 5 minutes to complete protein denaturation before being loaded onto polyacrylamide gels.

3.6.4 *SDS-PAGE*

The homogenised protein extracts were separated by SDS-PAGE using 12% bis-acrylamide 1:29 (BioRad) gels, with the volume in each well equalised to 20µl with the addition of 1x

sample buffer. Electrophoresis was conducted using 4°C electrolyte buffer (25mM Tris Base, 192 mM Glycine, 2mM SDS) at a constant 150V in an ice bath for all experiments except for the initial gel which was run at room temperature. Acrylamide gels were then washed in a 25mM Tris base, 192mM Glycine, 20% Methanol buffer and then transferred to a 0.2µm-pore nitrocellulose membrane for 1 hour at 100V. Membranes were washed in TBST and blocked for 30 minutes in a 1% BSA/5% Milk TBST blocking solution and probed with primary anti-LC3 (Novus) antibody for 1 hour; For optimisation a variety of antibody dilutions were attempted including 1:500, 1:1000, 1:2000 and 1:4000. Following primary antibody incubation membranes were blocked for 30 minutes in blocking solution followed by a 30 minute incubation in goat raised anti-rabbit IgG antibody (1:5000), which was HRP conjugated (Thermo scientific). Bands where visualised using West Femto (ThermoFisher Scientific) Enhances Chemiluminescent (ECL) substrate and imaged via a Syngene G:Box with GeneSys software.

A variety of protein loads were used in the optimisation of the protocol to detect LC3B, which was expected to yield bands at ~15kDa and ~17kDa, which necessitated the use of a miniium of a 12% acrylamide gel for resolution. Initially a Bradford assays were used to quantify the protein concentrations of the samples. This was achieved by comparing a 2.5µl of sample diluted in 997.5ul distilled water against standards made up of Bovine Serum Albumin in 2.5µl of RIPA buffer to create protein concentrations of 1µg/ml, 2µg/ml, 4µg/ml, 6µg/ml, 8µg/ml, 10µg/ml, 15µg/ml, 20µg/ml and 25µg/ml creating a protein curve.

To visualise the protein load G250-Coomassie Blue (Pierce, ThermoScientific) reagent was added in equal quantities to protein standard/sample and the optical density measured at 595nm. However, in later experiments this found to produce many false negative results

(i.e. no detectable protein) which were contradicted by incubating gel/membranes with Coomassie blue reagent for 10-minutes. Therefore, later studies used similar volumes to load and use a β-actin as a control to normalise the marker results.

To strip and reprobe the membranes for the β-actin loading control, membranes were washed 4 times for 5 minutes in TBST and then incubated for 10 minutes in a high pH stripping buffer (15.38mM Glycine, 0.1% SDS, 1% Tween 20, pH2.2). Membranes were washed another 4 times in TBST before being blocked for 30 mins in 1% BSA in TBST and then were incubated with a 1:5000 or 1:10000 dilution of the primary β-actin antibody (Pierce, ThermoFisher), at room temperature for 1 hour. Washing was repeated followed by another 30 minute block in 1% BSA in TBST solution and then the membrane was incubated for 1 hour at room temperature in anti-mouse IgG HRP antibody, before the membrane was rewashed and proteins were visualised using the ECL method as previously described.

4 Pathology

4.1 Introduction and Aims

In accord with the tissue request agreement it was important to ensure the hippocampus would provide variability in the marking of pathological proteins for degradation, so p62 immunohistochemistry was used to assess the present of pathological proteins in the subregions of the hippocampus and will be outlined in this chapter. There was also an aim to assess the pathological proteins themselves, however this was not completed due to mitigating circumstances of this project, but the initially attempts to conduct immunohistochemistry for TDP43 and using AT8 for tau will be included.

4.2 Case Overview

Case No.	Sex	Age at death	Clinical Diagnosis	Pathological Diagnosis	Mutation	APOE status
2009026	M	85	No Disease	No Disease		33
2009031	F	94	No Disease	No Disease		33
2011015	F	87	No Disease	No Disease		33
2011022	F	90	No Disease	No Disease		33
2014004	F	87	No Disease	No Disease		34
2014008	M	85	No Disease	No Disease		33
2014009	M	84	No Disease	No Disease		33
2014016	F	76	No Disease	No Disease		34
2014020	F	90	No Disease	No Disease		33
DPM95/32	F	58	FTD	FTLD-tau MAPT	MAPT	33
DPM96/21	M	55	FTD	FTLD-tau MAPT	MAPT	34
DPM99/01	M	70	FTD	FTLD-tau MAPT	MAPT	34
DPM01/01	F	65	FTD	FTLD-tau MAPT	MAPT	33
DPM07/09	F	60	FTD	FTLD-tau MAPT	MAPT	33
DPM09/32	F	58	FTD	FTLD-tau MAPT exon 10 +16 mutation	MAPT	33
DPM12/30	F	63	FTD (MAPT mutation)	FTLD-tau exon 10 +16 mutation	MAPT	33
NSP87/81	F	71	FTD	FTLD-TDP A	GRN	33
NSP90/80	F	61	FTD	FTLD-TDP A	GRN	
DPM94/13	F	66	FTD	FTLD-TDP A	GRN	33
DPM97/33	F	67	FTD	FTLD-TDP A	GRN	33
DPM01/02	M	66	FTD	FTLD-TDP A	GRN	33
DPM12/02	M	73	Pick's Disease	FTLD-TDP Type A (PGRN)	GRN	33
DPM13/04	M	72	PNFA	FTLD-TDP Type A	GRN	34
N114/92	M	58	FTD	FTLD-TDP A	C9ORF72	33
DPM01/06	F	64	FTD	FTLD-TDP A	C9ORF72	33
DPM09/08	F	70	FTD	FTLD-TDP type B	C9ORF72	33
DPM09/29	M	82	FTD	FTLD-TDP type A	C9ORF72	33
DPM13/26	M	65	FTD	FTLD-TDP type A	C9ORF72	33
NSP88/82	M	59	FTD+MND	FTLD-TDP B	C9ORF72	33
DPM11/18	F	73	MND/FTD	FTLD-TDP type B	C9ORF72	33
2010010	M	82	Alzheimer's Disease	Alzheimer's Disease		34
2011002	F	70	Alzheimer's Disease	Alzheimer's Disease		44
2011028	F	71	Alzheimer's Disease	Alzheimer's Disease		44
2012003	F	72	Alzheimer's Disease	Alzheimer's Disease		34
2012005	M	73	Alzheimer's Disease	Alzheimer's Disease		44
2012017	M	76	Alzheimer's Disease	Alzheimer's Disease		44
2012029	F	81	Alzheimer's Disease	Alzheimer's Disease		33
2013045	M	79	Alzheimer's Disease	Alzheimer's Disease		33

Table 4.1 Overview of the clinicopathlogical information of the cases used in the present study.

Table 4.1 outlines the cohort as provided by Manchester Brain Bank. As expected all 7 of the cases with a MAPT mutation had pathological FTLD-tau and a clinical diagnosis of FTD, whilst all of the 7 GRN mutations cases were pathologically FTLD-TDP Type A with a diagnosis of FTD, it is noted that one is listed at Pick's Disease however clinically this is sometimes used to refer to bvFTD. The C9orf72 expansion cases have a FTLD-TDP43 subtype of type A or B, which is in keeping with the literature as previously described and a clinical diagnosis of and FTD variant, two of these cases had co-morbid MND. For all of the cases in the no disease group there were no a clinical or pathological diagnoses of a neurological or neurodegenerative disease, whilst the AD group only had AD as a clinical and pathological diagnosis. Overall for FTLD mutations and their pathological diagnosis are in keeping with the literature and clinically there are no atypically presenting cases.

4.3 P62 immunohistochemistry

Following successful optimisation of p62 immunohistochemistry, the inclusion types were characterised for scoring. Within the AD and control cohort, neuronal inclusions similar to neurofibrillary tangles (figure 4.1) were noted in grey matter areas. In addition, in the white matter (WM) of the FTD cases oligodendroglial coiled bodies were observed (figure 4.2), characterised by immunoreactivity curling around the glial cell nucleus with a thin 'tail'. Final observations, where a slightly different neuronal inclusion in some of the FTD cases (figure 4.3), which in some cases demonstrated a more bulbous or swollen cell body and/or a flame-like appearance. Astrocytic and plaque pathology was not observed in any of the cases but the presence of argyrophilic grain like structures was also recorded.

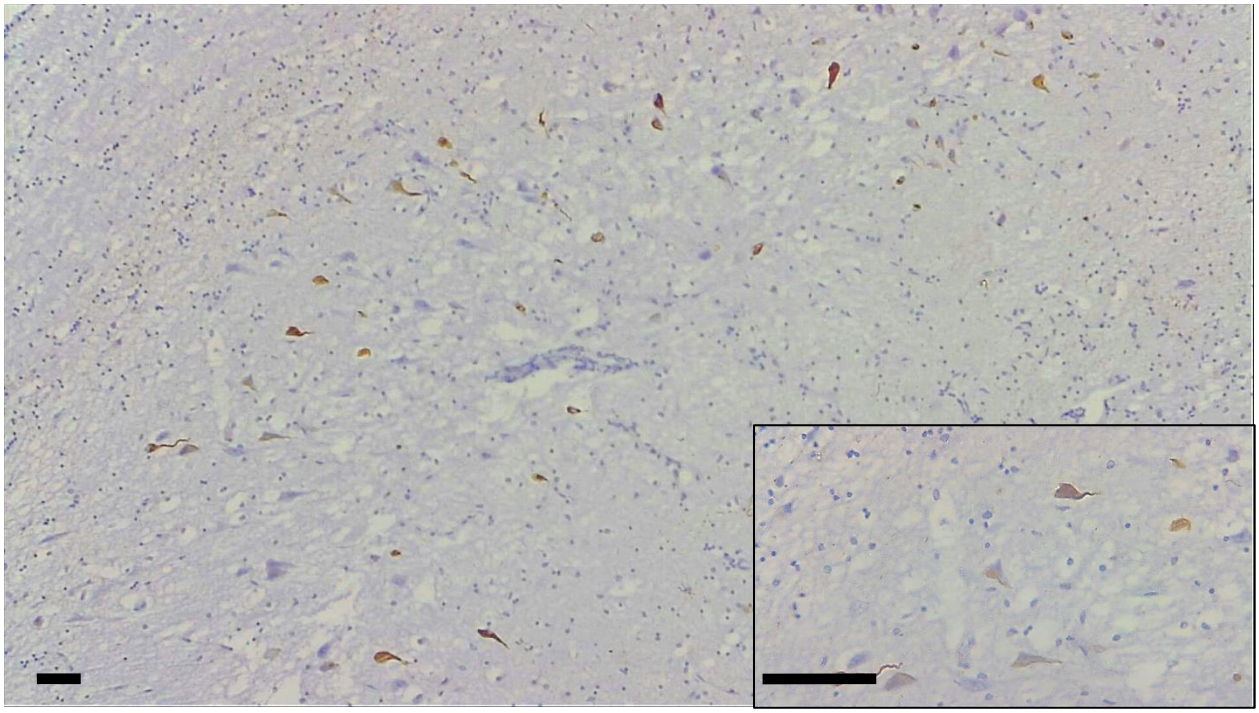

Figure 4.1: x100 micrograph of AD neuronal p62 pathology, inset x400 micrograph of the same case and region. Bar indicates 100µm.

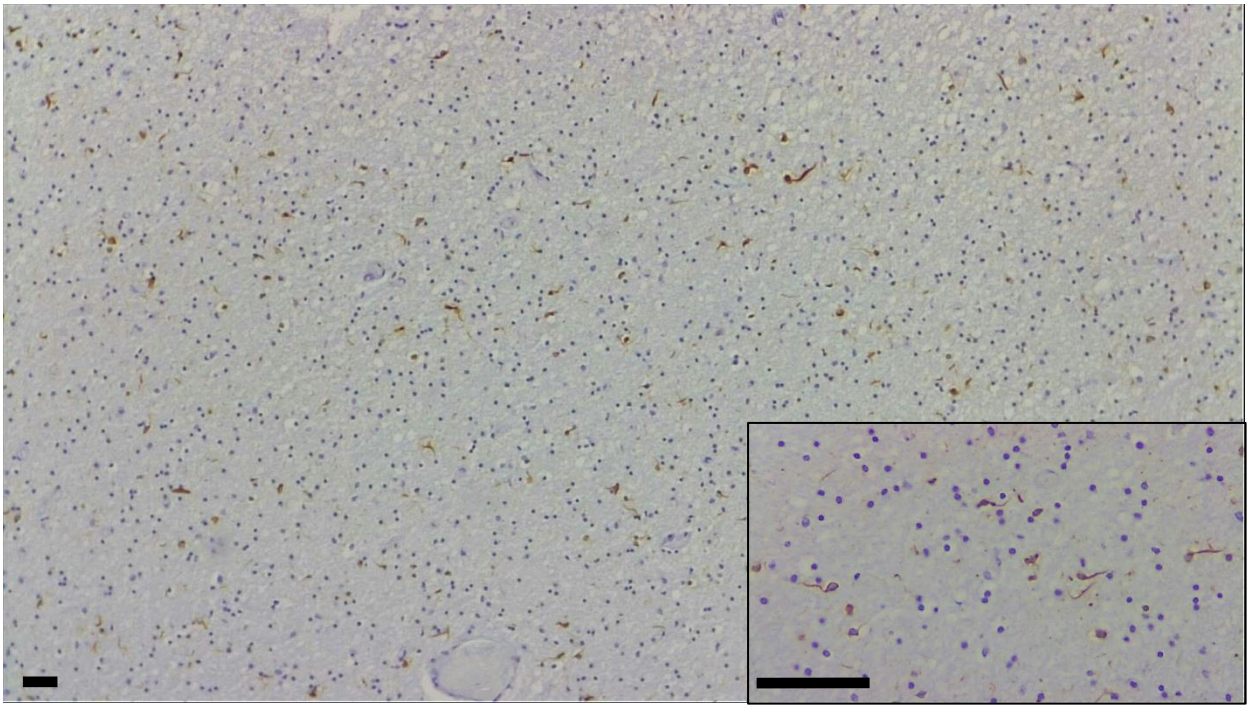

Figure 4.2: x100 micrograph of oligodendroglial coiled bodies. Inset x400 micrograph of the same case and region. Bar indicates 100µm

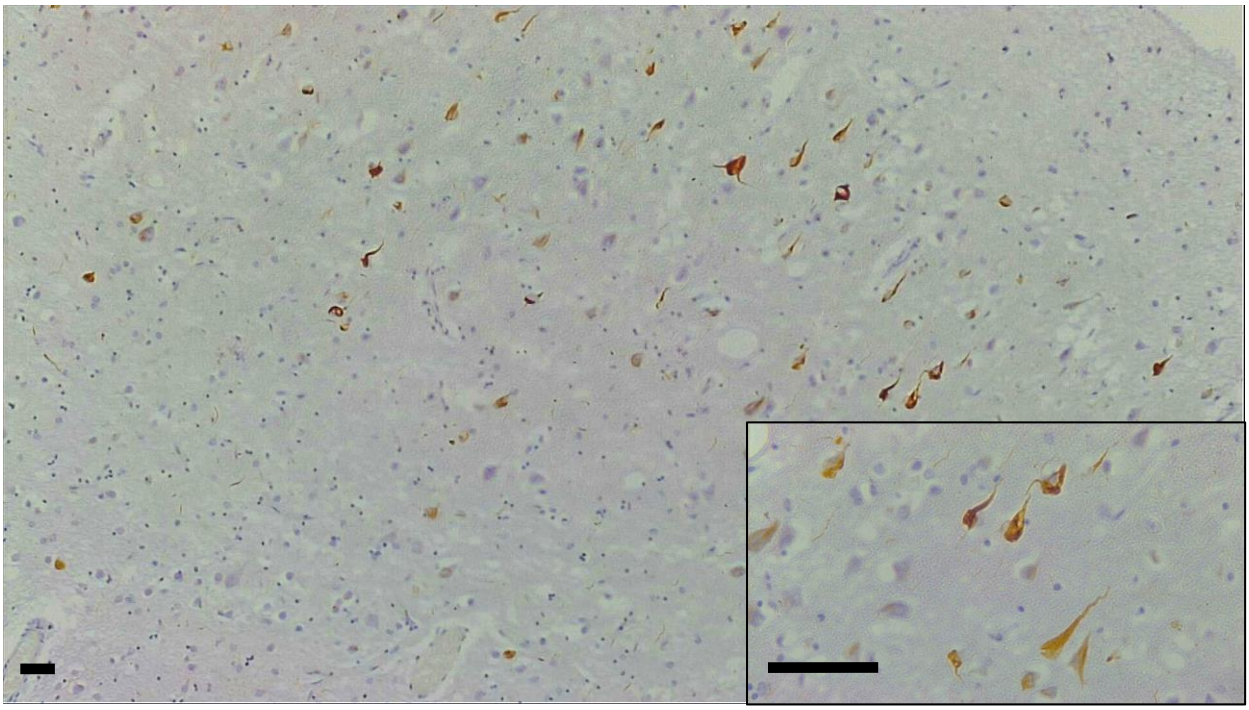

Figure 4.3: x100 micrograph of neuronal inclusions in an FTLD-Tau case, inset a x400 micrograph of the same case and region. Bar indicates 100µm

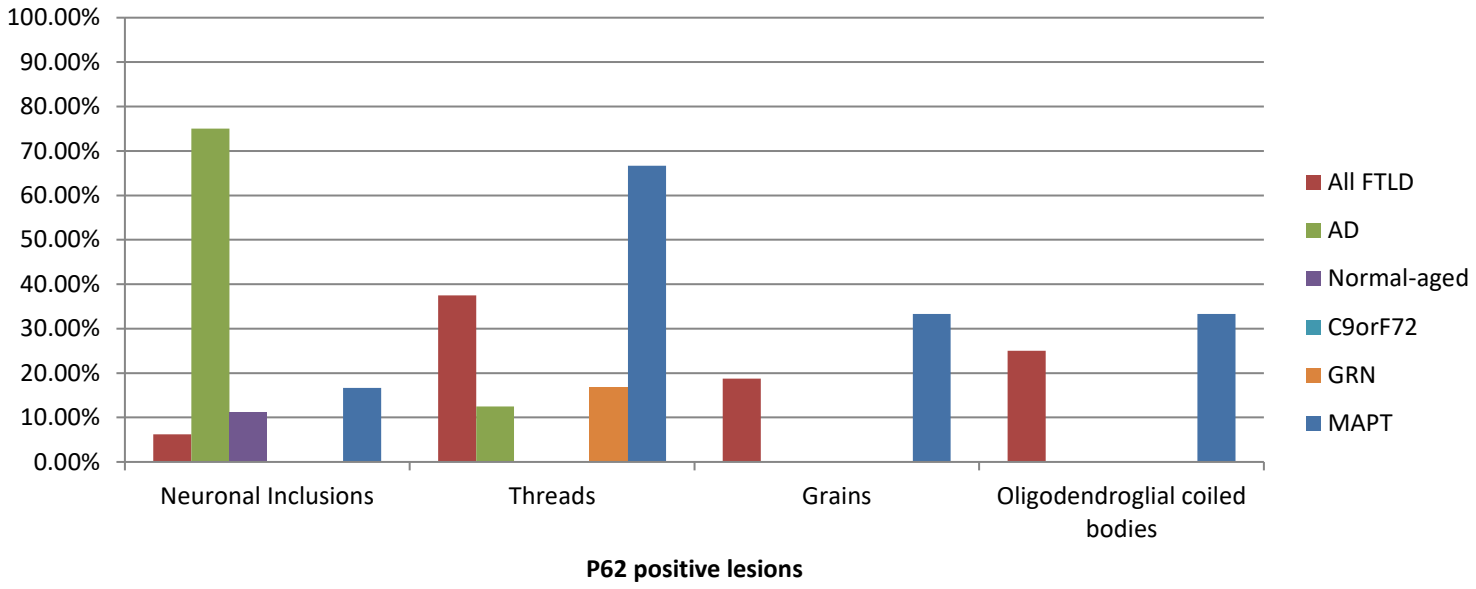

Figure 4.4: Bar chart showing the distribution of the different p62 positive lesions by temporal lobe sub-region; "All FTLD" groups all four mutations; AD Alzheimer's disease

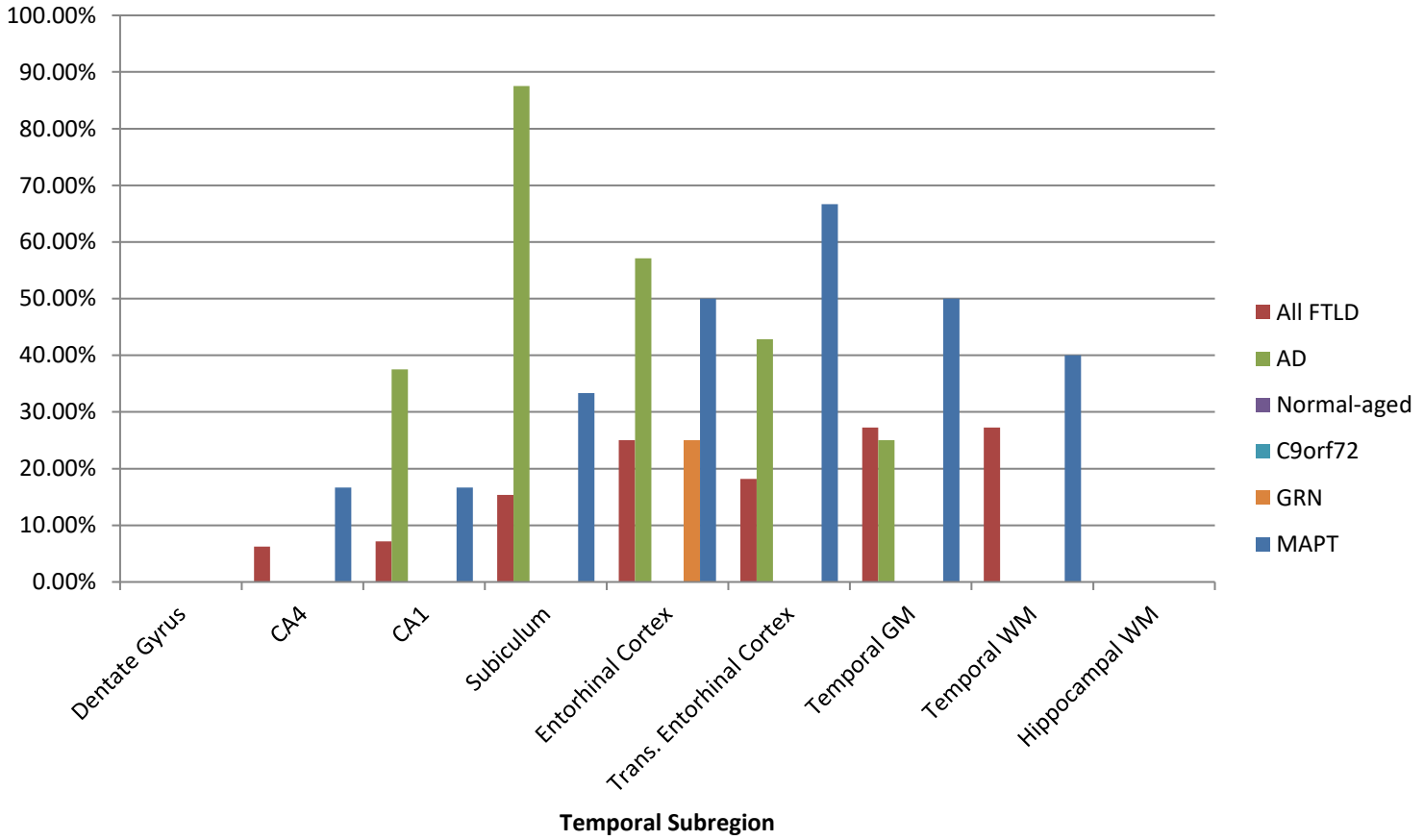

Figure 4.5: Bar chart showing the percentage of cases showing significant p62 immunopositivity (in consideration of all lesion type) by temporal lobe sub-region; "All FTLD" groups all four mutations; AD Alzheimer's disease

From the C9orf72 subgroup 3 of the cases failed to successfully stain for p62 due to the integrity of the tissue from cases N114/92, DPM 01/06 and DPM 09/08. For MAPT this was also true case DPM96/21 and case NSP87/81 from the GRN cohort.

In the first instance, the different sub-types of FTLD were grouped for comparison with AD and the no disease control to allow an overall view of these cases as part of the FTLD spectrum (noted as 'all FTLD' on figure 4.4), this was done initially due to small sample sizes, especially when considering missing brain regions from the tissue provided. With respect to the prevalence of the aggregate types detected, neuronal inclusions were present in all three disease groups, however they were most common in AD, present in 6 out of 8 of cases, and least common in across the FTLD group with only 1 out 16 detecting significant neuronal p62, with the normal-aged group also detecting significant pathology in 1 out of 9 groups. Both FTLD and AD demonstrated the presence of P62 positive threads, in 6 out of 16 and 1 out of 8 cases respectively, whilst none of the no disease controls showed any P62 positive thread pathology. Only the FTLD cases showed the presence of P62 positive argyrophilic grain-like structures or white matter oligodendroglial coiled body pathology in 3 out of 16 and 4 out 16 of cases respectively.

Investigating the FTLD mutations most of the p62 immunoreactivity was found within the *MAPT* cases (N=6) with 1 case out of the 6 demonstrating neuronal inclusions, 4 out 6 cases demonstrating p62 positive threads, 2 cases showing grains and 2 having oligodendroglial coiled bodies. *C9orf72* (N=4) cases showed no p62 immunoreactivity and the *GRN* cases (N=6) presented with threads in 1 of the cases.

In terms of the regional distribution, the most commonly affected subregion in *MAPT* mutant cases was the trans-entorhinal cortex (2 cases), however this area was only available in 3 cases

due to the way the tissue section had be sectioned and provided. Other regions which demonstrated p62 immunoreactivity in the *MAPT* group included the temporal grey matter (50.00%, 2 out of 4), subiculum (50.00%, 2 out of 4), temporal white matter (40.00%, 2 out of 5 cases), CA1 (1 out of 6) and CA4 (1 out of 6). In the *GRN* mutant group only the entorhinal cortex demonstrated significant p62 immunopositivity, with 1 out of the 4 cases having some degree of significant pathology. None of the *C9orf72* mutant cases had a significant amount of immunoreactivity in the temporal lobe (n=4).

In terms of regional distribution (figure 4.5), none of the ND, AD or FTLD cases showed significant- pathology in the dentate gyrus or hippocampal white matter. Whilst in the AD group, pathology was most predominantly focused around the hippocampal, entorhinal and temporal grey matter areas, negating CA4. In the dentate gyrus, hippocampal white matter and temporal white matter none of the AD cases had significant p62 pathology, whilst, for AD cases, p62 pathology was most prevalence in the subiculum (7 out of 8 cases), entorhinal cortex (4 out of 7 cases), transentorhinal cortex (3 out of 7 cases), CA1 (3 out of 8 caes) and finally temporal grey matter (2 out of 8 cases).

When all FTLD groups are considered together they had a lower prevalence of P62 pathology compared to AD in CA1, the subiculum, and the entorhinal cortex, but a higher prevalence in CA4 and temporal WM when compared to the AD and normal-aged groups. Significant temporal grey matter pathology was similar in both AD (2 out of 8 cases) and FTLD (2 out of 11 regions scored) whilst in normal-aged brains was not evident in any of the case (n=9). 3 of the FTLD cases (n=11) showed Temporal WM pathology (where this region was available), which comprised of OCB and threads, whilst the AD and normal-aged groups showed no such pathology.

In conclusion, the *MAPT* FTLD group harboured some distinct P62 positive lesions, namely the OCB and grains, that were not detected in the other groups investigated, along with a particularly high detection of P62 positive thread pathology. The P62 positive neurons detected in AD were significantly less prevalent across the FTLD and control group. A regional variation of P62 immunopositivity was also noted across the normal-aging, AD and different FTLD subgroups.

4.4 AT8 immunohistochemistry

The brain tissue provided by the Manchester Brain bank had already been Braak staged as part of their tissue collection process, but an assessment of the accumulation of tau pathology in the different anatomical sub-regions and cell layers across the different study groups was a complementary piece of work that was initiated but not completed due to the mitigating circumstances associated with this project.

AT8 immunohistochemistry was first optimised using a 1:500 (image 4.19a) antibody dilution using the FTLD-*MAPT* tissue, however in order to compare tissue with the no-disease controls and AD, which had been previously stained as part of another project, further optimisation was needed since the previous AD and no-disease controls experiments used a 1:750 dilution (image 4.19b). When the FTLD tissue was stained using this antibody dilution, the results were not consistent with the other study (Images 4.19 c&d). Therefore, due to the time and tissue constraints in association with the mitigating circumstances of this study, along with the fact that the known inconsistency of pathogenic tau presence in no-disease aged and some of the FTLD sub-groups, AT8 immunohistochemistry was not pursued across this cohort.

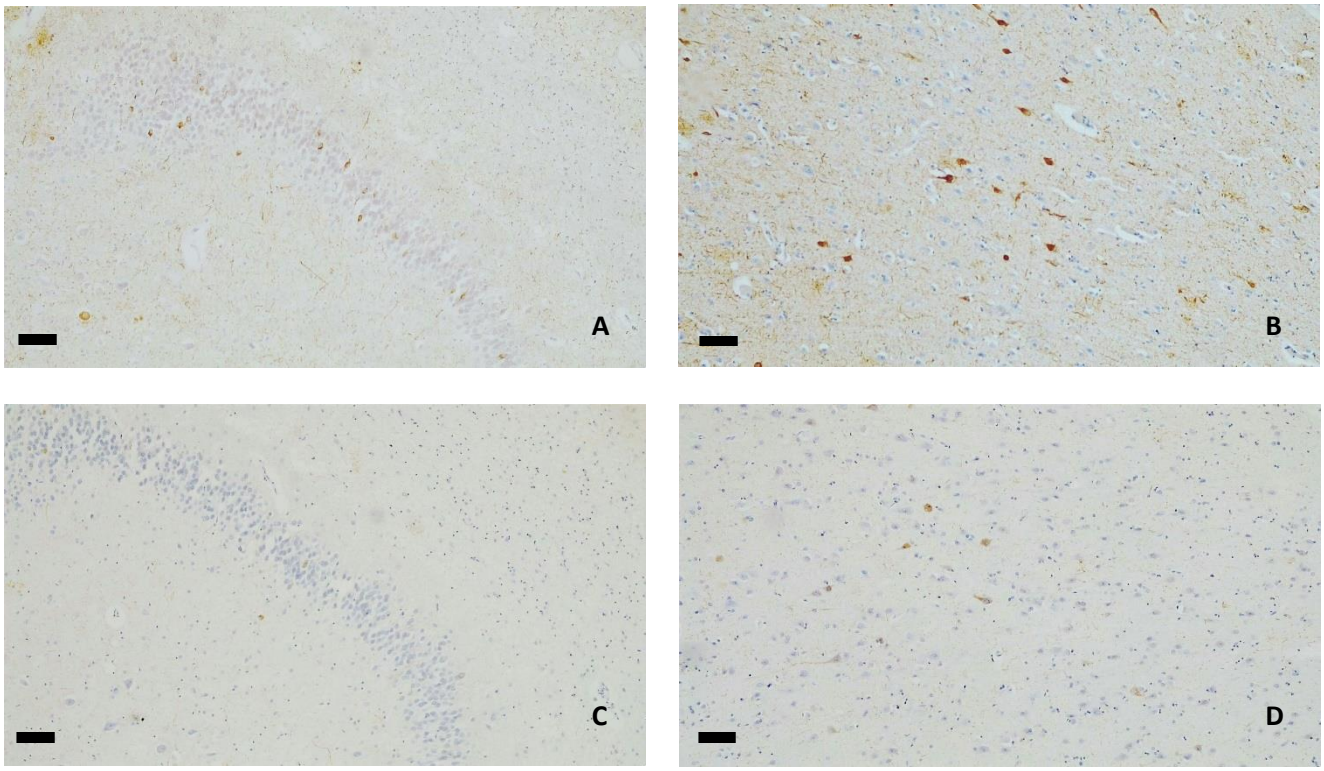

Figure 4.6: Examples **of** AT8 immunohistochemistry, figure A shows Neuronal inclusions in the dentate gyrus of a MAPT mutation case using 1:500 dilution, whilst B shows an AD case with neurofibrillary tangles in the temporal grey matter using 1:750, C shows the same case and region as A but using 1:750 dilution whilst D shows the same AD case as B within the same experimental run as C. Bars indicate 100µm

4.5 TDP43 immunohistochemistry

TDP43 immunohistochemistry was also completed across all cases in the temporal lobe tissue, as part of a complimentary project to understand abnormal protein accumulation across the different dementia sub-groups, in the different brain sub-regions and cell layers that had been investigated for autophagy marker distribution (see figure 5.7.). Due to the mitigating circumstances associated with this project, the scoring was not completed, and full analysis was not made.

However some preliminary analysis evidenced neuronal inclusions and dystrophic neurites in an FTLD-TDP43 A and an FTLD-TDP43 B case, which were similar in morphology to those described in Lashley et al. (2015).

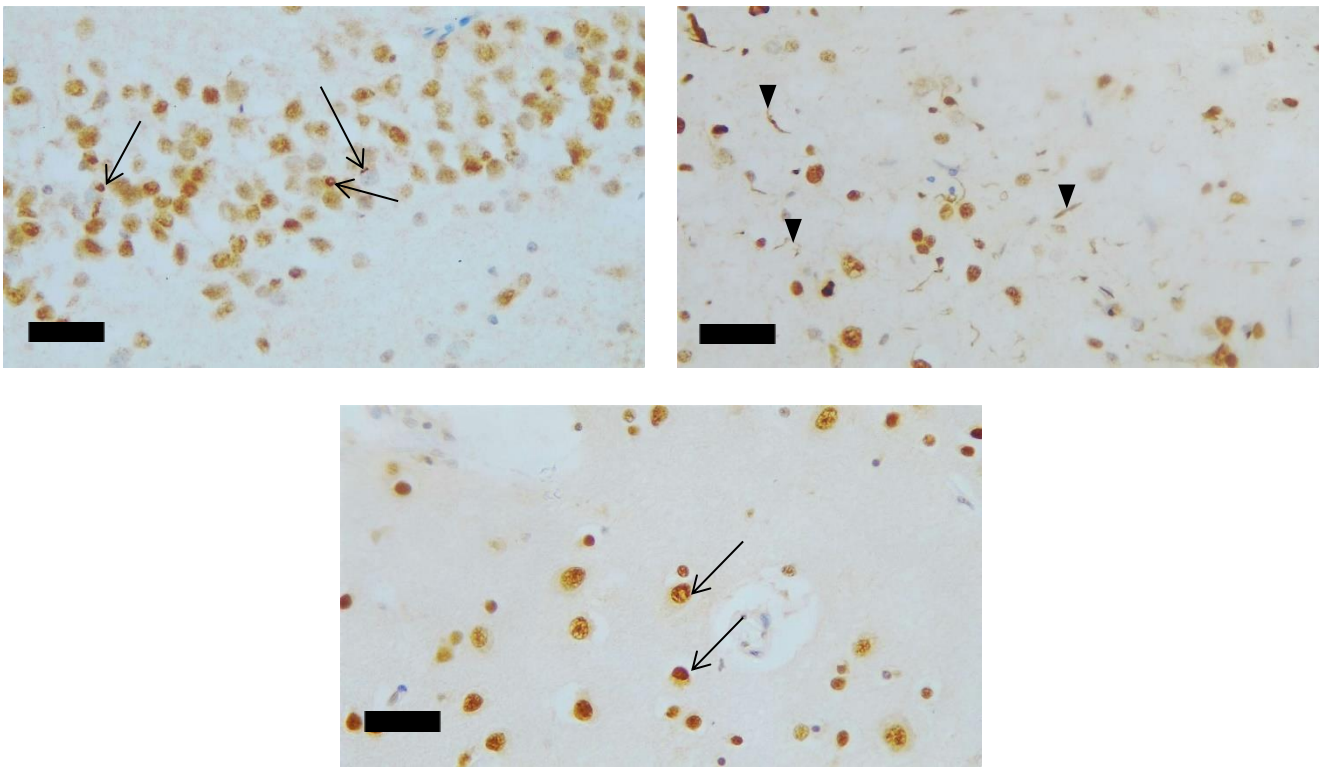

Figure 4.7: Micrographs showing the staining using anti-TDP43 antibody. Arrows show neuronal inclusions, whilst arrowheads denote dystrophic neurites. **Top Row:** FTLD-TDP43 Type A pathology in the same case. *Bottom Row*: FTLD-TDP43 Type B neuronal inclusions.

5 Macroautophagy

5.1 Introduction and Aims

As described in section 1.2 and 1.3 damaged proteins and organelles can be degraded via a cellular process, macroautophagy which is a multi-step process, with Beclin-1 being associated with initiation and LC3 being involved in autophagosome maturation, however availability of these proteins in the brain regions associated with FTLD need further investigation.

In order to assess this anti-LC3 and anti-Beclin-1 immunohistochemistry was used in order to observe the regional difference in macro autophagy marker distribution across ND, *C9orf72*, *MAPT*, *GRN* and AD groups.

5.2 LC3 Immunohistochemistry

LC3 immunohistochemistry was conducted on sections of the frontal and temporal lobe (including the hippocampus) of the normal ageing, AD and FTLD groups to allow a gross regional comparison of this key MA associated marker, across different types of dementia inducing disease.

The immunoreactivity detected was noted to appear with a varying intensity despite the control section remaining consistent, as described previously (see figure 3.2). Further examples of the LC3 staining can be seen in the temporal lobe in figure 5.1 and in the frontal in figure 5.3.

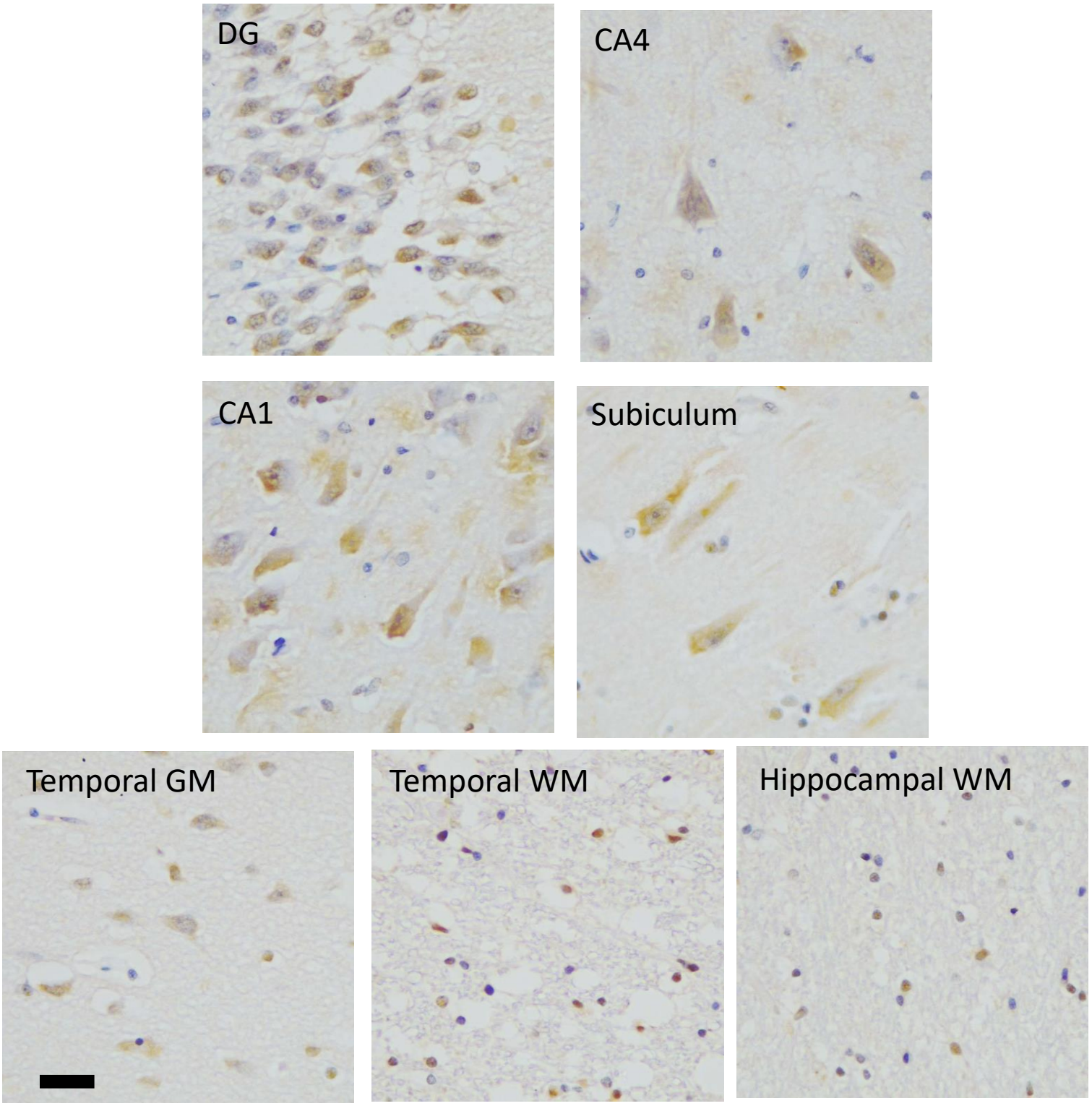

Figure 5.1: Demonstrating the immunohistochemistry using anti-LC3 antibody in the hippocampal/temporal regions shown. Bar indicates 50µm

Figure 5.1 therefore demonstrates the variation in LC3 staining across the different sub-regions, between the FTLD mutations (*MAPT, C9orf72*, and *GRN*), AD and no-disease (ND) controls.

In the Dentate gyrus no-disease (Mdn= 3, IQR= 4) and AD (Mdn= 3, IQR= 3) had similar levels of LC3 detected with moderate variation in the scores for cases in these two groups. FTLD groups tended to have lower LC3 scores (FTLD-*GRN Mdn=1, IQR= 1;* FTLD-*C9orf72, Mdn= 0, IQR= 2;* FTLD-*MAPT,* Mdn= 0, IQR= 2) suggestin lower LC3 protein immunoreactivity and low variation in these groups. In CA4 scores on average were higher in each group, with less variation in No-disease (Mdn=5, IQR= 1) and AD (Mdn= 5, IQR= 1) groups compared to FTLD-*GRN* (Mdn= 3, IQR, 2), FTLD-*C9orf72* (Mdn= 4, IQR= 5) and FTLD-*MAPT* (Mdn= 4, IQR= 2); However, the FTLD groups still had low levels of variation with the exception of FTLD-*C9orf72* which demonstrated much more variation. In CA1, all average scores where moderate but again there were differences in the spread. No-disease (Mdn= 4, IQR= 2) and AD (Mdn= 4, IQR= 3) demonstrated mildly less variability in their LC3 scores thant FTLD-*GRN* (Mdn= 3, IQR= 4), FTLD-*C9orf72* (Mdn= 4, IQR= 5), FTLD-*MAPT* (Mdn=3, IQR= 4), with FTLD-*C9orf72* showing the most variation. For the subiculum FTLD-*GRN* (Mdn= 0, IQR= 0), and FTLD-*C9orf72* (Mdn= 2, IQR= 4) had low levels of LC3, with the *GRN* group only having one case with a score above 0; This is compared to the relatively higher detected levels of LC3 no-disease (Mdn= 5, IQR=3), AD (Mdn= 5, IQR= 1) and FTLD-*MAPT* (Mdn= 4,5, IQR= 5), in this region all groups apart from FTLD-*GRN* had high levels of variation in their scores. No-disease (Mdn= 3.5, IQR= 3) and AD (Mdn= 3, IQR= 4) both moderate scores and spread in

the temporal grey matter, with a similar degree of variation in the levels of LC3 detected in FTLD-*GRN* (Mdn= 1, IQR= 3), FTLD-*C9orf72* (Mdn= 2, IQR= 3), and FTLD-*MAPT* (Mdn= 0, IQR= 2), but in these latter three groups the median score tended to be lower.

White matter areas had much lower scores for LC3 in general; In the temporal white matter No-disease (Mdn= 1, IQR= 2), AD (Mdn= 0, IQR= 1) and FTLD-*C9orf72* (Mdn= 0, IQR=1), had low levels detected on average with a small amount of variation, whilst FTLD-*GRN* (Mdn= 0, IQR= 0), and FTLD-*MAPT* (Mdn= 0, IQR= 0) had very little immunoreactivity. Similar trends where found in the hippocampal white matter with No-disease (Mdn= 1, IQR= 2), AD (Mdn= 0, IQR= 1) and FTLD-*C9orf72* (Mdn= 0, IQR=2) having low scores and limited variability within the groups and FTLD-*GRN* (Mdn= 0, IQR= 0),and FTLD-*MAPT* (Mdn= 0, IQR= 0) tending to fall below detection for LC3 immunoreactivity, with the exception of one outlier in the FTLD-*MAPT* group. These data suggest there is limited LC3 available in the white matter structure of the hippocampus and temporal lobe.

Kruskal-Wallis test was used to demonstrate no statistically significant differences in the dentate gyrus, CA1, temporal grey matter, temporal white matter and the hippocampal white matter ($p > .05$). However there was an observed difference in two of the subregions CA4 and the subiculum where the output gave $H(4)= 11.941$, $p= .018$ and $H(4)=11.493$, $p= .022$ respectively, which indicated that there was at least two subgroups would be different in this region, but *post hoc* analysis is required. Variation of scores in the CA4 can also be seen in figure 5.2.

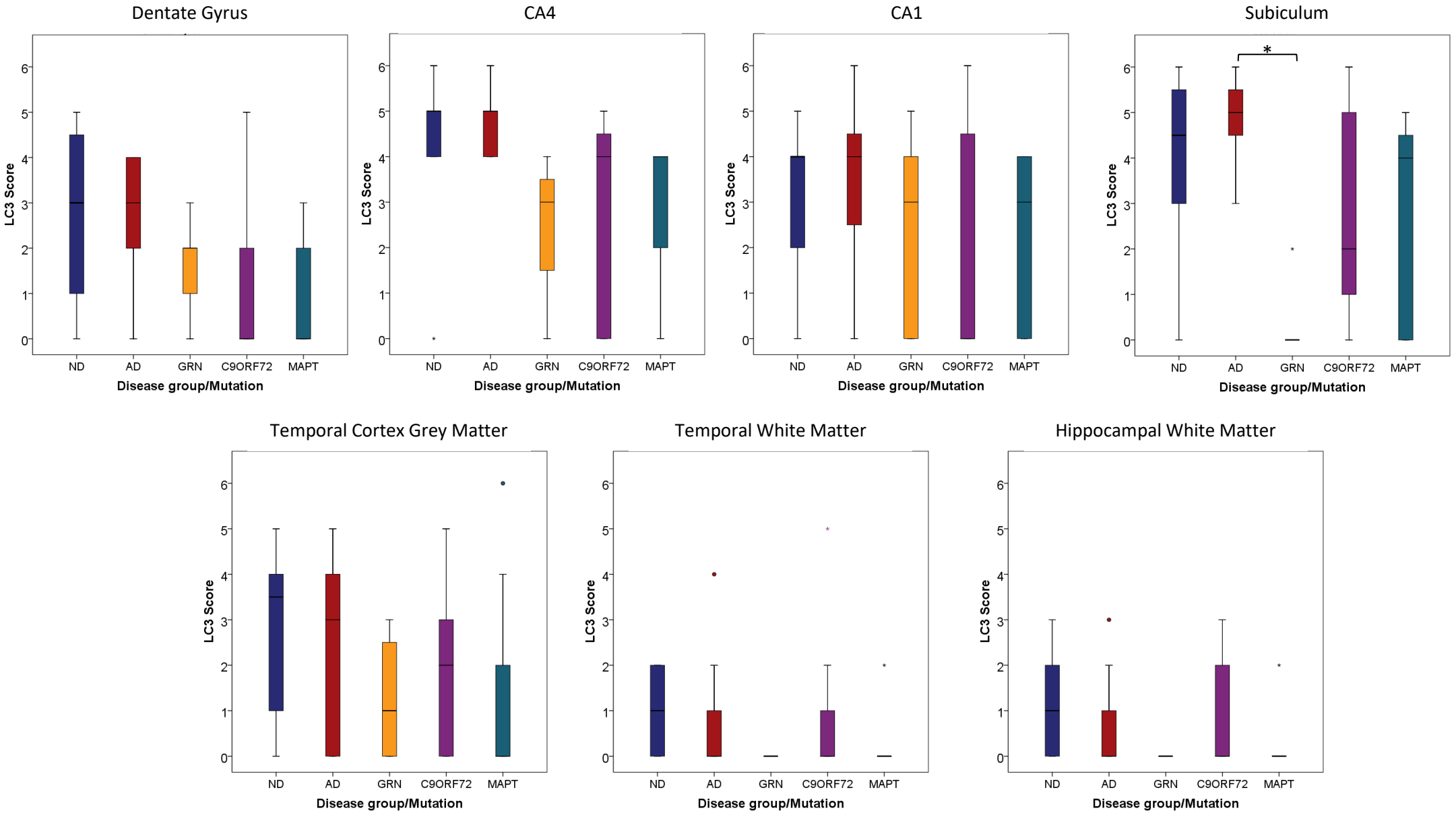

Figure 5.2: Boxplots for each region of the hippocampus scored for LC3 immunoreactivity grouped by the mutation/disease group. ND, No disease; AD, Alzheimer's Disease * p< .05

To further investigate the nature of the exact differences detected in relation to which disease group was driving the variation, Dunn's-Bonferroni test for *post hoc* analysis was applied. In CA4 no specific group differences could be discovered after adjusting for multiple testing. Meanwhile in the subiculum there was a statistically significant difference between the AD and the GRN group was found ($p = .017$), suggesting the AD had significantly higher scores (Mdn=5), which was significantly higher than for the *GRN* group (Mdn= 0).

Immunohistochemistry and analysis for LC3 has been completed in frontal lobe in addition to the temporal lobe since these are regions predominantly impacted by FTLD. The different cell layers of the frontal lobe were assessed independently, given their variation in anatomical connectivity, variation in physiological characteristics (such as neurotransmitter predominance) and variable involvement in different stages in neurodegenerative disease (Mackenzie & Neumann, 2016, Duyckaerts, 2009), examples of how the Layers stain can be seen in figure 5.3.

In Layer I of the frontal grey matter no-disease and AD groups had fairly similar spreads of detection (Mdn=0, IQR = 3, and Mdn = 0, IQR = 5 respectively), with generally low levels of LC3 protein available in this area but some variation. In the FTLD groups, the *GRN* and *MAPT* cases had similar scores with low amounts of spread (Mdn= 0, IQR= 0 and Mdn= 0, IQR= 0 respectively) meanwhile the FTLD-C9orf72 group also had relatively low scores (Mdn= 0, IQR= 2) but more variance compared to FTLD-*MAPT* and FTLD-*GRN* groups. It was also noted that both the *MAPT* and *GRN* groups had one outlier with a score 3 and *C9orf72* had an outlier with a score of 5.

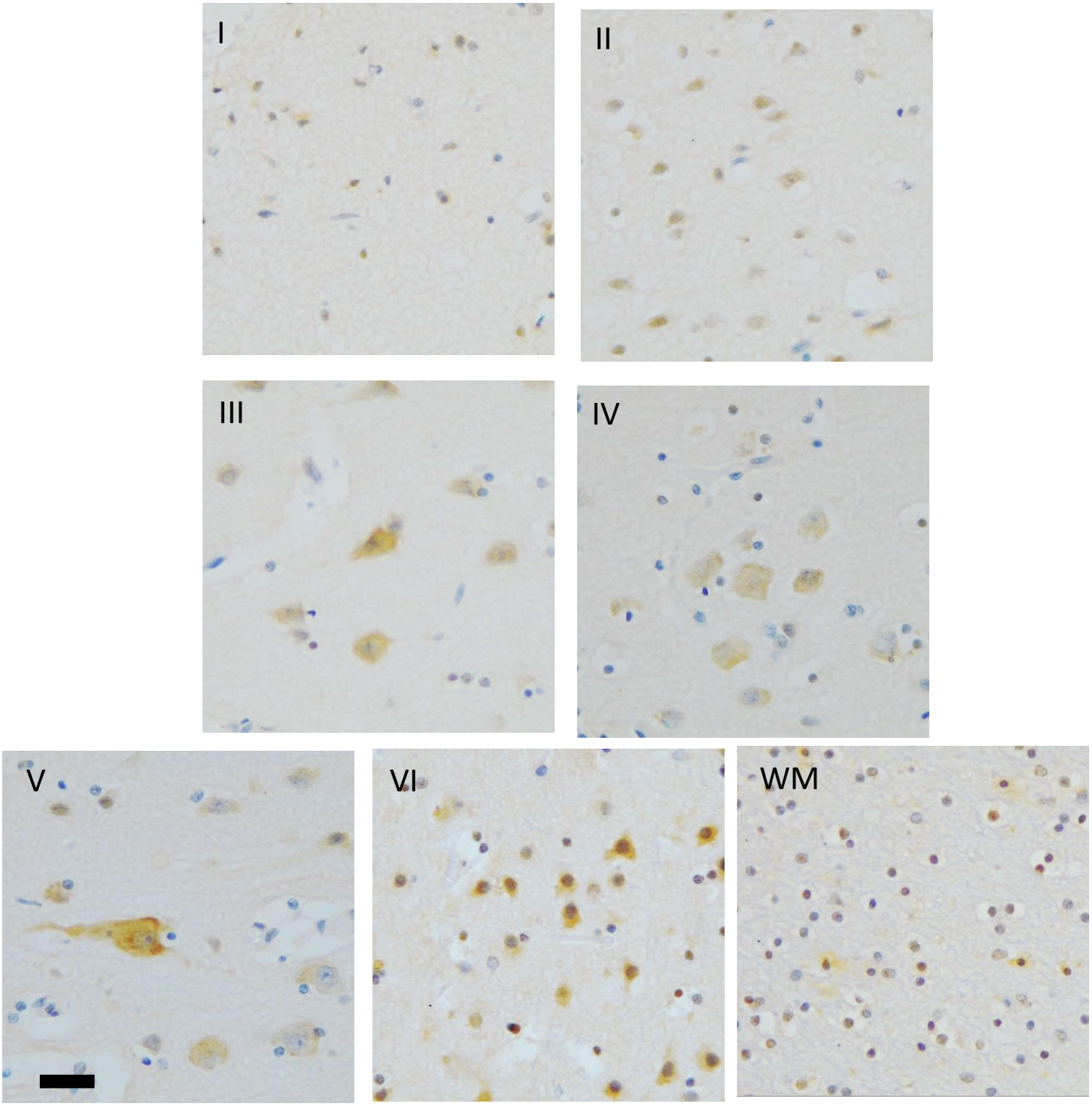

Figure 5.3: Demonstrating immunohistochemistry using anti-LC3 antibody in the frontal grey matter layers and frontal white matter. Bar indicates 50µm

Within layer II scores, cases demonstrated similar variance in all groups, with the no-disease groups having a slightly higher average score (Mdn= 2.5, IQR =4) with AD, FTLD-*GRN,* FTLD-*MAPT* and FTLD-*C9orf72* groups having a median of 0 (IQR= 6, 3, 3, and 4 respectively). Median Layer III scores were similar in all groups (No-disease Mdn= 3, IQR=3; AD Mdn= 4, IQR= 2; FTLD-*GRN* Mdn= 3, IQR= 3; FTLD-*C9orf72* Mdn= 3, IQR= 1; FTLD- *MAPT* Mdn= 3, IQR = 5), whilst the IQRs suggest variation in the no-disease, AD, FTLD-*GRN* and FTLD-*MAPT*, but comparative heterogeneity in the FTLD-*C9orf72* group in this region. In Layer IV no disease (Mdn, 3, IQR= 4) and AD (Mdn= 3, IQR= 5) had higher average scores and moderate spread compared to the average lower scores of FTLD-*MAPT* (Mdn=1, IQR= 3) and FTLD-*GRN* (Mdn= 0, IQR = 3) groups which also had some variability within their groups, whilst FTLD-*C9orf72* was more uniform in layer IV (Mdn= 0, IQR= 1) suggesting lower levels of LC3 protein. All of the groups in layer V showed moderate LC3 staining and with some variation, no-disease (Mdn= 3.5, IQR= 2), AD (Mdn= 3, IQR= 3) and *GRN* (Mdn= 2, IQR= 3) all had a similar degree of LC3 staining, with the latter have a slightly lower average score; however, whilst there was a moderate level of staining in FTLD-*C9orf72* (Mdn= 3, IQR= 4) and FTLD-*MAPT* (Mdn= 3, IQR= 5) their IQRs imply more variability around this average. In Layer VI, average scores tended to be low, with the no-disease and AD groups having (Mdn= 3), FTLD-*C9orf72 Mdn= 2*, and FTLD-*MAPT* all have Mdn= 1 suggesting slightly less LC3 positivity and FTLD-*GRN* have no LC3 immunoposivity on average (Mdn= 0). No-disease and AD cases had similar spreads, with each groups have an IQR= 2, whilst FTLD-*GRN,* FTLD-*C9orf72,* and FTLD-*MAPT,* all had IQRs of 3 suggesting a slightly higher degree of variability in the FTLD groups compared to no disease or AD. Finally, in the frontal white matter, immunoposivity was scared with both FTLD-*MAPT,* and FTLD-*GRN* tending to show no LC3 immunopositively cells

(Mdn= 0, IQR= 0 and Mdn= 0, IQR= 0), with only one case in the FTLD-*GRN* having detectable LC3. Meanwhile both AD (Mdn= 0, IQR= 3) and FTLD-*C9orf72* (Mdn= 0, IQR= 1) had similar scores, but the AD group had more spread than FTLD-*C9orf72*, and it was only the no-disease groups that usually had detectable LC3 (Mdn= 2.5, IQR = 4), they also had the highest IQR indicating this is a regional with variable LC3 levels when no neurological disease is present.

When exploring variation across normal-aging, AD, FTLD-*MAPT*, FTLD-*GRN* and FTLD-*C9orf72* groups, Kruskal-Wallis testing showed no significant differences in the LC3 immunopositivity scores across the frontal cortex grey matter layers I, II, III, IV and V However, layer VI and the frontal white matter showed significant variation ($H(4)=10.951$, $p= .027$, and $H(4)=10.129$, $p= .038$ respectively) and required further analysis to assess the statistical relevant differences between each of the disease groupings which was conducted via Dunn-Bonferroni test.

A summary of the LC3 scores in frontal lobe regions is shown in figure 5.4. Briefly, *post hoc* analysis did to reveal any significant difference between groups in Layer VI of the frontal grey matter, however, in the frontal white matter, Dunn-Bonferonni tests showed that the No-Disease group's LC3 score (Mdn=2.5) was significantly higher than the FTLD-*MAPT* group (Mdn=0, p=0.037).

It was also noted that both the FTLD-*GRN* and FTLD-*MAPT* groups had LC3 levels below detection in the frontal white matter, with only one of the FTLD-*GRN* cases showing an observable level and none of the MAPT mutation groups showing detection. Meanwhile the

no-disease and AD had a comparably larger amount of spread in the frontal white matter (see figure 5.4).

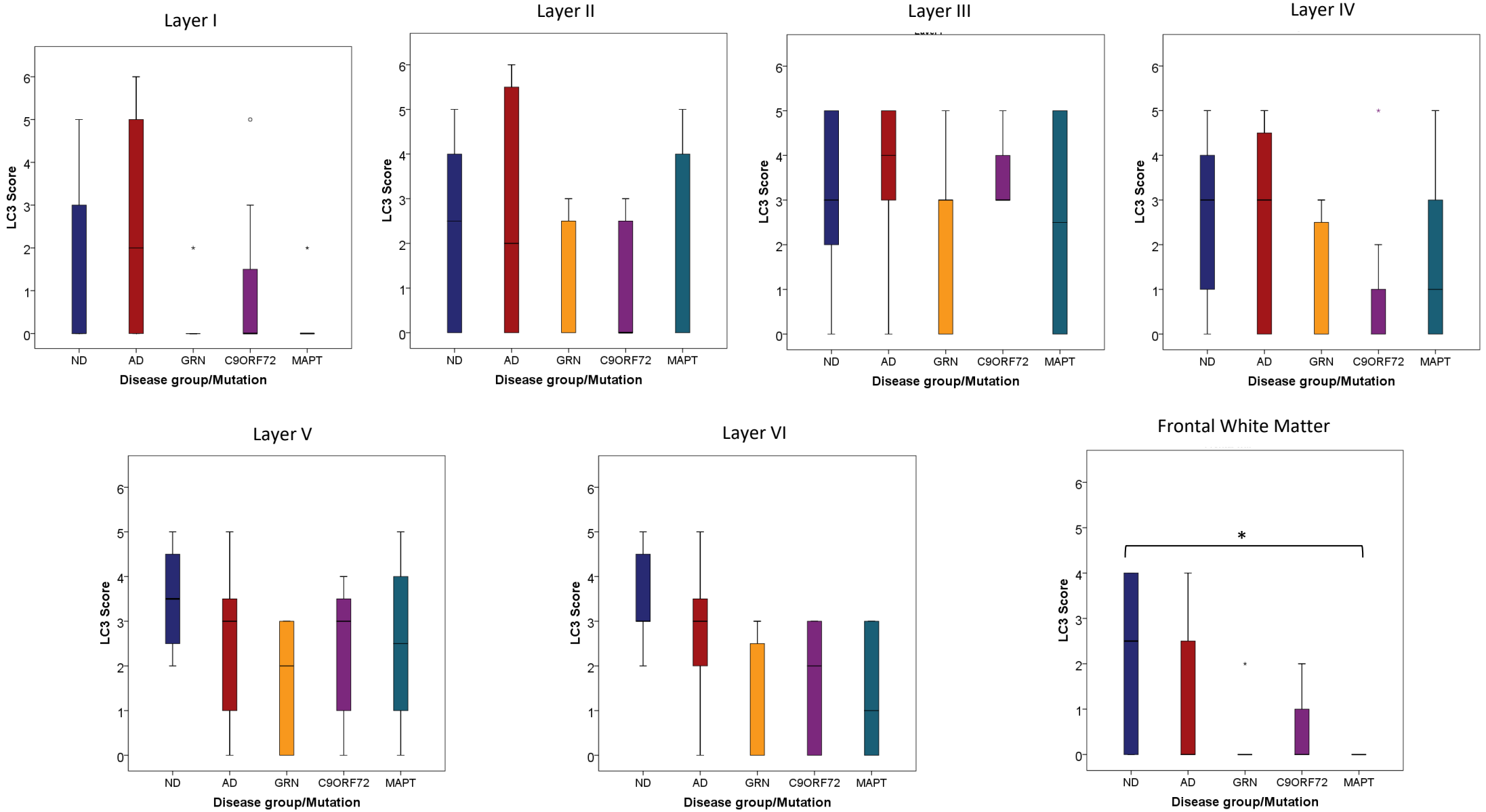

Figure 5.4: Boxplots for the distribution of scores in the frontal lobe grey matter cell layers and white matter. ND, No Disease; AD, Alzheimer's Disease; *p<.05

5.3 Beclin-1 Immunohistochemistry

Beclin-1 immunohistochemistry was conducted and analysed in the temporal lobe and frontal lobe as an additional marker of MA.

Assessment of the temporal lobe allowed investigation of anatomically distinct sub-regions that are known to have variable involvement in the different types of neurodegenerative disease including AD and FTLD, with pathological deposition occurring at different stages of disease (Charles Duyckaerts et al., 2009; Mackenzie & Neumann, 2016). The sub-regions investigated included dentate gyrus, CA4, CA1, subiculum, temporal cortex grey matter, temporal white matter and hippocampal white matter. Figure 5.5 demonstrates an example of the typical Beclin-1 immunoreactivity seen in temporal lobe neurons. Like the other autophagy antibodies it stained with a varying intensity despite the staining control being of consistent staining. Sections were therefore scored in the same way as described for LC3, with both % of cells and intensity being considered to give an overall score of 6.

In the dentate gyrus no-disease (Mdn= 4, IQR= 1), AD (Mdn= 4, IQR= 0) and FTLD-*GRN* (Mdn= 3, IQR= 2) had similar levels of Beclin-1 detected with only a small variation in the scores for cases within these two groups meanwhile FTLD-*C9orf72* (Mdn= 3, IQR= 3) and FTLD-*MAPT* (Mdn= 4, IQR= 3) also had moderate Beclin-1 scores, but greater variation. In CA4 scores on average were higher in each group, with less variation in No-disease (Mdn=5, IQR= 1), AD (Mdn= 5, IQR= 1) and FTLD-*GRN* (Mdn= 4.5, IQR= 1) groups compared to FTLD-*C9orf72* (Mdn= 4, IQR= 2) and FTLD-*MAPT* (Mdn= 5, IQR= 3). In CA1, all average scores were high with were differences in the spread; No-disease (Mdn= 4.5, IQR= 1), AD (Mdn= 5, IQR= 2) and FTLD-*MAPT* (Mdn=3, IQR= 4) demonstrated less variability in their Beclin-1 scores than FTLD-*GRN* (Mdn= 4, IQR= 3) and FTLD-*C9orf72* (Mdn= 4, IQR= 4), suggesting that whilst

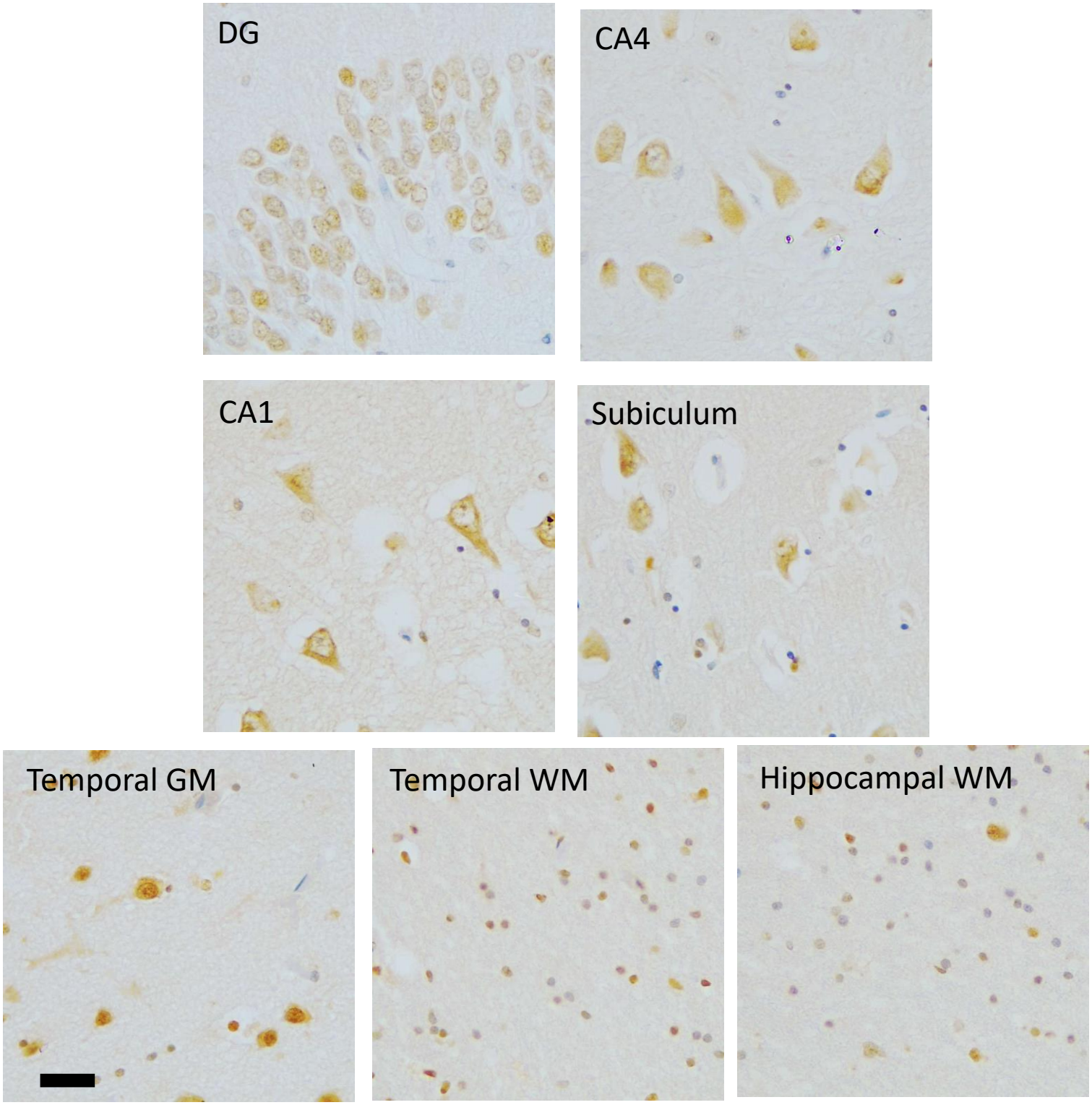

Figure 5.5: Demonstrating the immunohistochemistry using anti-Beclin-1 antibody in the hippocampal/temporal regions scored. Bar indicates 50µm

Beclin-1 is relatively abundant, there is some within group variation for FTLD-*GRN* and FTLD-*C9orf72*.

For the subiculum a similar trend to CA4 was observed; No-disease (Mdn= 5, IQR=2), AD (Mdn= 5, IQR= 1), FTLD-*GRN* (Mdn= 4.5, IQR= 3), FTLD-*C9orf72* (Mdn= 5, IQR= 3), and FTLD-*MAPT* (Mdn= 5, IQR= 1) all had moderate-to-high average scores, indicating a stable level of Beclin-1, variation was for ND, AD and FTLD-*MAPT* was lower than for FTLD-*GRN* and FTLD-C9orf72.

No-disease (Mdn= 5, IQR= 2), AD (Mdn= 4, IQR= 5), FTLD-*GRN* (Mdn= 3.5, IQR= 3), FTLD-*C9orf72* (Mdn= 4, IQR= 5), and FTLD-*MAPT* (Mdn= 5, IQR= 1) all had high scores in the temporal grey matter, however there was a more variability in Beclin-1 scores for AD, and FTLD-*C9orf72* compared to the other groups.

The temporal white matter No-disease (Mdn= 5, IQR= 2), AD (Mdn= 4, IQR= 5) and FTLD-*MAPT* (Mdn= 4, IQR=2) has higher levels of Beclin-1 compared to FTLD-*GRN* (Mdn= 1.5, IQR= 5),and FTLD-*C9orf72* (Mdn= 0, IQR= 4) had very little immunoreactivity and a large amount of variation this suggests between and within disease variation in Beclin-1 scores. Finally the hippocampal white matter showed at least moderate beclin-1 staining with a large amount of data spread indicated by the IQRs (No-disease, Mdn= 5.5, IQR= 3;, AD Mdn= 3, IQR=5; FTLD-*GRN* Mdn= 2, IQR= 4; FTLD-*C9orf72,* Mdn= 3, IQR=5; FTLD-*MAPT* Mdn= 5, IQR= 2) suggesting a typically high level of Beclin-1 but a lack of heterogeneity within diseases.

Kruskal-Wallis test was used to identify regions with statistically significant differences between the control, healthy-ageing, FTLD-*MAPT*, FTLD-*GRN* and FTLD-*C9orf72* groups. This analysis identified only the temporal lobe grey matter (see figure 5.6) as having statistically

significant differences ($c^2(4)= 11.326$, $p= .023$) meanwhile all other regions had no significant differences ($p> .05$) and so were not appropriate for further *post hoc* investigation.

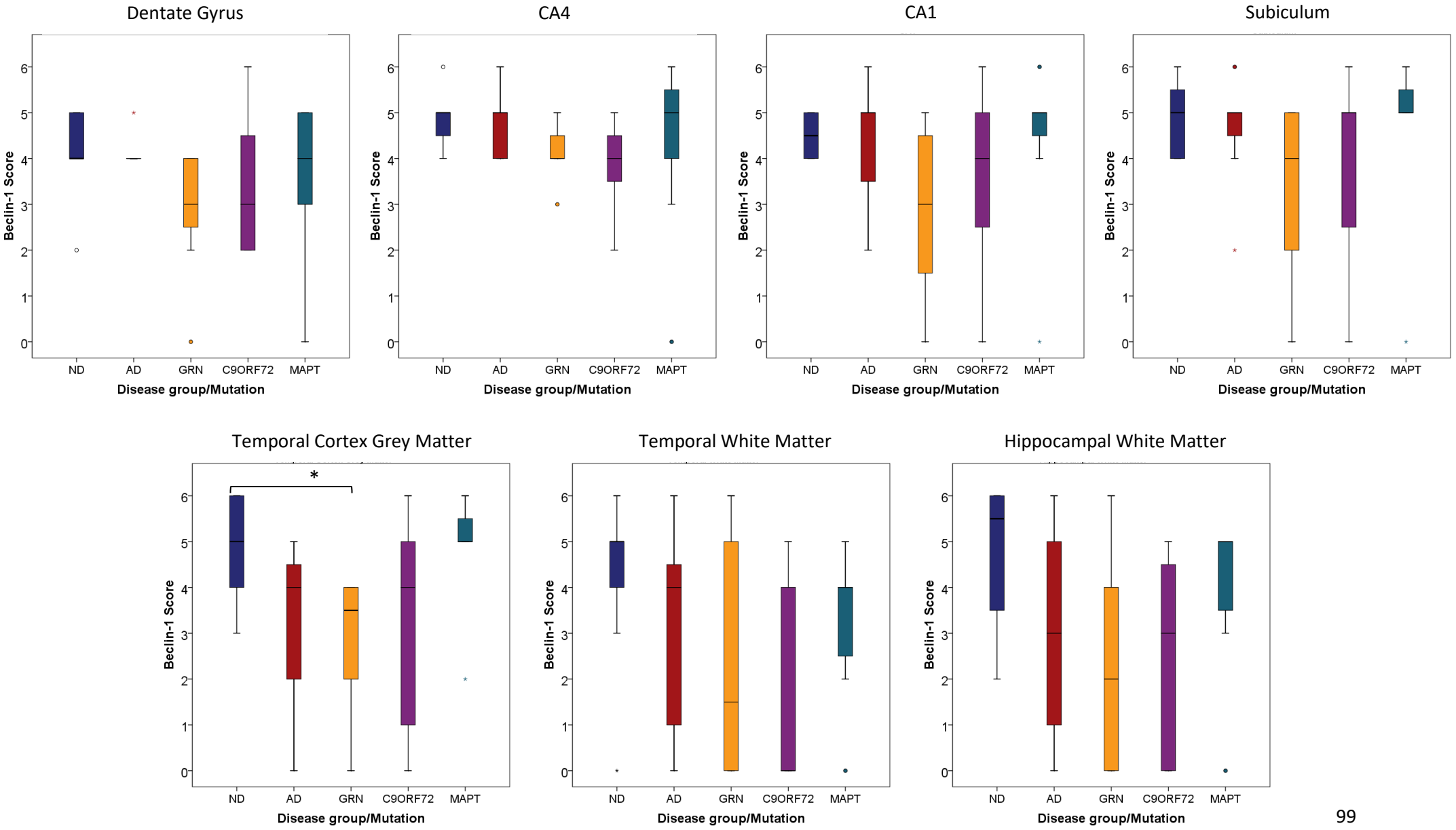

Figure 5.6: Beclin-1 immunoreactivity scores in the hippocampal subregions. ND, No Disease; AD, Alzheimer's Disease; *p< .05

Anti-Beclin-1 immunohistochemistry was also conducted using in the frontal lobe with the different cell layers being independently scored in the same way as for LC3 (see in figure 5.7). Kruksal-Wallis tests demonstrated significant differences in layer I of the frontal grey matter ($H(4)=11.416$, $p= .022$, $n=28$)), with *post hoc* testing indicating and significant difference between AD groups (Mdn=5.5) and FTLD-*C9orf72* (Mdn=0), suggesting significantly more immunopositivity for Beclin-1 in Layer I for AD cases compared to FTLD-*C9orf72* expansion cases.

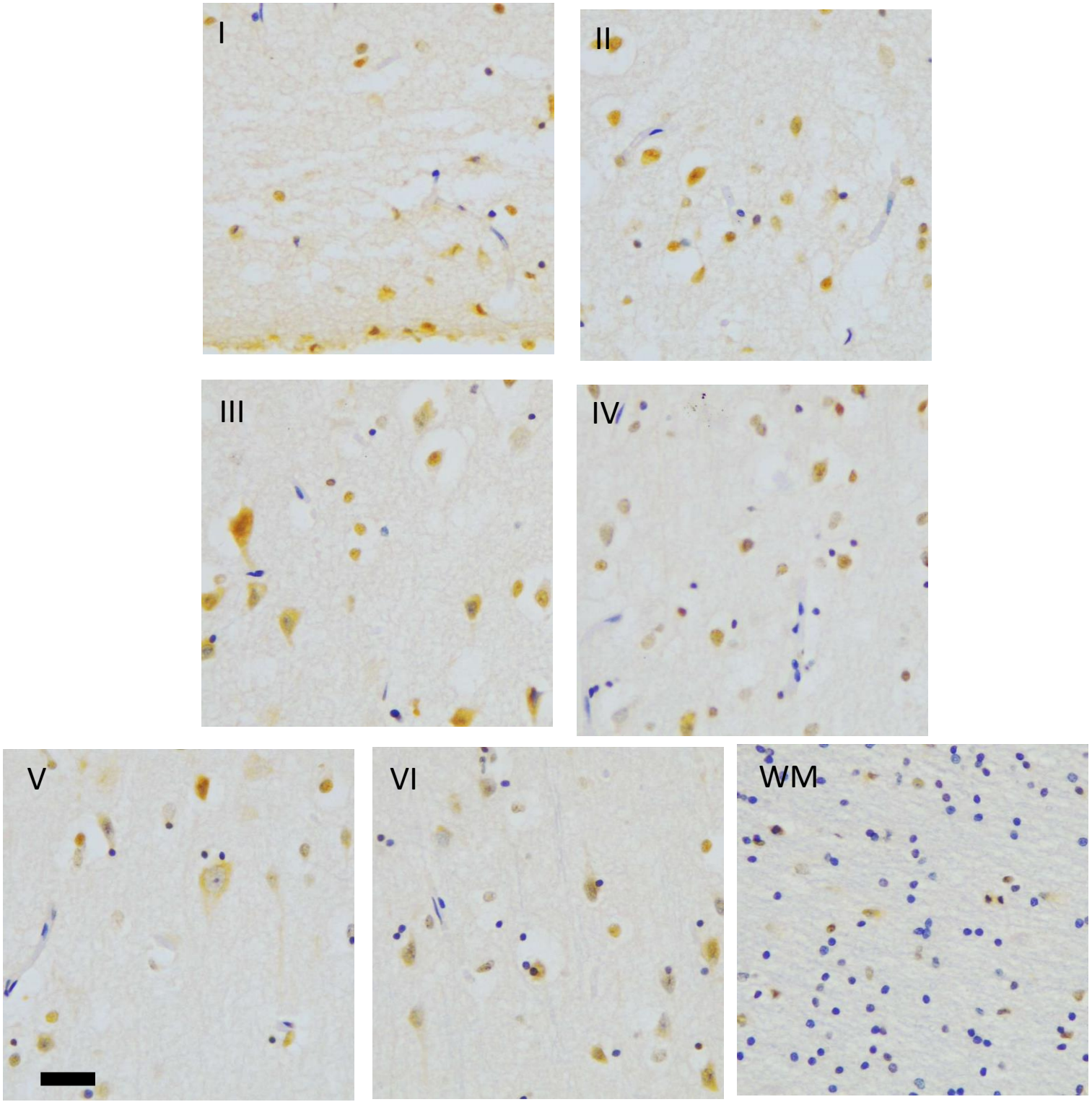

Figure 5.7: the six frontal grey matter layers and WM demonstrating the staining with anti-beclin-1 immunohistochemistry. Bar indicates 50µm.

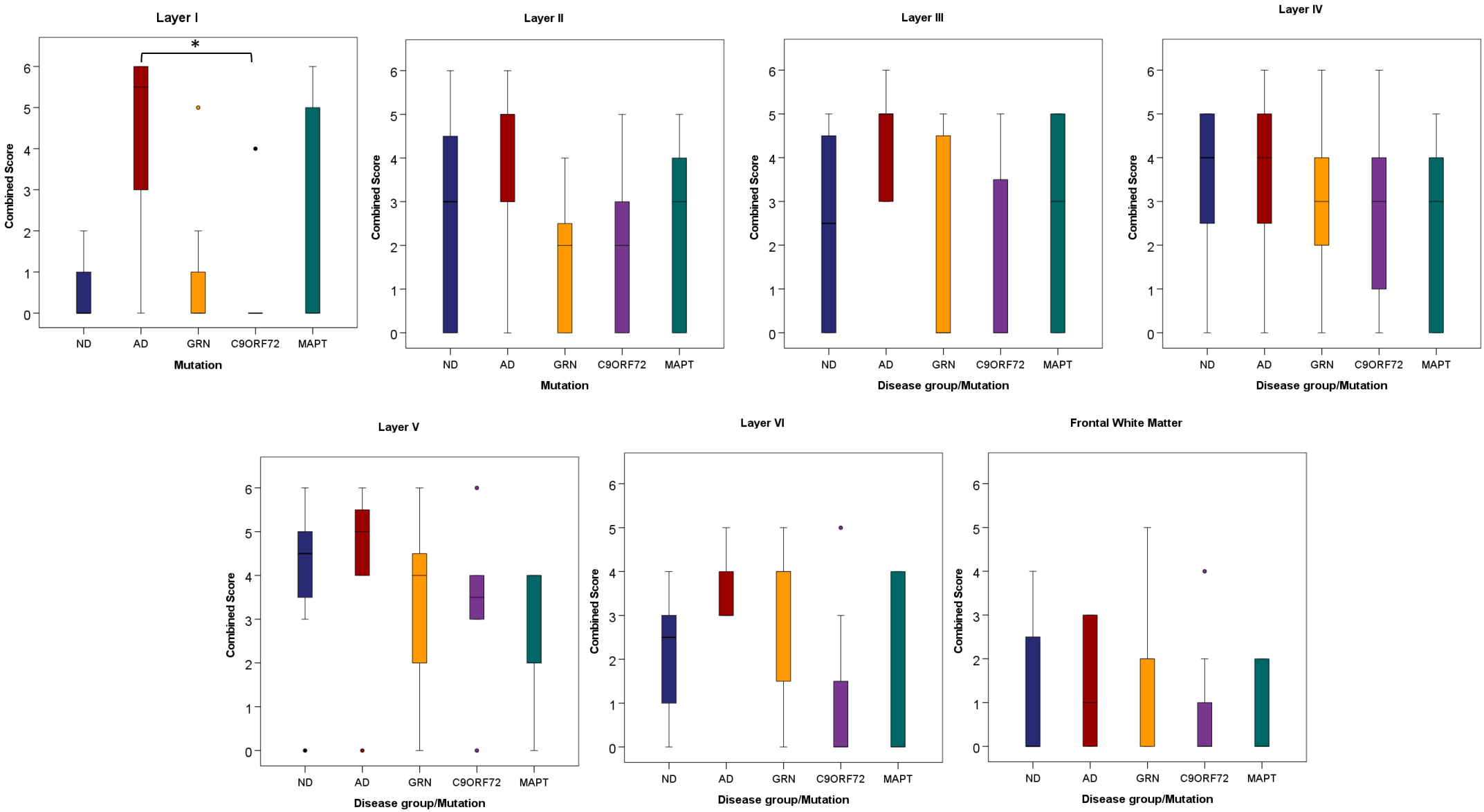

Figure 5.8: Beclin-1 immunoreactivity scores in the frontal lobe subregions. ND, No Disease; AD, Alzheimer's Disease; *p< .05

6 Chaperone Mediated Autophagy

6.1 Introduction and Aims

Macroautophagy is just one of the ways of the ways cells can degrade proteins and as previously described primarily involves on aggregate proteins and organelles, however some proteins can be degraded before they aggregate via CMA.

In this section the aim was to use IHC to assess the distribution of the CMA associated proteins LAMP2a and Hsc70 in the different FTLD mutation groups and compare them to AD and ND.

6.2 LAMP2a immunohistochemistry

LAMP2a is a marker of the CMA process as described in section 1.2.2 immunohistochemistry and was first assessed in the temporal lobe, and example of the staining can be found in figure 6.1. As with LC3 and Beclin-1, key anatomically distinct subregions were scored in consideration of the % cells stained as well as the staining intensity. No statistically significant variations were observed when investigation the comparisons between the groups by looking the mutations groups using Kruskal-Wallis test, the variations in these scores can be seen in figure 6.2. Average Dentate gyrus LAMP2a scores in no-disease (Mdn= 4, IQR= 4), and AD (Mdn= 4, IQR= 3) where similar moderate variation within whilst FTLD-*GRN* (Mdn= 0, IQR= 2), FTLD-*C9orf72* (Mdn= 2, IQR= 3) and FTLD-*MAPT* (Mdn= 2, IQR= 2) where lower with moderate within group variation. CA4 had higher levels of LAMP2a detected in no-disease (Mdn=4, IQR= 2), AD (Mdn= 4, IQR= 3), FTLD-*C9orf72* (Mdn= 4, IQR= 1) and FTLD-*MAPT* (Mdn= 4, IQR= 1) compared to FTLD-*GRN* (Mdn= 1, IQR= 4). A similar trend was found in with CA1 no-disease (Mdn=4, IQR= 4), AD (Mdn= 5, IQR= 3), FTLD-*C9orf72* (Mdn= 4, IQR= 1) and FTLD-*MAPT* (Mdn= 4, IQR= 2) compared to FTLD-*GRN* (Mdn= 1.5, IQR= 4), this indicates

a lack of available LAMP2a in both CA4 and CA1 in FTLD-*GRN.* The subiculum suggests more consistency between diseases with LAMP2a detection tending to be high with low variation within each group (No-disease, Mdn= 4, IQR= 2; AD, Mdn= 5, IQR=2; FTLD-*GRN* Mdn= 4, IQR= 1; FTLD-*C9orf72,* Mdn= 4, IQR= 3; FTLD-*MAPT* Mdn= 5, IQR= 2).
No-disease (Mdn= 4, IQR= 1), AD (Mdn= 5, IQR= 2), and FTLD-*MAPT* (Mdn= 5, IQR= 1) all had moderate-to-high LAMP2a scores with a very narrow variability whilst FTLD-*GRN* (Mdn= 3, IQR= 3), and FTLD-*C9orf72* (Mdn= 0, IQR= 3), had larger variation with FTLD-*C9orf72* also having a low score in this region and all had high scores in the temporal grey matter, however there was a more variability in Bcl-1 scores for AD, and FTLD-*C9orf72* compared to the other groups.

In the temporal white matter No-disease (Mdn= 2.5, IQR= 3), AD (Mdn= 2, IQR= 4) and FTLD-*C9orf72* (Mdn= 0, IQR=0), FTLD-*GRN* (Mdn= 0, IQR= 3), and FTLD-*MAPT* (Mdn= 3, IQR= 3). Similar trends where found in the hippocampal white matter with No-disease (Mdn= 2, IQR= 2), AD (Mdn= 3, IQR= 3), FTLD-*C9orf72* (Mdn= 0, IQR=2), FTLD-*GRN* (Mdn= 1, IQR= 3), and FTLD-*MAPT* (Mdn= 2, IQR= 4). These two white matter regions together suggest a typically low level of LAMP2a in white matter regions and a lack of heterogeneity within diseases.

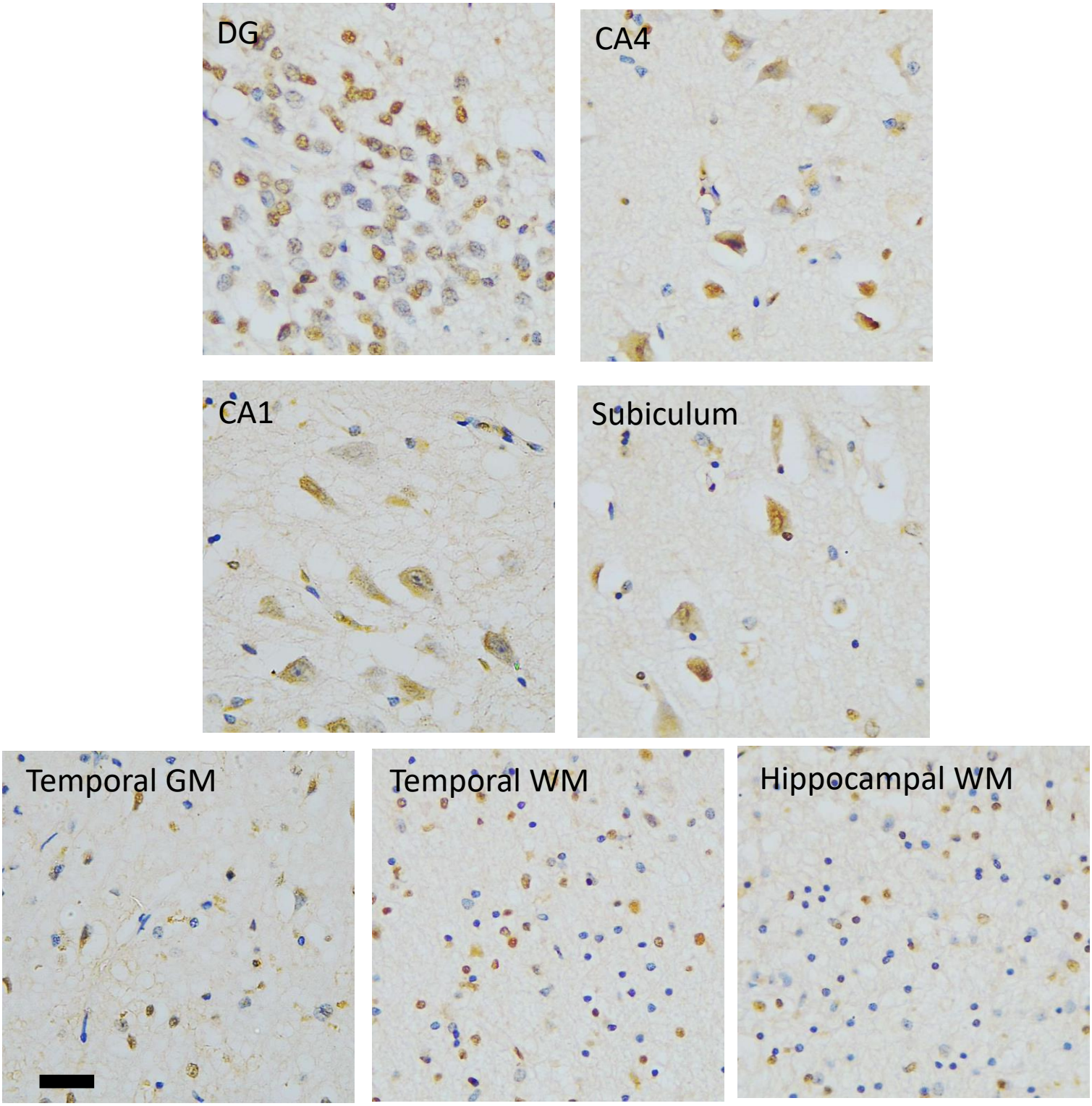

Figure 6.1: Demonstrating the immunohistochemistry using anti-LAMP2a antibody in the hippocampal/temporal regions scored. Bar indicates 50µm

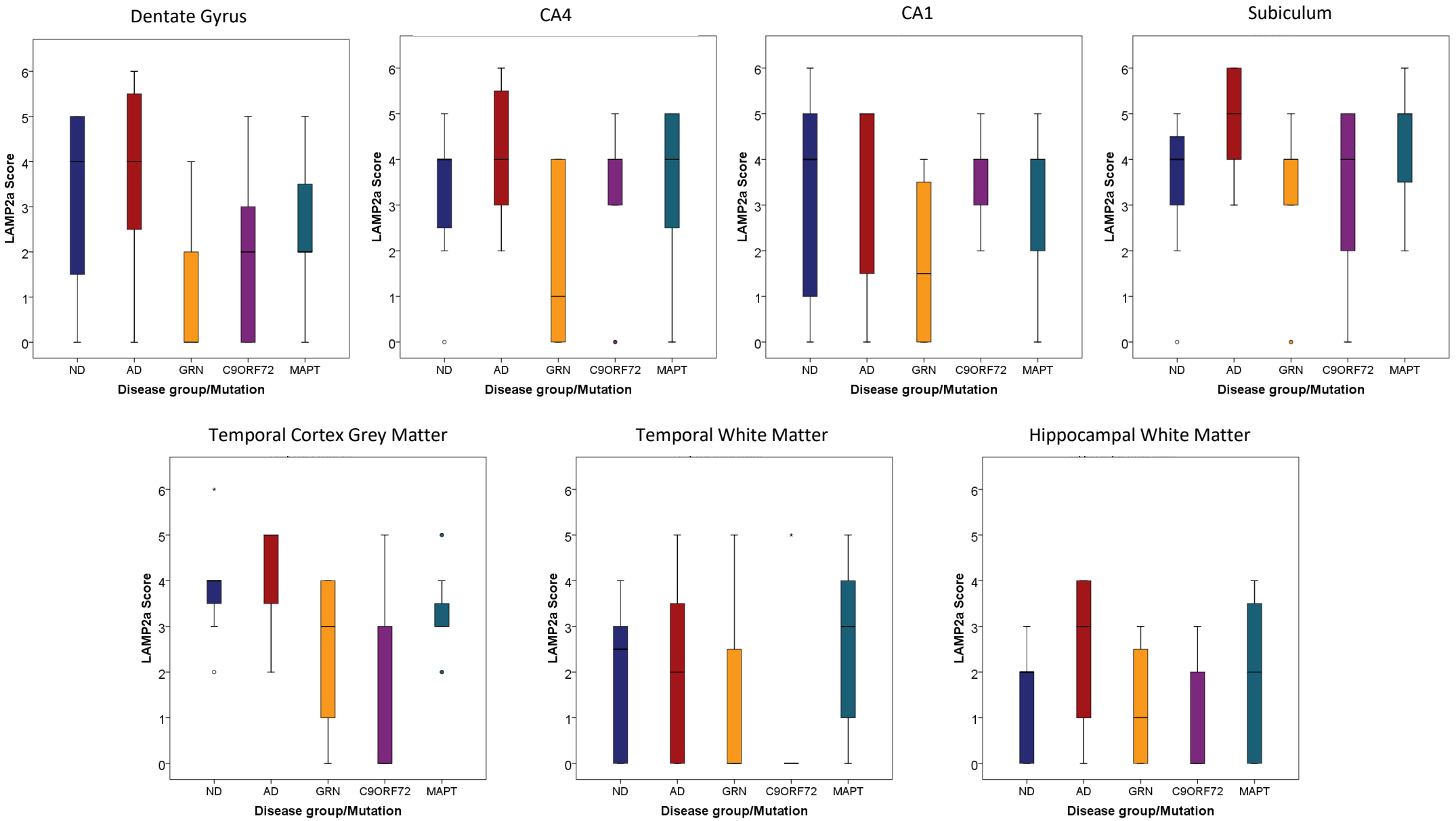

Figure 6.2: Distribution of LAMP2a scores in the hippocampal and temporal subregions. ND, No Disease; AD, Alzheimer's Disease.

Anti-LAMP2a immunohistochemistry was also assessed in the frontal lobe and the distribution of immunopositivity can be seen in figure 6.4. Kruksal-Wallis analysis did not elucidate any significant different in any of the frontal grey or white matter layers ($p>.0.05$). Examples of frontal staining with anti-LAMP2a antibody can be found in figure 6.3.

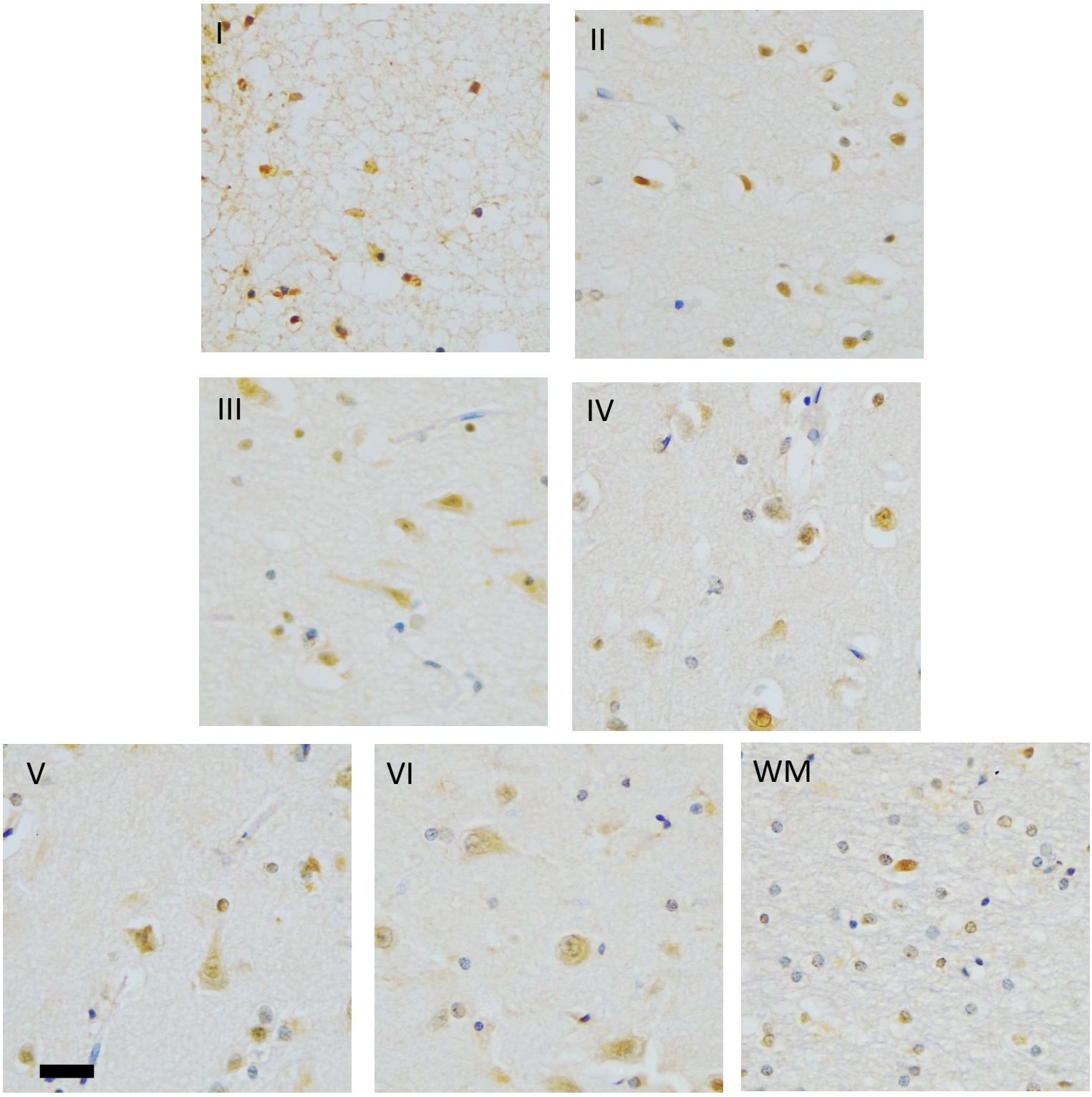

Figure 6.3: Anti-LAMP2a immunohistchemistry in the frontal cortex and WM. Bar indicates 50µm.

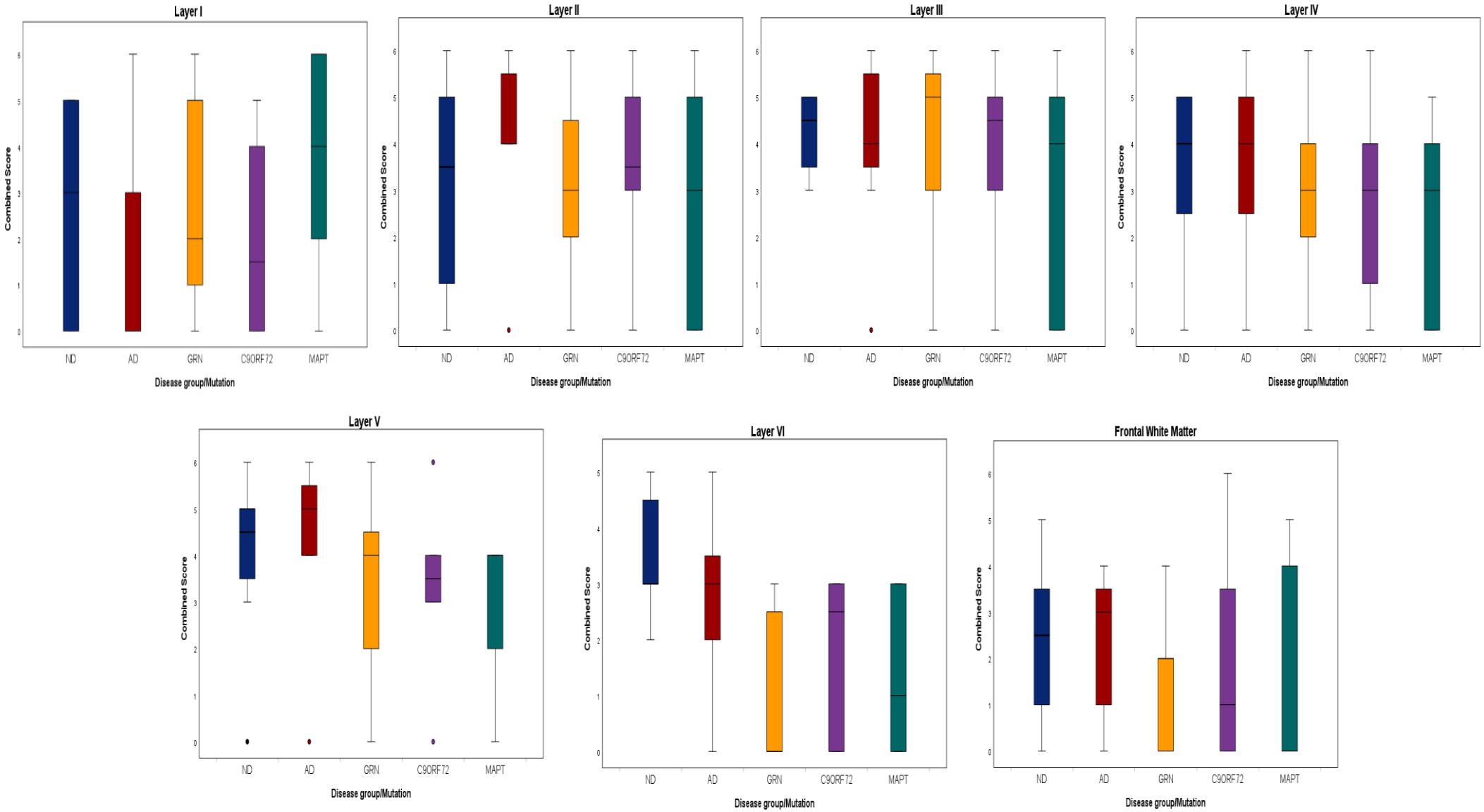

Figure 6.4: Distribution of LAMP2a scores in the frontal grey and white matter layers. ND, No Disease; AD, Alzheimer's Disease.

6.3 Hsc70 immunohistochemistry

Hsc70 immunohistochemistry was used as marker of the CMA process and this assessment was conducted in both in the temporal lobe and frontal lobe, as per the other autophagy markers under investigation. The same anatomical sub-regions and cell layers were assessed as per LC3, Beclin-1 and LAMP2A. No statistically significant differences could be elucidated by comparing the clinical (no-disease, AD and all of the FTLD) groups or by comparing no-disease and AD to the FTLD mutation groups (GRN, C9orf72 and MAPT). An example of staining see across the temporal lobe can be seen in figure 6.4 and the distributions of the Hsc70 scores can be found in figure 6.5, demonstrating the variation of hsc70 scores by the disease grouping.

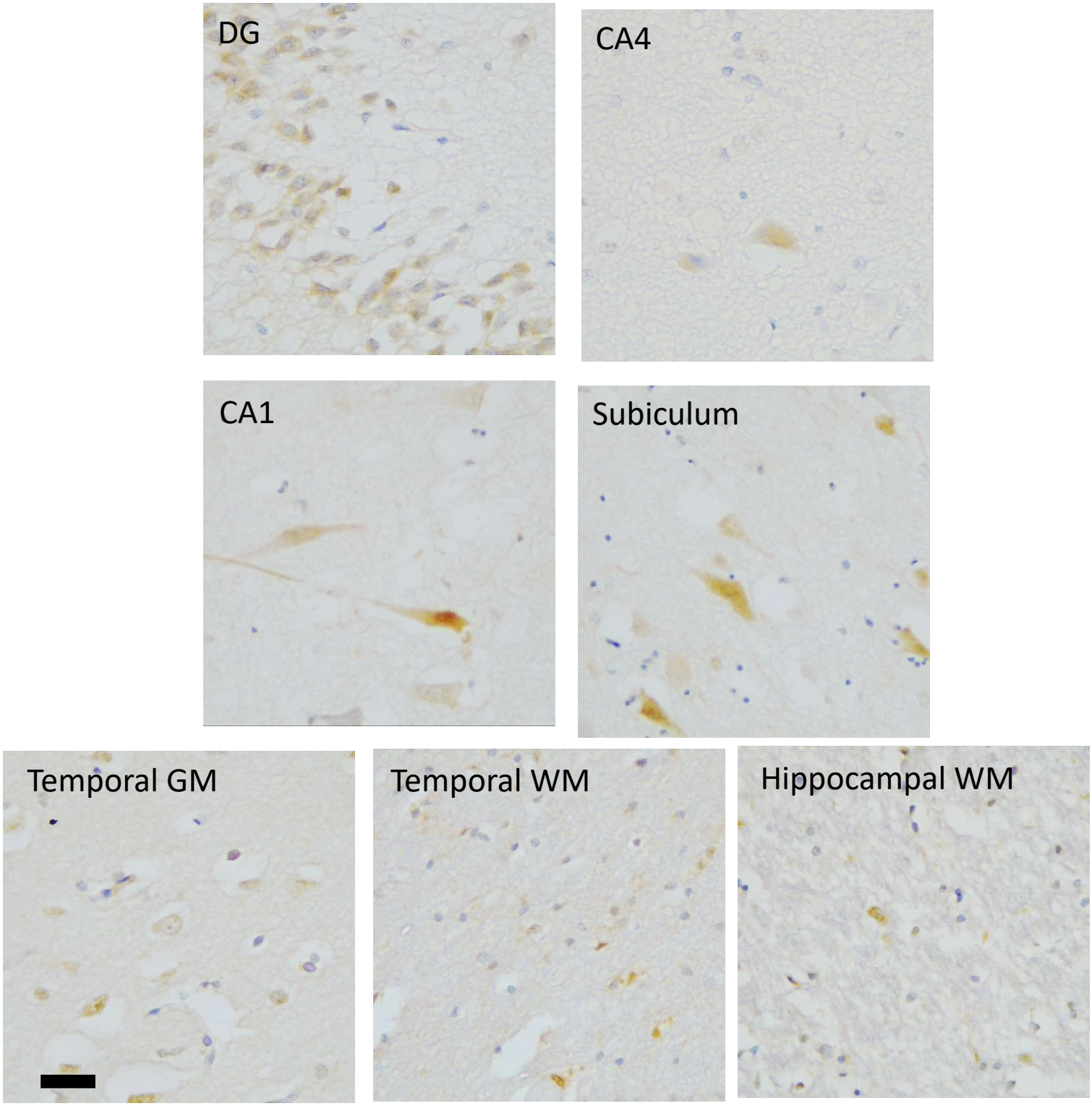

Figure 6.5: Demonstrating the immunohistochemistry using anti-hsc70 antibody in the hippocampal/temporal regions scored. Bar indicates 50µm

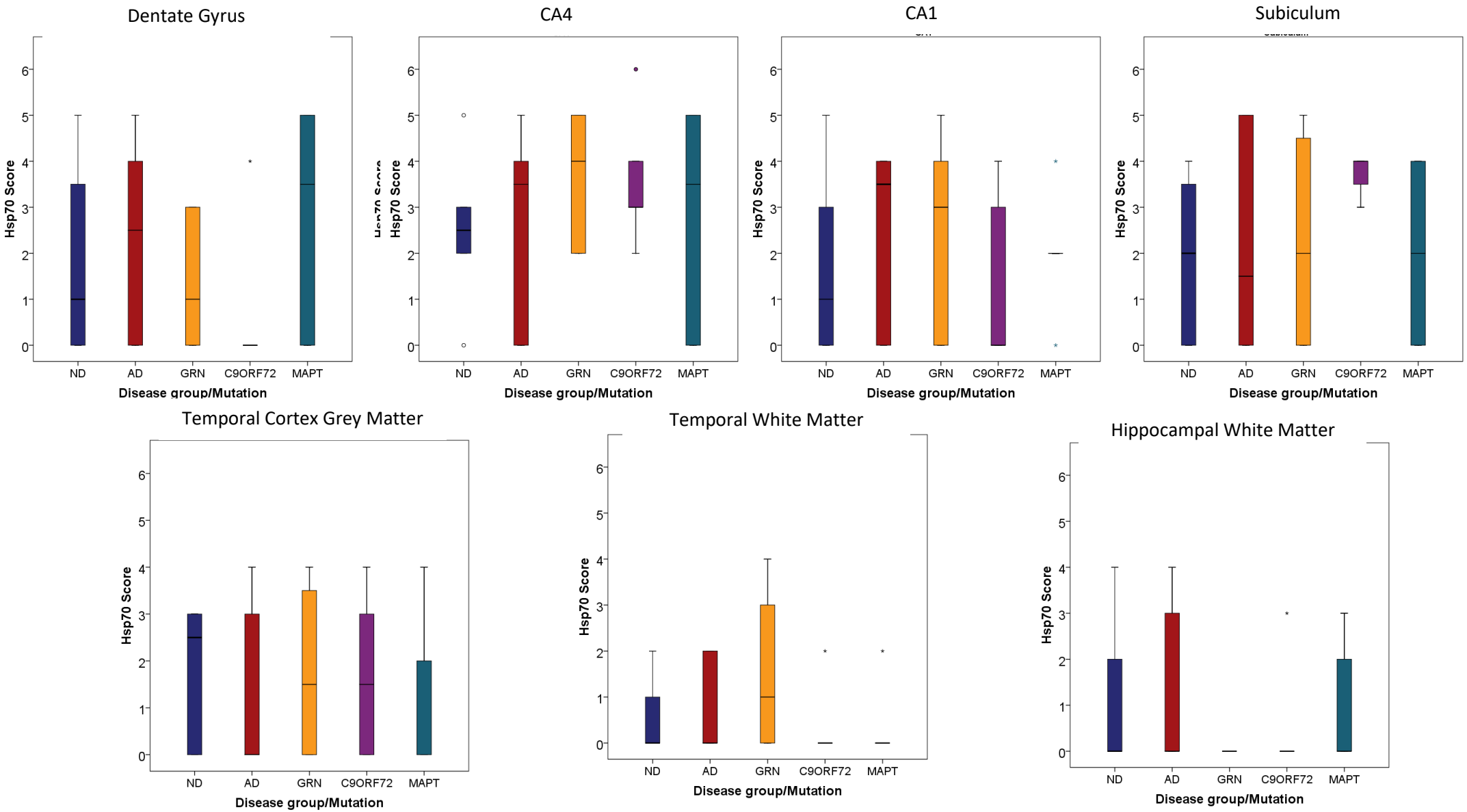

Figure 6.6: Distribution of Hsc70 scores in the hippocampal and temporal subregions. ND, No Disease; AD, Alzheimer's Disease.

The distribution of anti-Hsc70 immunohistochemistry in the frontal lobe can be seen in figure 6.6. Analysis of the values in the frontal region using Kruskal-Wallis testing indicated differences in grey matter layers III ($H(4)=9.804$, $p= .044$, $N=36$), IV ($H(4)=13.244$, $p= .010$, $n=36$), V ($H(4)=14.928$, $p= .005$, $n=36$), and VI ($H(4)=13.830$, $p =.008$, $n=36$) in addition to white matter ($H(4)=10.8880$, $p= .028$, $n= 36$). *Post hoc* analysis failed to find any significant differences between groups in Layers III, IV, V and the frontal white matter ($p>0.05$). In layer VI Dunn-Bonferroni testing demonstrated that no disease group had significantly greater scores (Mdn=4) when compared to the FTLD-*MAPT* group (Mdn=0, $p= .022$). In conclusion, there is a clear trend for decreased HSc70 in the FTLD groups in comparison to the AD and control groups.

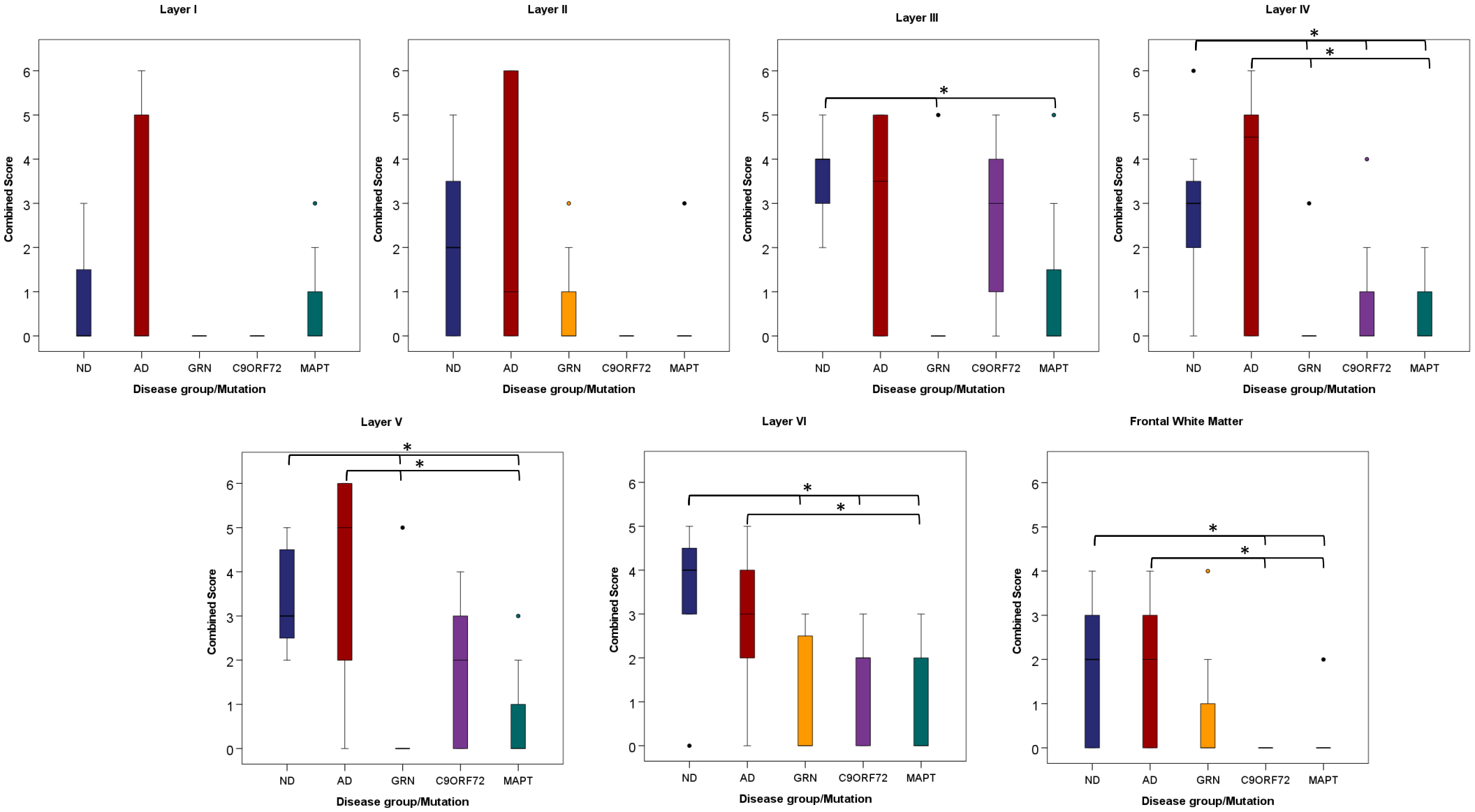

Figure 6.7: Distribution of Hsc70 scores in the frontal lobe grey and white matter. ND, No Disease; AD, Alzheimer's Disease. * denotes $p<0.05$

7 Western Blotting

7.1 Introduction and Aims

IHC is just one of the techniques that can be employed to assess autophagy markers and whilst it has the benefit giving visualisation of subregional distribution, it has the limitation of lacking the ability to quantify proteins. Moreover there is the specific issue for LC3 that is visualises both isoforms (LC3-I and LC3-II) of the protein, but the ratio of these two isoforms gives insight in the autophagic flux, as described in section 1.2. Therefore one of the aims of this project was to optimise a protocol to be able to observe this in human brain tissue.

7.7 LC3 Western Blotting Optimisation

Understanding variation in autophagy marker distribution across the different genetic FTLD subtypes, in relation to AD and no-disease controls was the principle aim of this study, however, the immunohistochemical analysis is not without limitation (to be discussed later) and so another aim of this study was to explore the potential utility of western blotting as a tool to understand autophagic flux, using LC3 marker detection in western blotting of human brain tissue.

The initial stage for the optimisation of the western blot aimed to assess the suitability of the available human tissue samples given that these were post-mortem derived samples where factors such as post-mortem delay have been known to impact analysis of proteins via western blot. An attempt to detect both bands of LC3 in both human brain tissue (including fractions of the whole tissue extract, a lysosomal and microsomal enriched extracts and the waste pellet and cytosolic supernatant were included for completeness, see section 3.6)) no-disease control patient fibroblasts was performed.

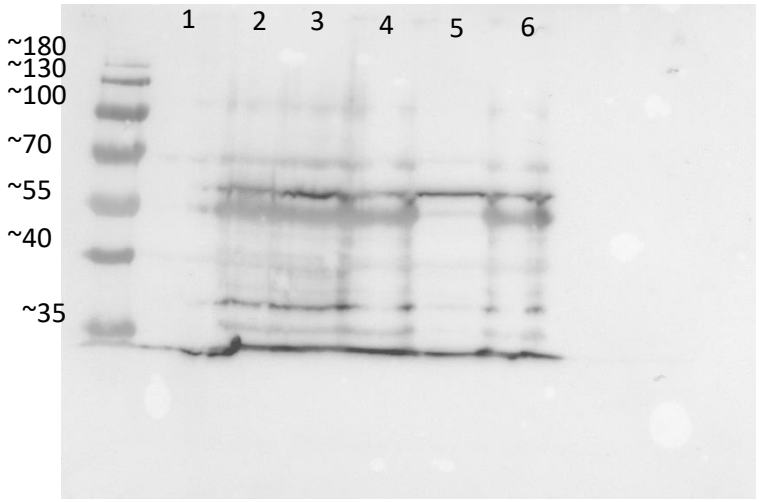

Figure 7.1: Western blot assessing the suitability of the fractions **1)** fibroblast, **2)** waste pellet, **3)** whole tissue (WT), **4)** Microsomal enriched, **5)** cytosolic supernatant, **6)** lysosomal enriched pellet.

The conditions were as described in the methods section using 1% BSA blocking solution and a 1:2000 anti-LC3 dilution and samples loaded at 10ug/ml. The presence of non-specific bands detected in the first experiments (not all data shown) suggested incomplete blocking, thus it was decided to add 5% milk powder to the blocking solution (see figure 7.1). As a consequence of this, there was no detected protein in the fibroblast sample. The cytosolic fraction was mostly devoid of protein whilst the other fractions had a detectable level of

protein but bands at the correct molecular weight could not be observed as the gel did not run down far enough due to overheating.

Repeated experiments explored a range of primary antibody dilutions and different overall protein loading amounts including 5µg, 15µg and 30µg of total protein the results of which can be seen in Figure 7.2. All gels showed some degree of non-specific binding; however, this was to be expected according to the manufacturer's information (Novus Bio) and are possible due to lysate preparation or post translational modifications.

The 1:2000 primary antibody dilution seemed to give the best results, coupled with loading the smallest amount of sample as there was no patchiness to the band as seen in the 1:4000 blot. However, the second band was still not detected under these conditions.

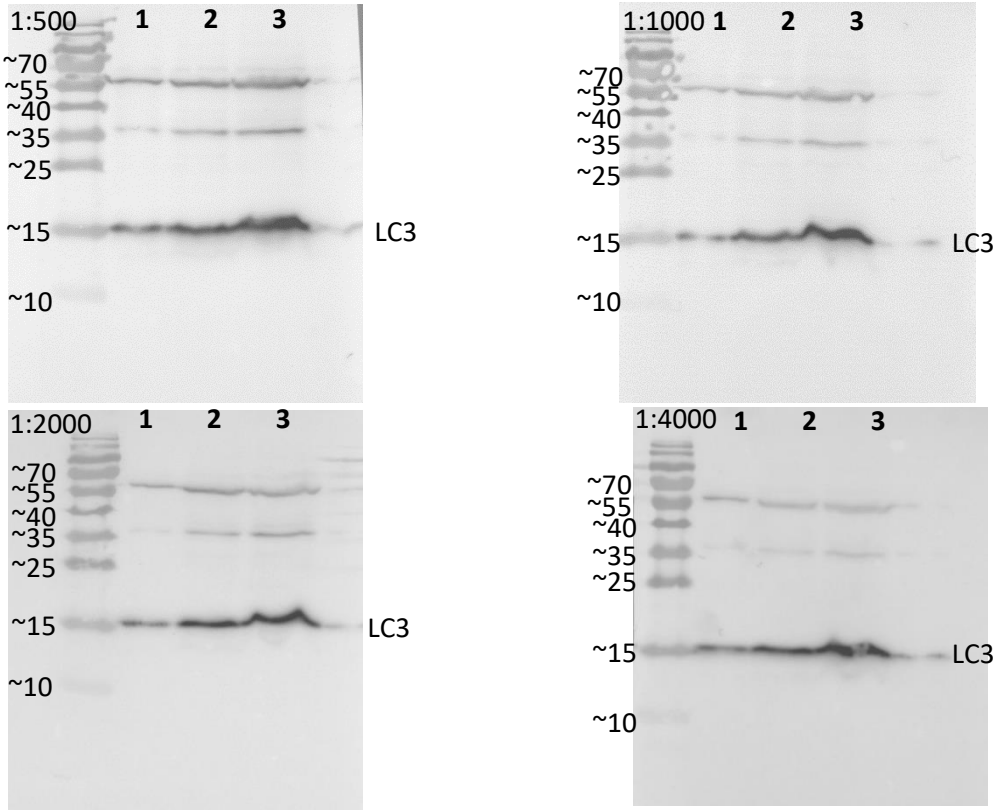

Figure 7.2: Assessment of different antibody dilutions, samples were cell culture lysates loaded at **1** 5µg, 2 15µg and **3** 30µg from left to right. Scale indicates approximate molecular weights in kDa

Figure 7.3 shows a blot with using a variety of AD and control skin-derived human fibroblast cell lines repeating the previous conditions using 1:2000 antibody dilution and 20µl of each sample. A few of the cell lines showed clear bands for both LC3-I and LC3-II which can be used to shed light on autophagic flux.

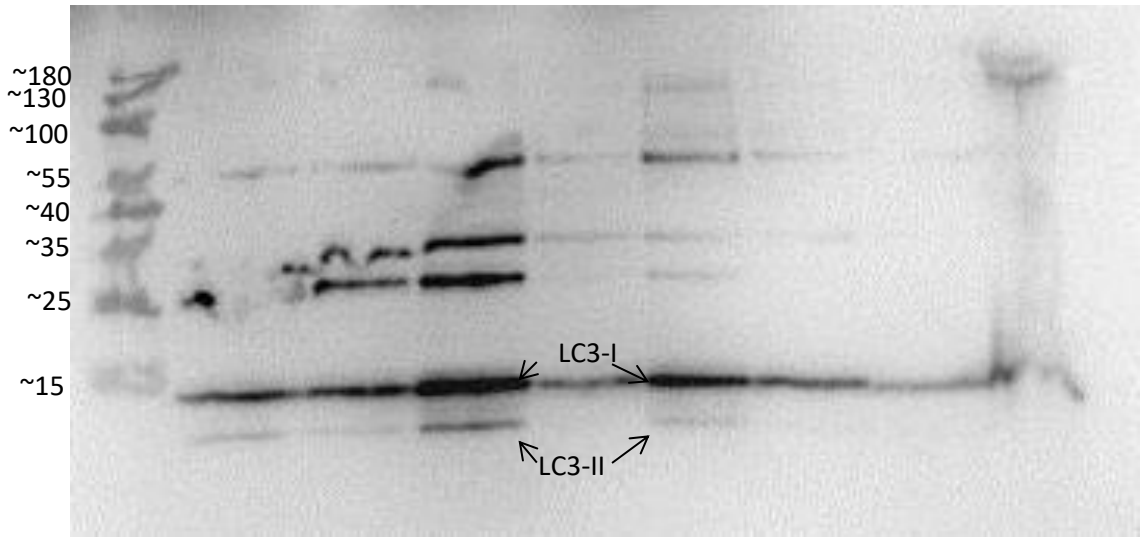

Figure 7.3: LC3 western blot using 1:2000 antibody dilution using several human fibroblast lysates to detect both LC3-I and LC3-II bands. Scale indicates approximate molecular weight sizes in kDa

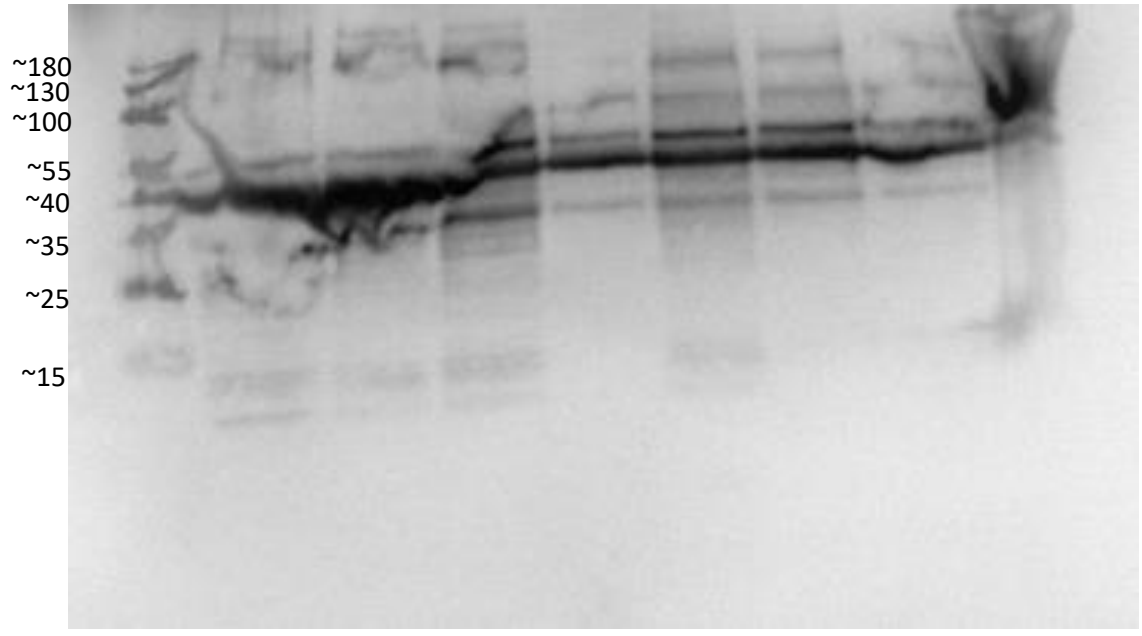

Figure 7.4: Beta-actin western blotting following strip and reprobe using a primary antibody dilution of 1:5000. Scale indicates approximate molecular weight sizes in kDa

Further western blotting was conducted for LC3 using 1:2000 and 1:4000 primary antibody dilutions as show in figure 7.5. Samples were the fibroblast “controls” identified in the previous blot and loaded at 5, 10 and 15µl and a whole tissue human brain extract loaded at 10µl. 1:2000 gave the best results, detecting both isoforms of LC3 with minimal non-specific bands shown. Meanwhile 1:4000 gave no detectable bands. Beta-actin gave a large degree of non-specific binding at both 1:5000 and 1:10000 antibody dilutions (Figure 7.5).

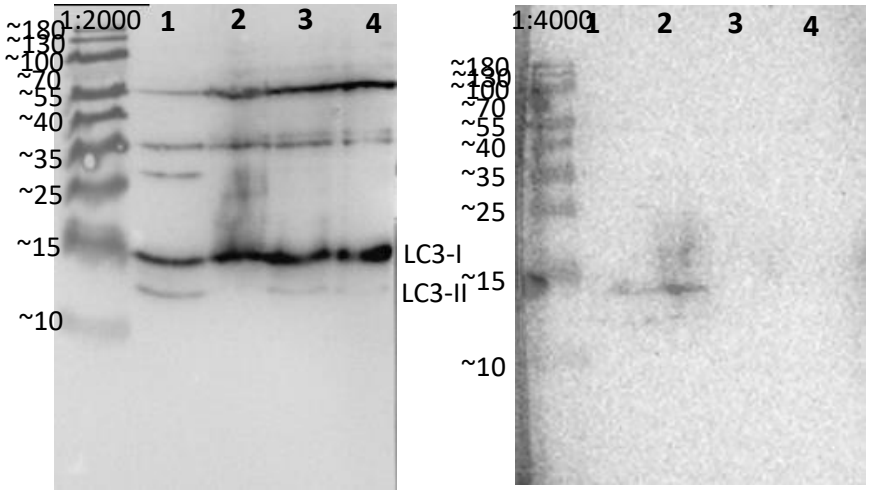

Figure 7.5: LC3 western blot using dilutions of 1:2000 and 1:4000. **(1)** 10µl of human brain whole tissue extract, and **(2-4)** Human fibroblast extract loaded at 20µl, 10µl, and 5µl of sample respectively. Scale indicates approximate molecular weight sizes in kDa

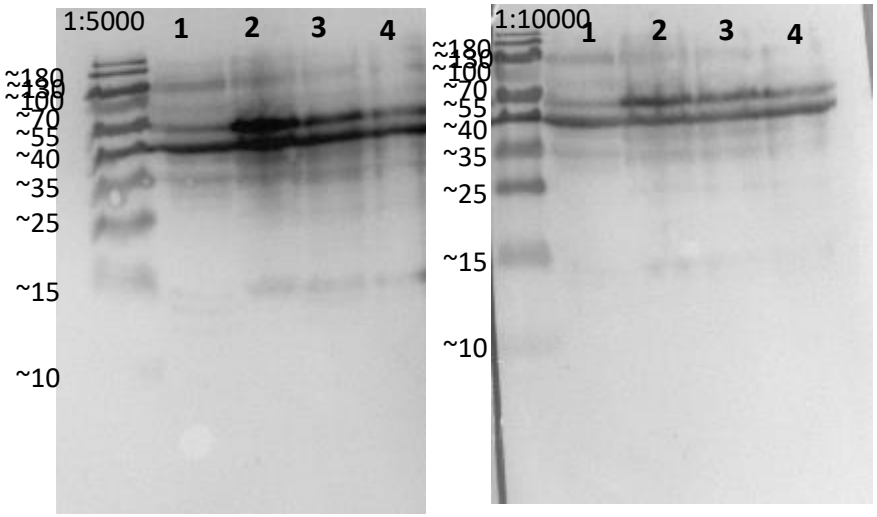

Figure 7.6: Beta-actin blots using antibody dilutions of 1:5000 and 1:10000. **(1)** 10µl of human brain whole tissue extract, **(2)** 20µl human fibroblast extract, **(3)**10µl of human fibroblast sample and **(4)** 5µl of human fibroblast sample. Scale indicates approximate molecular weight sizes in kDa.

8 Discussion

The aim of this project was to review the distribution of both MA and CMA markers in different forms of FTLD, specifically, those linked to *MAPT*, *C9orf72* and *GRN* mutations. Understanding variation in the detection of key autophagy markers could shed light on potential impairments in theses protein degradation pathways which may underlie some of the pathogenic protein accumulations associated with these neurodegenerative diseases. Comparative human brain studies have not been performed in relation to MA and CMA and so this study provides a novel insight to the potential role of protein degradation pathway disruption in disease. By furthering understanding of the variation in the MA and CMA it could uncover targets for future researchers to develop specific therapeutics for FTD and AD.

8.1 Macroautophagy

8.1.1 *P62 immunohistochemistry*

P62 immunohistochemistry allowed for the observation of the different morphologies and regional distributions of proteinaceous aggregates across the FTLD disease groupings, specifically showing protein aggregates that have been marked for degradation by macroautophagy. The differences noted between the lesion types within the disease grouping are consistent with what is expected of the literature into the pathology of the diseases, with white matter lesions being more prevalent in FTLD cases whilst neuronal inclusions were present in FTLD, AD and ND groups (Dickson et al., 2011; Charles Duyckaerts et al., 2009; Sha et al., 2006). The majority of the FTLD cases expressing p62 immunoreactivity lesions were the cases harbouring *MAPT* mutations suggesting a high

affinity of p62 for marking tau aggregates, given FTLD-*MAPT* commonly presents with tau positive lesions (Bodea et al., 2016; Dickson et al., 2011; Snowden et al., 2007; Sposito et al., 2015). The regional distributions of neuronal staining in AD was consistent the Braak staging criteria for classification as asymptomatic (aged-controls/ND) and prevalent AD with neuronal staining being predominant in the subiculum, EC and TEC of AD cases (Braak & Braak, 1995), whereas in the FTLD groups the EC, TEC and temporal grey matter most commonly harboured P62 positivity (Mackenzie & Neumann, 2016).

The full range of the protein aggregates such as TDP-43, tau, and Aβ that have been observed in other studies was not observed, due to the choice of antibody, anti-p62 (Mouse, Abcam), which was demonstrated by Kuusisto et al. (2001) to only show specific types of tau lesions, particularly NFTs and NTs but not astrocytic tau pathology. This was also the case in this current investigation, however a later study by Kuusisto et al. (2008) identified both tufted astrocytes and astrocytic plaques using a different p62, but in the putamen and amygdala of case with a diagnosis of CBD and PSP. This might suggest the p62 marker and method used in this study might not have been sufficient for the detection of astrocytic pathology or there may have been issues with respect to unmasking or choice of section. The lack of detection of astrocytic lesions may also have be due to the brain region in which the p62 immunochemistry was conducted as Kuusisto et al. (2008) which used sections including the basal ganglia and amygdala, which were not available in the present study.

The higher amount of p62 white matter staining in the FTLD group was as expected, given white mater glial inclusions have been more commonly reported in FTLD compared to no-disease control and AD brains (Duyckaerts et al., 2009). Due to the function of p62, this

suggests that these lesions are being marked for degradation by macroautophagy, but they are not being degraded by this pathway, and this could be due to an impaired initiation of macroautophagy or a downstream process such as autophagosome formation.

Double labelling immunofluorescence would be an interesting approach to use to explore if LC3 protein is interacting with p62, which is required to complete the engulfment of the marked autophagic cargo for degradation (Menzies et al., 2015; Schlafli et al., 2015; Sharifi et al., 2015). If the protein marked for degradation fails to be fully engulfed by the autophagosome, that could explain the abnormal accumulation of protein seen across the different forms of FTLD, however, there was insufficient tissue remaining in this study to allow of complex interactions between these key protein degradation associated proteins.

By investigating the exact nature of the macroautophagy deficits, it could identify potential therapeutic targets that can rescue protein degradation by restarting macroautophagy, however the small group sizes at present means the cohort lacks the power to do this.

The differences in the group based prevalence of these are of interest as neuronal inclusions are associated with cell loss, cellular dysfunction and worsened cognition (Nelson et al., 2012; Wilson et al., 2013), however the role of the other lesions is unclear (Miller et al., 2004), with cell culture investigations into oligodendroglial cells showing that aggregated tau does not impair the cells ability to function (Leyk et al., 2015).

TDP43 lesions would be expected in the FTLD-*C9orf72* and FTLD-*GRN* groups and studies have indicated that P62 detects TDP43 pathology in FTLD (Kuusisto et al., 2008; Tanji et al., 2012; Webster et al., 2016). The data from this study suggests P62 positive aggregates were `not widely detected in the FTLD-*C9orf72* and FTLD-*GRN* cases, which most often present with TDP-43 lesions, but this may be due the method for p62 antigen retrieval as another

study used a lower dilution (1.:100) to detect p62 positive dipeptide repeats (Mann et al., 2013), another possibility is incomplete antigen unmasking in this cohort and may have necessitated chemical antigen retrieval such as with formic acid or the use of a pressure cooker in the HEIR method; this may have been missed when optimising protocols due the blinding in place. In other studies, p62 positive, TDP43 negative, neuronal inclusions have been reported in the hippocampus of FTLD-*C9orf72* cases (Al-Sarraj et al., 2011) but given p62 itself is a substrate for autophagy, the story here is complex. TDP43 data was not available for the cases used in this study, but it would have been interesting to correlate TDP43 burden with p62 across the subgroups (and indeed, in relation to Braak stage in the AD cases) to see if this relationship varied.

Lashley et al. (2015) recommend for the assessment of TDP43 lesions the use of an antibody that stains both abnormal and normal TDP43 and using the cellular location and distribution to distinguish the two types from each other and noting this in relation to p62 would shed light on whether proteins marked for clearance were in face being effectively degraded.

In addition, it should be considered that p62 is also part of the Ubitquitin-Proteosome degradation system (UPS). This means that whilst the observed immunoreactivity could be marked abnormal ubitiquitinated protein intended for degradation by macroautophagy, these proteins could also be degraded via this alternative pathway, which has also been shown to be dysfunctional in some studies of neurodegenerative disease (Bedford et al., 2008).

There is lots of evidence linking p62 to the autophagy pathways in relation to FTLD. A very recent study demonstrated ALS-FTLD associated *SQSTM1/P62* mutations had the capacity to interrupt autophagy (Deng et al., 2020), with mutations impacting p62 being identified in

ALS-FTLD (Goode et al., 2016). Given p62 is only one of the 'marker' proteins for macroautophagy, (Menzies et al., 2015) one that is well known for its ability to bind to most abnormal tau and TDP43 deposits, it is interesting to note the variation in detection across the different genetic subtypes of FTLD. Alone however, this marker forms part of a complex story that cannot fully explain the role of autophagy in abnormal protein accumulation.

LC3 and Beclin-1 are other, more stringent MA markers, given their exclusive involvement within this pathway and clear association with specific phases in the process. With Beclin-1 being a requirement for MA initiation and LC3 being associated with autophagosomal formation (Menzies et al., 2015; Russell et al., 2013).

8.1.2 LC3 immunohistochemistry

Findings with LC3 immunohistochemistry suggest FTLD-*MAPT* cases had lower LC3-immunopositivity than controls in the frontal white matter. This is interesting, since high levels of LC3 in white matter has been linked to autophagy associated cell death in cerebral autosomal dominant arteriopathy with subcortical infarcts and leukoencephalopathy (CADASIL) (Hase et al., 2018) yet in myelinating disorders, LC3 and Beclin-1 has also been reported to be decreased (for review see Nutma et al., 2021) which is significant since myelin disturbances have also been reported in FTLD (Wang et al., 2018; Wu et al., 2021). This reduced LC3 immunopositivity in the white matter in the FTLD-*MAPT* cases may be linked to the tau mutation driven axonal malfunctioning, thought the exact nature of this relationship is something that could be explored as part of a further study. By designing interventions to address the LC3 deficit seen in the FTLD-*MAPT* cases, it may be possible to aim MA protein clearance as LC3 is necessary to complete autophagosomal maturation in

order to degrade the damaged proteins and organelles (Menzies et al., 2015; Russell et al., 2013).

In other brain regions, omnibus testing indicated variance in CA4 and the subiculum in LC3 assessment, however it was not possible to identify which groups this was attributed to, due to the small sample size presented in this study. CA4 is a particularly interesting area of the hippocampus that is relatively spared of abnormal protein accumulation in both AD and FTLD (Hatanpaa et al., 2014) and so the decrease of LC3 across the FTLD disease groupings compared to AD and control may suggest a reduction in autophagosome formation in this region. The data collected in this study also suggest a general variation in the amount of LC3 detected in temporal and frontal sub regions rather than a general trend of decrease or increase across hippocampus or frontal lobe (Menzies et al., 2015).This could be a consequence of these different areas being associated with different physiological roles and thus, they may have different levels of autophagic flux in relation to the protein clearance needs of the region.

In the frontal lobe, different cells layers were investigated due to their different physiological roles with respect to information processing and functional connectivity, as well as their differential involvement in neurodegenerative disease (Briggs, 2010; C. Duyckaerts et al., 2009). Layer VI is a cortical layer known to have a variety of cell types and processes information coming in and out of local neural networks, as well has having connections with deeper structures such as the thalamus (Briggs, 2010).

Meanwhile, the association fibers in the region of white matter scored contain short axons that connect neighbouring brain regions (Oishi et al., 2008). An impairment in the functioning of cells in this area could prevent neuronal networks from communicating and

thus give rise to an impairment in functions associated with the frontal cortex such as language production and behavioural regulation (Neubert et al., 2014). This inference should be taken with caution and cell loss protein aggregation have not been analysed therefore it is difficult to draw a stringent conclusion.

The difference between AD and the FTLD-*GRN* cases in CA4 is difficult analyse as there is no differences between the no-disease controls and AD or the no-disease controls and FTLD-*MAPT* groups. One potential explanation could be that because the AD and ND groups are statistically similar, and the presence of the outlier in the ND group for CA4 may have affected the mean rank score of the ND group in the ND vs MAPT comparisons, meaning it resulted in a non-significant difference. However, it must be considered that the group sizes were small, and variation within the groups large and this may be a reflection of the pathological heterogeneity, even within disease groups driven by the same mutation. Expansion of this study to include a much larger cohort would be extremely beneficial, as would the sue of serial sectioning and double staining immunofluorescence to explore the relationship between L3 and some of the FTLD associated pathogenic proteins.

8.1.3 *Beclin-1 immunohistochemistry*

Beclin-1 immunoreactivity indicated variance in the temporal lobe grey matter, however due to the sample size *post hoc* analysis failed to identify specific differences between the study groups, due to the size of the cohort. This might indicate disease associated variability in the initiation of the formation of the autophagosome from the pre-autophagosomal structures which is a key role of Beclin-1 (Menzies et al., 2017; Russell et al., 2013).

While Beclin-1 has not specifically been investigated previously in FTLD, a pathogenic role has been suggested in ALS, where in both cellular and animal models expressing mutant SOD1, Beclin-1 was found to be upregulated (Nassif et al., 2014). Other studies have also indicated that Beclin-1 can be upregulated in cellular stress conditions, such as those that occur as a consequence of trauma (Diskin et al., 2005).

FTLD-TDP associated with GRN cases normally results in Type A Classification(DeJesus-Hernandez et al., 2011; Renton et al., 2011); Whitwell et al. (2010) stated that FTLD-TDP type A cases show more lateral temporal lobe atrophy compared to controls and other FTLD subtypes . Whilst the temporal gyrus scored (collateral) is not in this region, the more generic findings showed that FTLD-Type A has more generic pattern of temporal atrophy whilst the other types showed more focal patterns of loss. This means any cases with a type B classification, commonly seen in those with *C9orf72* expansions (DeJesus-Hernandez et al., 2011; Renton et al., 2011), would have very specific regions of protein accumulation and cell loss which may not have been included in the sections that were scored in this study. This would need to be further investigated with respect to the pathological lesions to assess whether the temporal lobe decrease in Beclin-1 immunoreactivity is a response to a lack of abnormal protein or due to a pathological role. The novel insight into the reduced detection of Beclin-1 and in the *GRN* indicates there could be some benefit addressing the specific deficit In the MA initiation, and this may also be true on *C9orf72* however the lack of statistically significant different to controls makes this harder to elucidate.

Moreover, when comparing the results between Beclin-1 and LC3 immunohistochemistry there is no overlap between the mutation affected and the region that the decrease is observed; no region showed a significant difference in both MA markers, though this could

be suggestive that in some cases failure of abnormal protein clearance could be being driven by differential and specific pathway deficits; in some cases a failure of initiation of the autophagosome formation or in other cases, the failure of the maturation of the autophagosome and subsequent protein degradation.

This makes the identifying the exact nature of the autophagy deficit more difficult without quantifying the absolute autophagy protein levels in relation to each other, as well as pathogenic protein accumulation. Given the variation detected, exploration of the potential utility of western blotting as a tool for the assessment of autophagic flux was explored as a subsidiary aim of this project. (Menzies et al., 2015; Russell et al., 2013; Rosenfeldt et al., 2012)

8.1.4 *Western Blotting*

A number of optimisation conditions were explored to see if western blotting could be used to detect LC3-I and LC3-II, the ratio of which has been commonly used to assess autophagic flux, however other researchers have reported difficulties in using this approach in human brain tissue due to the sensitivity of the protein to degradation and the impact of post-mortem delay (insert ref).

This study identified an optimum approach for detecting the LC3 doublet, using a 1% BSA/5% Milk blocking solution prior to a 1:2000 one hour incubation with anti-LC3 antibody at room temperature. This method allowed the detection of the LC3 bands at 15 and 17 kDa as expected (Novus, 2017; Schlafli et al., 2015). Whilst this did also have some non-specific bands, this recognised by the antibody manufacturer (Novus, 2017).

Whilst the aim to successfully optimise the conditions for LC3 western blot analysis of human brain tissue were achieved, this was not performed across the study cohort as the

frozen brain tissue was not released in time for this element of the project work to be completed. However, LC3 analysis via western blot would give an indication of variation in autophagic flux across the different subtypes of FTLD. A recent study indicated that C9orf72 depletion reduced in enhanced autophagic flux (Ji et al., 2017) and so one might predict a more significant impact on flux in the FTLD-*C9orf72* disease group because of this. Understanding the overall impact of how the MA 'machinery' detection and variation relates to overall autophagic flux would give a much stronger picture regarding how proteostasis could be improved in the different forms of FTLD.

8.2 Chaperone-Mediated Autophagy

To date there are no studies exploring the variation in key CMA markers in FTLD and given the role of CMA in the clearance of key FTLD associated proteins such as tau and TDP43, this is an increasingly important area of research.

8.2.1 LAMP2a

Investigation into CMA using LAMP2a failed to yield any statistically significant results with respect to different FTLD mutations. (Salvador et al., 2000). These finding with LAMP2a suggest there no differences in amount of protein, when investigated by mutation, suggesting in all groups have the same availability of LAMP2a for the forming of the lysosomal receptor to transport to abnormal protein into the lysosome for degradation (Bandyopadhyay et al., 2008).

LAMP2a exists in both monomer and oligomer forms, and it is the formation of the LAMP2a receptor from several monomers that creates the receptor that allows for the transport of protein through the lysosomal membrane (Salvador et al., 2000). The current analysis does not assess the different forms of LAMP2a due to the unavailability of such specialised markers, and alternative techniques, such specialised gel electrophoresis as implemented in Bandyopadhyay et al. (2008), may be able to distinguish between these different forms. Should any variation in LAMP2a have been identified between the different FTLD disease groups, then it would have been interesting to pursue variation in monomeric and oligomeric forms to allow consideration of functional receptor formation.

Furthermore, the current analysis only gives rudimentary information on the amounts of these proteins, whereas other studies have shown it is not the amount of protein but other factors such as tau fragments of the exterior of the lysosome could contribute to the pathogenesis of the disease (Wang et al., 2009); Meanwhile Orenstein et al. (2013) found that α-synuclein protein was not translocated into the lysosome, and therefore not degraded, rather than the availability of the LAMP2a protein being the limiting factor. This suggests that the cellular location of the pathological proteins and the CMA markers in relation to each other is also important in the study of CMA in neurodegenerative disease and this poses a challenge, particularly when working with human brain tissue.

8.2.2 Anti-Hsc70 Immunohistochemistry

Investigations into Hsc70 in the hippocampal and temporal lobe did not find any evidence for a variance in the amount of Hsc70 protein in any of the hippocampal or temporal subregions studied. A lack of significance with the amount of Hsc70 detected suggests that is expressed at the same levels in all groups, meaning suitable abnormally folded proteins

should be able to bind to co-chaperone complex and this is important to know since this could be a rate limiting factor in the CMA process (Bain et al., 2018).

Meanwhile in the frontal lobe variances in the Hsc70 immunopositivity were identified in Layers III, IV, V and VI in addition to the frontal white matter. However, the only specific difference that could be identified between in the no-disease and FTLD-*MAPT* mutation groups was that in the disease group, Hsc70 detection was lower than in the no-disease group which could therefore mean decreased targeting of damaged proteins (namely tau), to the lysosome for degradation.

Firstly, Hsc70 is responsible for biding to the KFERQ-like motif on the tau protein (Wang et al., 2009), and so any decrease in chaperone levels my decrease may reduce the targeting of the pathogenic protein form for degradation via CMA (Bejarano & Cuervo, 2010). Hsc70 is known to rapidly interact with tau once it detached from the microtubule and so given it exists in a hyperphosphorylated state in disease, once might expect this interaction to increase assuming the chaperone is available in abundance (Jinwal et al., 2010). Another implication would be that a lack of availability of Hsc70 could also mean that there is no receptive protein inside the lysosome to ensure the tau protein straights out and enters the lysosome for degradation (Jinwal et al., 2010, Salvador, 2000, Wang, 2009). Given the decreased Hsc70 noted in the FTLD-*MAPT* group of this study, it could be speculated could be speculated that there is insufficient chaperone to direct hyperphosphorylated tau for degradation and this could contribute to the aggregation of this protein. Chaperone restoring therapies might therefore be a viable therapeutic avenue to explore, specifically in FTLD-*MAPT*.

8.3. Overall findings

Overall this study has added to the understanding of autophagy recruitment pathways in FTLD. Specifically it has highlighted variation markers for macroautophagy (LC3 and Beclin-1) and CMA (Hsc70 and LAMP2a) in the frontal and temporal lobes and that there are differences between FTLD mutation groups (*GRN,MAPT* and *C9orf72*). It has also laid out a basis for better quantifying autophagic flux using the LC3 western blotting using fresh-frozen human brain tissue.

9 Limitations

A limitation of the current analysis is due the small sample at present. These small group sizes means that the p62 prevalence rates cannot be assessed by chi-square for statistical significance due to many expect cell counts of zero. This could be remedied by increasing the cohort size, which will also increase the power of the statistics conducted for the autophagy markers (as outline in section 7.1). Given the relative scarcity of human brain tissue, particularly in the rarer forms of neurodegenerative disease such as FTD, studies such of this that provide a 'proof of concept' are important to see if the release of further tissue and cohort expansion is warranted. Given the variation reported in this study, this expansion of the study would give a valuable insight on to the variation in autophagy deficit in FTLD.

With respect to the methodology used, it is important to acknowledge that the scoring of IHC is subjective, even when using a semi-quantitative scale. To limit the impact of this at the current stage, each section was scored twice to ensure the scoring was consistent throughout, if any scores where different they would be scored a third time.

Another issue with the use of IHC that was noted with regards to the p62 protocol, the use of the microwave to boil the sections for HIER for anti-p62 IHC damaged a significant amount of the tissue. This of particular importance with FTLD-*C9orf72* cases leading to only 4 of the total 8 cases with tissue suitable for scoring and many regions damaged in other cases. This was not an issue with the Labvision™ PT module (Thermo Scientific) preparations in later protocols, hence all future HEIR will be conducted using the latter method to preserve tissue.

Furthermore, since the autophagy markers LC3, Beclin-1, LAMP2a, and Hsc70 stain with a varying intensity, there is a lower threshold for detection meaning that some of the variation may be lost. This is occurred due to the optimisation phase for the immunochemistry, in which only few cases are used to set the protocol and antibody dilution. This was completed using mid-Braak stage sections in another study and is necessary to preserve the very limited supply of tissue. To correct this Western blotting could be employed, using the developed protocol, which allow for further quantification of smaller levels of protein and differences between groups.

In addition, the use of anti-LC3 antibodies in immunohistochemistry stain all isoforms of LC3, whilst this gives some insight into the alterations in autophagy it is very difficult to draw definitive conclusions. Whilst a low amount of LC3 could indicate a problem with the MAP1LC3B gene expression/transcription it does not necessarily indicate a problem with autophagy as this is best studied by looking at the different isoforms of LC3. Whilst this is not been analysed, it will be via western blotting (as discussed in section 7.2).

With respect to protein quantification, neither IHC nor Western blot are the ideal methods to use, for example an ELISA would be the best option for the analysis of specific protein amounts. However this is expensive and with respect to LC3 suffers from the same issue as IHC in that it will only quantify total LC3 and not the different the LC3-I and LC3-II isoforms that give a better insight into autophagic flux (Schlafli et al., 2015; Sharifi et al., 2015). For comparison of the different autophagy markers it is better to conserve the scientific methods employed, hence the intended use of western blotting as we have demonstrated that it is a viable technique to identify the different isoforms of LC3.

Finally, in the pathology of these diseases it is often noted that within a given region, some cells will demonstrate pathology, whilst their neighbouring will not, neither the use of IHC or western blotting allows for the analysis of this. The way in which the IHC has been assessed so far only allows for an overall score of the region and cell counting would be swayed by individual variation in cell numbers, meanwhile western blotting lacks more spatial resolution than IHC as it uses several gyri from a brain region in a homogenisation form. One way to study abnormal protein and changes in autophagy between single cells is via the use of double-labelling immunofluorescence which visuals two proteins of interest at the same time; plans to follow this are outlined in section 7.3.

10 Future work

10.1 Further Immunohistochemical assessment

Future immunohistochemical studies could include pathological protein analysis using the markers initiated in this project (AT8 and TDP43) and compare these markers to the autophagic proteins. For the AD cohort this would also include amyloid-beta pathology marker such as 4G8 (Baghallab et al., 2018). An alternative approach if protein analysis using these markers is not possible would be to use Braak staging (Braak & Braak, 1995; Braak et al., 2006)(ref) and Thal phases (Thal et al., 2002) as a quasi-measure of pathology in well characterised tissue from sources such as Brains for Dementia Research, this is possible due to AD pathology having well characterised progression throughout the brain unlike FTLD (Ferrari et al., 2011; Mackenzie & Neumann, 2016)

Further considerations would be to compare to other neurodegenerative diseases or subtypes. An obvious comparison would be to compare to MND variants due to the link between FTLD and MND as previously described (Bak, 2010; Tiryaki & Horak, 2014). An example of this would include those with a SOD1 mutation as in these cases SOD1 aggregates have been observed in the neuronal and glia cells, predominantly in the motor cortex (Forsberg et al., 2019; Nolan et al., 2020). Currently the mechanism linking SOD1 aggregates to cell death is thought to be oxidative stress (An et al., 2014; Mahoney et al., 2006; Tu et al., 1997).

Alternatively, the more specific mutations in the pathological proteins could be studied where the tissue is available such as missense mutations in TARDBP (Gendron et al., 2013; Moreno et al., 2015, Floris, 2015) and MAPT (Forrest et al., 2019) as mentioned previously.

This would provide insight into how these mutations affect the further effect the protein degradation pathways in *post-mortem* samples.

Another avenue for future research would be to stain an area not usually involved in the early stages of diseases that cause dementia such as the occipital lobe (Braak & Braak, 1995; Braakman et al., 2006 ; Kril & Halliday, 2011). Including the occipital lobe into study would allow for a within case control region, as this area of the brain is not normally as heavily affected in FTLD by cell loss or protein aggregation, adding a further level of complexity to the understanding of autophagy pathways in FTLD.

The tissue request for this study did include provisions to expanded to include 96 cases, this will consist of a total 64 FTLD, 13 AD and 13 control cases and given this study has identified a number of key variations between the different genetic forms of FTLD, then this work will now be continued in the larger group. The FTLD groups will include 11 MAPT mutations, 11 C9orf72 expansions and 11 GRN mutations. It also included a number of sporadic cases for FTLD- TDP-43, with 17 FTLD-TDP type A, 6 FTLD-TDP type B and 8 FTLD-TDP type C cases, the use of genetic and sporadic cases would allow for the comparison of different underlying associations of FTLD and their impact of autophagy, as well as have implications for autophagy altering treatments.

Furthermore, an expanded cohort would allow for the analysis would allow for the comparison of changes in autophagy markers and clinical phenotypes such as bvFTD, PFNA and SD. The utility of this is at present there are no diagnostic tests other than *post mortem* analysis for assessing the aggregate protein in sporadic FTD cases (Bruun et al., 2019; Greaves & Rohrer, 2019; Ntymenou et al., 2021 542; Sancesario & Bernardini, 2015) and genetic testing is usually reserved for cases with a family history of FTD or MND (Greaves &

Rohrer, 2019). If a link between specific autophagy deficits could be demonstrated, it would improve access to any approved treatments that would aim to correct the autophagy impairment.

By including groups of the same pathological diagnosis but having both genetic and sporadic causes, the study will compare the differences between the familial and sporadic forms of FTLD with respect with their proteinopathy, this will help gain understanding of whether any autophagy marker changes are associated with the presence of abnormal protein or if there are differences between the sporadic and familial causes of the disease. Finally, conducting analysis between the different clinical phenotypes will allow for the observation of changes in autophagy by FTLD presentation, which if syndrome specific could be useful for tailoring autophagy-based therapeutics for FTD in the future.

10.2 Western Blotting

Western blotting analysis would allow for the further quantification autophagic protein markers such as LC3, Beclin-1, LAMP2a and Hsc70.

This would be especially useful for LC3 as this this would allow for the analysis of the LC3-I to LC3-II ratio which is a superior marker of autophagic flux compared to total LC3 as demonstrated by the immunohistochemical assessment (Schlafli et al., 2015; Sharifi et al., 2015). As previously discussed, LC3-I is cleaved into LC3-II and bound to the autophagosome as it engulfs the autophagic cargo (Kabeya et al., 2004; Sou et al., 2006). A lower LC3-II to the LC3-I ratio, compared to controls, would suggest a slower or impaired autophagosomal formation, whilst a however an increased ratio would suggest the inverse, possibly as a response to the abnormal protein load. This can also be compared to other markers of macroautophagy such as p62 (Pankiv et al., 2007; Schlafli et al., 2015; Wooten et al., 2008)

or Beclin-1. Comparison to degradation marking proteins such as P62 would allow for insight into effective proteins marked for degradation are being broken down by MA, where a high p62 to LC3 ratio indicated an impairment in MA (Masuda et al., 2019 545). Beclin-1 western blotting would indicate that the abnormal protein is initiating the MA response (Pickford et al., 2008; Russell et al., 2013).

In addition, western blotting for LAMP2a would be a useful as a marker of CMA; LAMP2a is the receptor protein that forms a pore in the lysosome membrane, allowing singular abnormal proteins to pass through for degradation (Bandyopadhyay et al., 2008)(Bandyopadhyay et al., 2008)(Bandyopadhyay et al., 2008)(Bandyopadhyay et al., 2008). A lack of LAMP2a would inhibit the ability of the protein to enter the lysosome which would prevent it from being degradation via the CMA pathway (Bandyopadhyay et al., 2008). Western blotting under non-reducing conditions (such as used inBandyopadhyay et al., 2008) would also demonstrate if the monomer LAMP2a is polymerising into the tetramer which is crucial for the formation of the lysosomal pore allowing proteins to directly enter the lysosome (Bandyopadhyay et al., 2008; Salvador et al., 2000).

Further investigating Hsc70 with western blotting would allow for more quantitative measures of the protein and would allow for further insight in the availability of the protein, which is crucial for the abnormal proteins to chaperoned to the lysosome (Bandyopadhyay et al., 2008; Chiang et al., 1989; Salvador et al., 2000).

An alternative approach would be use ELISAs which would provide a more accurate quantification of the protein levels, this would be especially useful for Beclin-1, LAMP2a and Hsc70 analysis. However due to the aforementioned LC3-I and LC3-II ratio the use of an ELISA would be limited as there aren’t any antibodies currently available that can distinguish

between the two isoforms, however a sandwich ELISA technique has been demonstrated in cell culture models (Oh et al., 2017). For LAMP2a it would also not assess the polymerisation of the monomers (Bandyopadhyay et al., 2008).

10.3 Double Immunofluorescence analysis

Using double labelling immunofluorescence would allow for the observation of the direct interaction of the autophagy markers (LC3, LAMP2a, Hsc70 and Beclin-1) and pathological markers (AT8 and TDP-43), it would allow for the observation of two markers within a single cell; this could be the observe the localisation of an autophagic marker in relation to pathogenic protein such as abnormal TDP-43, Aß or Tau, or it could be used to identify stages of the autophagy processes. Such techniques have been previously used, for example some studies have shown that LC3 will aggregate around abnormal TDP-43 in cell culture models (Wang, Ma, et al., 2015)(Wang, Ma, et al., 2015). Analysis could also focus on cells with a high and low abnormal protein burden within the same region and case, this may improve understanding of why some cells in a given area will be heavily affect by abnormal protein whilst their neighbours show no pathology, as seen in the variation of inclusions in our study and in diagnostic criteria (Braak et al., 2006; Braak & Braak, 1997; Mackenzie et al., 2011).

11 Summary

Overall, the project has addressed the aim of conducting immunochemistry for four autophagy markers and observing differences in protein aggregates in the hippocampus and confirming a variation of markers in the hippocampal subregions. Moreover, analysis has shown differences between MA and CMA recruitment which differentially affect hippocampal and frontal subregions with the mutation (MAPT, C9orf71, and GRN). Furthermore, the study has addressed its goal of having both a protein extraction and LC3 western blotting protocol optimised in preparation for investigations using fresh-frozen human brain tissue following a confirmatory experiment using the different brain fractions. Future work also includes the use of specific pathological protein markers (AT8 and anti-TDP43) and comparing them to autophagy markers via IHC and immunofluorescence.

References

Adams, S. J., DeTure, M. A., McBride, M., Dickson, D. W., & Petrucelli, L. (2010). Three repeat isoforms of tau inhibit assembly of four repeat tau filaments. *PLoS One*, *5*(5), e10810. https://doi.org/10.1371/journal.pone.0010810

Al-Sarraj, S., King, A., Troakes, C., Smith, B., Maekawa, S., Bodi, I., Rogelj, B., Al-Chalabi, A., Hortobagyi, T., & Shaw, C. E. (2011). p62 positive, TDP-43 negative, neuronal cytoplasmic and intranuclear inclusions in the cerebellum and hippocampus define the pathology of C9orf72-linked FTLD and MND/ALS. *Acta Neuropathol*, *122*(6), 691-702. https://doi.org/10.1007/s00401-011-0911-2

Alvarez-Erviti, L., Rodriguez-Oroz, M. C., Cooper, J. M., Caballero, C., Ferrer, I., Obeso, J. A., & Schapira, A. H. V. (2010). Chaperone-Mediated Autophagy Markers in Parkinson Disease Brains. *Archives of Neurology*, *67*(12), 1464-1472. https://doi.org/10.1001/archneuro1.2010.198

An, T., Shi, P., Duan, W., Zhang, S., Yuan, P., Li, Z., Wu, D., Xu, Z., Li, C., & Guo, Y. (2014). Oxidative stress and autophagic alteration in brainstem of SOD1-G93A mouse model of ALS. *Mol Neurobiol*, *49*(3), 1435-1448. https://doi.org/10.1007/s12035-013-8623-3

Aoki, N., Boyer, P. J., Lund, C., Lin, W. L., Koga, S., Ross, O. A., Weiner, M., Lipton, A., Powers, J. M., White, C. L., & Dickson, D. W. (2015). Atypical multiple system atrophy is a new subtype of frontotemporal lobar degeneration: frontotemporal lobar degeneration associated with α-synuclein. *Acta Neuropathol*, *130*(1), 93-105. https://doi.org/10.1007/s00401-015-1442-z

Arechavaleta-Velasco, F., Perez-Juarez, C. E., Gerton, G. L., & Diaz-Cueto, L. (2017). Progranulin and its biological effects in cancer. *Med Oncol*, *34*(12), 194. https://doi.org/10.1007/s12032-017-1054-7

Arenas, A., Kuang, L., Zhang, J., Kingren, M. S., & Zhu, H. (2021). FUS regulates autophagy by mediating the transcription of genes critical to the autophagosome formation. *Journal of Neurochemistry*, *157*(3), 752-763. https://doi.org/10.1111/jnc.15281

Armstrong, M. J., Litvan, I., Lang, A. E., Bak, T. H., Bhatia, K. P., Borroni, B., Boxer, A. L., Dickson, D. W., Grossman, M., Hallett, M., Josephs, K. A., Kertesz, A., Lee, S. E., Miller, B. L., Reich, S. G., Riley, D. E., Tolosa, E., Troster, A. I., Vidailhet, M., & Weiner, W. J. (2013). Criteria for the diagnosis of corticobasal degeneration. *Neurology*, *80*(5), 496-503. https://doi.org/10.1212/WNL.0b013e31827f0fd1

ARUK. (2018a). *Current Treatments*. Retrieved 02/01/2022 from https://www.dementiastatistics.org/statistics/current-treatments/

ARUK. (2018b). *Different Types of Dementia*. Retrieved 02/01/2022 from https://www.dementiastatistics.org/statistics/different-types-of-dementia/

Attems, J., & Jellinger, K. A. (2013). Neuropathology. In T. Dening & A. Thomas (Eds.), *Oxford Textbook of Old Age Psychiatry* (Second ed.). OUP Oxford.

Baghallab, I., Reyes-Ruiz, J. M., Abulnaja, K., Huwait, E., & Glabe, C. (2018). Epitomic Characterization of the Specificity of the Anti-Amyloid Abeta Monoclonal Antibodies 6E10 and 4G8. *J Alzheimers Dis*, *66*(3), 1235-1244. https://doi.org/10.3233/JAD-180582

Bain, H. D. C., Davidson, Y. S., Robinson, A. C., Ryan, S., Rollinson, S., Richardson, A., Jones, M., Snowden, J. S., Pickering-Brown, S., & Mann, D. M. A. (2018). The role of lysosomes and autophagosomes in frontotemporal lobar degeneration. *Neuropathol Appl Neurobiol*. https://doi.org/10.1111/nan.12500

Bak, T. H. (2010). Motor neuron disease and frontotemporal dementia: One, two, or three diseases? *Ann Indian Acad Neurol*, *13*(Suppl 2), S81-88. https://doi.org/10.4103/0972-2327.74250

Baker, M., Mackenzie, I. R., Pickering-Brown, S. M., Gass, J., Rademakers, R., Lindholm, C., Snowden, J., Adamson, J., Sadovnick, A. D., Rollinson, S., Cannon, A., Dwosh, E., Neary, D., Melquist, S., Richardson, A., Dickson, D., Berger, Z., Eriksen, J., Robinson, T., . . . Hutton, M. (2006). Mutations in progranulin cause tau-negative frontotemporal dementia linked to chromosome 17. *Nature*, *442*(7105), 916-919. https://doi.org/10.1038/nature05016

Bandyopadhyay, U., Kaushik, S., Varticovski, L., & Cuervo, A. M. (2008). The chaperone-mediated autophagy receptor organizes in dynamic protein complexes at the lysosomal membrane. *Mol Cell Biol*, *28*(18), 5747-5763. https://doi.org/10.1128/MCB.02070-07

Barbier, P., Zejneli, O., Martinho, M., Lasorsa, A., Belle, V., Smet-Nocca, C., Tsvetkov, P. O., Devred, F., & Landrieu, I. (2019). Role of Tau as a Microtubule-Associated Protein: Structural and Functional Aspects. *Front Aging Neurosci*, *11*, 204. https://doi.org/10.3389/fnagi.2019.00204

Barker, W. W., Luis, C. A., Kashuba, A., Luis, M., Harwood, D. G., Loewenstein, D., Waters, C., Jimison, P., Shepherd, E., Sevush, S., Graff-Radford, N., Newland, D., Todd, M., Miller, B., Gold, M., Heilman, K., Doty, L., Goodman, I., Robinson, B., . . . Duara, R. (2002). Relative frequencies of Alzheimer disease, Lewy body, vascular and frontotemporal dementia, and hippocampal sclerosis in the State of Florida Brain Bank. *Alzheimer Dis Assoc Disord*, *16*(4), 203-212. https://www.ncbi.nlm.nih.gov/pubmed/12468894

Barnes, J., Whitwell, J. L., Frost, C., Josephs, K. A., Rossor, M., & Fox, N. C. (2006). Measurements of the amygdala and hippocampus in pathologically confirmed Alzheimer disease and frontotemporal lobar degeneration. *Arch Neurol*, *63*(10), 1434-1439. https://doi.org/10.1001/archneur.63.10.1434

Bayraktar, O., Oral, O., Kocaturk, N. M., Akkoc, Y., Eberhart, K., Kosar, A., & Gozuacik, D. (2016). IBMPFD Disease-Causing Mutant VCP/p97 Proteins Are Targets of Autophagic-Lysosomal Degradation. *PLoS One*, *11*(10), e0164864. https://doi.org/10.1371/journal.pone.0164864

Bedford, L., Hay, D., Paine, S., Rezvani, N., Mee, M., Lowe, J., & Mayer, R. J. (2008). Is malfunction of the ubiquitin proteasome system the primary cause of alpha-synucleinopathies and other chronic human neurodegenerative disease? *Biochim Biophys Acta*, *1782*(12), 683-690. https://doi.org/10.1016/j.bbadis.2008.10.009

Bejarano, E., & Cuervo, A. M. (2010). Chaperone-mediated autophagy. *Proc Am Thorac Soc*, *7*(1), 29-39. https://doi.org/10.1513/pats.200909-102JS

Biffi, A., & Greenberg, S. M. (2011). Cerebral amyloid angiopathy: a systematic review. *J Clin Neurol*, *7*(1), 1-9. https://doi.org/10.3988/jcn.2011.7.1.1

Birsa, N., Bentham, M. P., & Fratta, P. (2020). Cytoplasmic functions of TDP-43 and FUS and their role in ALS. *Semin Cell Dev Biol*, *99*, 193-201. https://doi.org/10.1016/j.semcdb.2019.05.023

Bodea, L. G., Eckert, A., Ittner, L. M., Piguet, O., & Götz, J. (2016). Tau physiology and pathomechanisms in frontotemporal lobar degeneration. *Journal of Neurochemistry*. https://doi.org/10.1111/jnc.13600

Boeve, B. F. (2011). The multiple phenotypes of corticobasal syndrome and corticobasal degeneration: implications for further study. *J Mol Neurosci*, *45*(3), 350-353. https://doi.org/10.1007/s12031-011-9624-1

Bose, J. K., Huang, C. C., & Shen, C. K. (2011). Regulation of autophagy by neuropathological protein TDP-43. *J Biol Chem*, *286*(52), 44441-44448. https://doi.org/10.1074/jbc.M111.237115

Bouhouche, A., Tibar, H., Ben El Haj, R., El Bayad, K., Razine, R., Tazrout, S., Skalli, A., Bouslam, N., Elouardi, L., Benomar, A., Yahyaoui, M., & Regragui, W. (2017). LRRK2 G2019S Mutation: Prevalence and Clinical Features in Moroccans with Parkinson's Disease. *Parkinsons Dis*, *2017*, 2412486. https://doi.org/10.1155/2017/2412486

Boxer, A. L., & Boeve, B. F. (2007). Frontotemporal dementia treatment: current symptomatic therapies and implications of recent genetic, biochemical, and neuroimaging studies. *Alzheimer Dis Assoc Disord*, *21*(4), S79-87. https://doi.org/10.1097/WAD.0b013e31815c345e

Braak, E., & Braak, H. (1995). Staging of Alzheimer ' s Disease-Related Neurofibrillary Changes. *Neurobiology of Aging*, *16*(3), 271-278.

Braak, H., Alafuzoff, I., Arzberger, T., Kretzschmar, H., & Del Tredici, K. (2006). Staging of Alzheimer disease-associated neurofibrillary pathology using paraffin sections and

immunocytochemistry. *Acta Neuropathol*, *112*(4), 389-404. https://doi.org/10.1007/s00401-006-0127-z

Braak, H., & Braak, E. (1997). Diagnostic criteria for neuropathologic assessment of Alzheimer's disease. *Neurobiol Aging*, *18*(4 Suppl), S85-88. https://doi.org/10.1016/s0197-4580(97)00062-6

Braakman, N., Matysik, J., van Duinen, S. G., Verbeek, F., Schliebs, R., de Groot, H. J., & Alia, A. (2006). Longitudinal assessment of Alzheimer's beta-amyloid plaque development in transgenic mice monitored by in vivo magnetic resonance microimaging. *J Magn Reson Imaging*, *24*(3), 530-536. https://doi.org/10.1002/jmri.20675

Briggs, F. (2010). Organizing principles of cortical layer 6. *Front Neural Circuits*, *4*, 3. https://doi.org/10.3389/neuro.04.003.2010

Bruun, M., Koikkalainen, J., Rhodius-Meester, H. F. M., Baroni, M., Gjerum, L., van Gils, M., Soininen, H., Remes, A. M., Hartikainen, P., Waldemar, G., Mecocci, P., Barkhof, F., Pijnenburg, Y., van der Flier, W. M., Hasselbalch, S. G., Lotjonen, J., & Frederiksen, K. S. (2019). Detecting frontotemporal dementia syndromes using MRI biomarkers. *Neuroimage Clin*, *22*, 101711. https://doi.org/10.1016/j.nicl.2019.101711

Buratti, E., & Baralle, F. E. (2001). Characterization and functional implications of the RNA binding properties of nuclear factor TDP-43, a novel splicing regulator of CFTR exon 9. *J Biol Chem*, *276*(39), 36337-36343. https://doi.org/10.1074/jbc.M104236200

Buratti, E., & Baralle, F. E. (2008). Multiple roles of TDP-43 in gene expression, splicing regulation, and human disease. *Front Biosci*, *13*, 867-878. https://www.ncbi.nlm.nih.gov/pubmed/17981595

Caballero, B., Bourdenx, M., Luengo, E., Diaz, A., Sohn, P. D., Chen, X., Wang, C., Juste, Y. R., Wegmann, S., Patel, B., Young, Z. T., Kuo, S. Y., Rodriguez-Navarro, J. A., Shao, H., Lopez, M. G., Karch, C. M., Goate, A. M., Gestwicki, J. E., Hyman, B. T., . . . Cuervo, A. M. (2021). Acetylated tau inhibits chaperone-mediated autophagy and promotes tau pathology propagation in mice. *Nat Commun*, *12*(1), 2238. https://doi.org/10.1038/s41467-021-22501-9

Caballero, B., Wang, Y., Diaz, A., Tasset, I., Juste, Y. R., Stiller, B., Mandelkow, E. M., Mandelkow, E., & Cuervo, A. M. (2018). Interplay of pathogenic forms of human tau with different autophagic pathways. *Aging Cell*, *17*(1). https://doi.org/10.1111/acel.12692

Castellani, R. J., Rolston, R. K., & Smith, M. A. (2010). Alzheimer disease. *Dis Mon*, *56*(9), 484-546. https://doi.org/10.1016/j.disamonth.2010.06.001

Casterton, R. L., Hunt, R. J., & Fanto, M. (2020). Pathomechanism Heterogeneity in the Amyotrophic Lateral Sclerosis and Frontotemporal Dementia Disease Spectrum: Providing Focus Through the Lens of Autophagy. *J Mol Biol*, *432*(8), 2692-2713. https://doi.org/10.1016/j.jmb.2020.02.018

Chang, M. C., Srinivasan, K., Friedman, B. A., Suto, E., Modrusan, Z., Lee, W. P., Kaminker, J. S., Hansen, D. V., & Sheng, M. (2017). Progranulin deficiency causes impairment of autophagy and TDP-43 accumulation. *J Exp Med*, *214*(9), 2611-2628. https://doi.org/10.1084/jem.20160999

Chen, H. J., & Mitchell, J. C. (2021). Mechanisms of TDP-43 Proteinopathy Onset and Propagation. *Int J Mol Sci*, *22*(11). https://doi.org/10.3390/ijms22116004

Chiang, H. L., Terlecky, S. R., Plant, C. P., & Dice, J. F. (1989). A role for a 70-kilodalton heat shock protein in lysosomal degradation of intracellular proteins. *Science*, *246*(4928), 382-385. https://www.ncbi.nlm.nih.gov/pubmed/2799391

Ciechanover, A., & Kwon, Y. T. (2015). Degradation of misfolded proteins in neurodegenerative diseases: therapeutic targets and strategies. *Exp Mol Med*, *47*, e147. https://doi.org/10.1038/emm.2014.117

Cohen, T. J., Hwang, A. W., Restrepo, C. R., Yuan, C. X., Trojanowski, J. Q., & Lee, V. M. (2015). An acetylation switch controls TDP-43 function and aggregation propensity. *Nat Commun*, *6*, 5845. https://doi.org/10.1038/ncomms6845

Coon, E. A., Sorenson, E. J., Whitwell, J. L., Knopman, D. S., & Josephs, K. A. (2011). Predicting survival in frontotemporal dementia with motor neuron disease. *Neurology*, *76*(22), 1886-1893. https://doi.org/10.1212/WNL.0b013e31821d767b

Couratier, P., Corcia, P., Lautrette, G., Nicol, M., & Marin, B. (2017). ALS and frontotemporal dementia belong to a common disease spectrum. *Rev Neurol (Paris)*, *173*(5), 273-279. https://doi.org/10.1016/j.neurol.2017.04.001

Courtney, C., Farrell, D., Gray, R., Hills, R., Lynch, L., Sellwood, E., Edwards, S., Hardyman, W., Raftery, J., Crome, P., Lendon, C., Shaw, H., Bentham, P., & Group, A. D. C. (2004). Long-term donepezil treatment in 565 patients with Alzheimer's disease (AD2000): randomised double-blind trial. *Lancet*, *363*(9427), 2105-2115. https://doi.org/10.1016/S0140-6736(04)16499-4

Coyle-Gilchrist, I. T., Dick, K. M., Patterson, K., Vazquez Rodriquez, P., Wehmann, E., Wilcox, A., Lansdall, C. J., Dawson, K. E., Wiggins, J., Mead, S., Brayne, C., & Rowe, J. B. (2016). Prevalence, characteristics, and survival of frontotemporal lobar degeneration syndromes. *Neurology*, *86*(18), 1736-1743. https://doi.org/10.1212/WNL.0000000000002638

Cruts, M., Gijselinck, I., van der Zee, J., Engelborghs, S., Wils, H., Pirici, D., Rademakers, R., Vandenberghe, R., Dermaut, B., Martin, J. J., van Duijn, C., Peeters, K., Sciot, R., Santens, P., De Pooter, T., Mattheijssens, M., Van den Broeck, M., Cuijt, I., Vennekens, K., . . . Van Broeckhoven, C. (2006). Null mutations in progranulin cause ubiquitin-positive frontotemporal dementia linked to chromosome 17q21. *Nature*, *442*(7105), 920-924. https://doi.org/10.1038/nature05017

Cuervo, A. M. (2010). Chaperone-mediated autophagy: selectivity pays off. *Trends Endocrinol Metab*, *21*(3), 142-150. https://doi.org/10.1016/j.tem.2009.10.003

Cuervo, A. M., Stefanis, L., Fredenburg, R., Lansbury, P. T., & Sulzer, D. (2004). Impaired degradation of mutant alpha-synuclein by chaperone-mediated autophagy. *Science*, *305*(5688), 1292-1295. https://doi.org/10.1126/science.1101738

Daniel, R., He, Z., Carmichael, K. P., Halper, J., & Bateman, A. (2000). Cellular localization of gene expression for progranulin. *J Histochem Cytochem*, *48*(7), 999-1009. https://doi.org/10.1177/002215540004800713

Darios, F., & Stevanin, G. (2020). Impairment of Lysosome Function and Autophagy in Rare Neurodegenerative Diseases. *J Mol Biol*, *432*(8), 2714-2734. https://doi.org/10.1016/j.jmb.2020.02.033

Dehay, B., Bove, J., Rodriguez-Muela, N., Perier, C., Recasens, A., Boya, P., & Vila, M. (2010). Pathogenic lysosomal depletion in Parkinson's disease. *J Neurosci*, *30*(37), 12535-12544. https://doi.org/10.1523/JNEUROSCI.1920-10.2010

DeJesus-Hernandez, M., Mackenzie, I. R., Boeve, B. F., Boxer, A. L., Baker, M., Rutherford, N. J., Nicholson, A. M., Finch, N. A., Flynn, H., Adamson, J., Kouri, N., Wojtas, A., Sengdy, P., Hsiung, G. Y., Karydas, A., Seeley, W. W., Josephs, K. A., Coppola, G., Geschwind, D. H., . . . Rademakers, R. (2011). Expanded GGGGCC hexanucleotide repeat in noncoding region of C9ORF72 causes chromosome 9p-linked FTD and ALS. *Neuron*, *72*(2), 245-256. https://doi.org/10.1016/j.neuron.2011.09.011

Deng, Z., Lim, J., Wang, Q., Purtell, K., Wu, S., Palomo, G. M., Tan, H., Manfredi, G., Zhao, Y., Peng, J., Hu, B., Chen, S., & Yue, Z. (2020). ALS-FTLD-linked mutations of SQSTM1/p62 disrupt selective autophagy and NFE2L2/NRF2 anti-oxidative stress pathway. *Autophagy*, *16*(5), 917-931. https://doi.org/10.1080/15548627.2019.1644076

Desmarais, J. A., Cao, M., Bateman, A., & Murphy, B. D. (2008). Spatiotemporal expression pattern of progranulin in embryo implantation and placenta formation suggests a role in cell proliferation, remodeling, and angiogenesis. *Reproduction*, *136*(2), 247-257. https://doi.org/10.1530/REP-08-0044

Devenney, E., Vucic, S., Hodges, J. R., & Kiernan, M. C. (2015). Motor neuron disease-frontotemporal dementia: a clinical continuum. *Expert Rev Neurother*, *15*(5), 509-522. https://doi.org/10.1586/14737175.2015.1034108

Dice, J. F., Terlecky, S. R., Chiang, H. L., Olson, T. S., Isenman, L. D., Short-Russell, S. R., Freundlieb, S., & Terlecky, L. J. (1990). A selective pathway for degradation of cytosolic proteins by lysosomes. *Semin Cell Biol*, *1*(6), 449-455. https://www.ncbi.nlm.nih.gov/pubmed/2103896

Dickson. (1999). Neuropathologic differentiation of progressive supranuclear palsy and corticobasal degeneration. *Journal of neurology*, *246 Suppl*, II6-I15. https://doi.org/10.1007/BF03161076

Dickson, Kouri, N., Murray, M. E., & Josephs, K. A. (2011). Neuropathology of frontotemporal lobar degeneration-tau (FTLD-tau). *Journal of molecular neuroscience : MN*, *45*(3), 384-389. https://doi.org/10.1007/s12031-011-9589-0

Dickson, Rademakers, R., & Hutton, M. L. (2007). Progressive supranuclear palsy: Pathology and genetics. *Brain Pathology*, *17*(56), 74-82. https://doi.org/10.1111/j.1750-3639.2007.00054.x

Dikic, I., & Elazar, Z. (2018). Mechanism and medical implications of mammalian autophagy. *Nat Rev Mol Cell Biol*, *19*(6), 349-364. https://doi.org/10.1038/s41580-018-0003-4

Diskin, T., Tal-Or, P., Erlich, S., Mizrachy, L., Alexandrovich, A., Shohami, E., & Pinkas-Kramarski, R. (2005). Closed head injury induces upregulation of Beclin 1 at the cortical site of injury. *J Neurotrauma*, *22*(7), 750-762. https://doi.org/10.1089/neu.2005.22.750

Dou, J., Su, P., Xu, C., Wen, Z., Mao, Z., & Li, W. (2020). Targeting Hsc70-based autophagy to eliminate amyloid beta oligomers. *Biochem Biophys Res Commun*, *524*(4), 923-928. https://doi.org/10.1016/j.bbrc.2020.02.016

Duyckaerts, C., Delatour, B., & Potier, M.-C. (2009). Classification and basic pathology of Alzheimer disease. *Acta Neuropathologica*, *118*, 5-36. https://doi.org/10.1007/s00401-009-0532-1

Duyckaerts, C., Delatour, B., & Potier, M. C. (2009). Classification and basic pathology of Alzheimer disease. *Acta Neuropathol*, *118*(1), 5-36. https://doi.org/10.1007/s00401-009-0532-1

Elia, L. P., Mason, A. R., Alijagic, A., & Finkbeiner, S. (2019). Genetic Regulation of Neuronal Progranulin Reveals a Critical Role for the Autophagy-Lysosome Pathway. *J Neurosci*, *39*(17), 3332-3344. https://doi.org/10.1523/JNEUROSCI.3498-17.2019

Esteves, A. R., & Cardoso, S. M. (2020). Differential protein expression in diverse brain areas of Parkinson's and Alzheimer's disease patients. *Sci Rep*, *10*(1), 13149. https://doi.org/10.1038/s41598-020-70174-z

Fell, J., Klaver, P., Lehnertz, K., Grunwald, T., Schaller, C., Elger, C. E., & Fernández, G. (2001). Human memory formation is accompanied by rhinal-hippocampal coupling and decoupling. *Nat Neurosci*, *4*(12), 1259-1264. https://doi.org/10.1038/nn759

Fernández-Matarrubia, M., Matías-Guiu, J. A., Moreno-Ramos, T., & Matías-Guiu, J. (2015). Biomarkers: a new approach to behavioural variant frontotemporal dementia. *Neurologia*, *30*(1), 50-61. https://doi.org/10.1016/j.nrl.2013.03.002

Ferrari, R., Kapogiannis, D., Huey, E. D., & Momeni, P. (2011). FTD and ALS: a tale of two diseases. *Curr Alzheimer Res*, *8*(3), 273-294. https://www.ncbi.nlm.nih.gov/pubmed/21222600

Floris, G., Borghero, G., Cannas, A., Di Stefano, F., Murru, M. R., Corongiu, D., Cuccu, S., Tranquilli, S., Cherchi, M. V., Serra, A., Loi, G., Marrosu, M. G., Chio, A., & Marrosu, F. (2015). Clinical phenotypes and radiological findings in frontotemporal dementia related to TARDBP mutations. *J Neurol*, *262*(2), 375-384. https://doi.org/10.1007/s00415-014-7575-5

Forrest, S. L., Halliday, G. M., McCann, H., McGeachie, A. B., McGinley, C. V., Hodges, J. R., Piguet, O., Kwok, J. B., Spillantini, M. G., & Kril, J. J. (2019). Heritability in frontotemporal tauopathies. *Alzheimers Dement (Amst)*, *11*, 115-124. https://doi.org/10.1016/j.dadm.2018.12.001

Forsberg, K., Graffmo, K., Pakkenberg, B., Weber, M., Nielsen, M., Marklund, S., Brannstrom, T., & Andersen, P. M. (2019). Misfolded SOD1 inclusions in patients with mutations in C9orf72 and other ALS/FTD-associated genes. *J Neurol Neurosurg Psychiatry*, *90*(8), 861-869. https://doi.org/10.1136/jnnp-2018-319386

Fyfe, I. (2018). Tau folds differently between diseases. *Nat Rev Neurol*, *14*(11), 633. https://doi.org/10.1038/s41582-018-0076-x

Garre-Olmo, J. (2018). [Epidemiology of Alzheimer's disease and other dementias]. *Rev Neurol*, *66*(11), 377-386. https://www.ncbi.nlm.nih.gov/pubmed/29790571 (Epidemiologia de la enfermedad de Alzheimer y otras demencias.)

Gendron, T. F., Rademakers, R., & Petrucelli, L. (2013). TARDBP mutation analysis in TDP-43 proteinopathies and deciphering the toxicity of mutant TDP-43. *J Alzheimers Dis*, *33 Suppl 1*, S35-45. https://doi.org/10.3233/JAD-2012-129036

Ghemrawi, R., & Khair, M. (2020). Endoplasmic Reticulum Stress and Unfolded Protein Response in Neurodegenerative Diseases. *Int J Mol Sci*, *21*(17). https://doi.org/10.3390/ijms21176127

Ghosh, R., & Pattison, J. S. (2018). Macroautophagy and Chaperone-Mediated Autophagy in Heart Failure: The Known and the Unknown. *Oxid Med Cell Longev*, *2018*, 8602041. https://doi.org/10.1155/2018/8602041

Gil, M. J., Manzano, M. S., Cuadrado, M. L., Fernandez, C., Gomez, E., Matesanz, C., Calero, M., & Rabano, A. (2018). Argyrophilic Grain Pathology in Frontotemporal Lobar Degeneration: Demographic, Clinical, Neuropathological, and Genetic Features. *J Alzheimers Dis*, *63*(3), 1109-1117. https://doi.org/10.3233/JAD-171115

Goedert. (2004). Tau protein and neurodegeneration. *Seminars in Cell & Developmental Biology*, *15*(1), 45-49. https://doi.org/http://dx.doi.org/10.1016/j.semcdb.2003.12.015

Goedert, & Jakes. (1990). Expression of separate isoforms of human tau protein: correlation with the tau pattern in brain and effects on tubulin polymerization. *EMBO J*, *9*(13), 4225-4230. https://www.ncbi.nlm.nih.gov/pubmed/2124967

Goode, A., Butler, K., Long, J., Cavey, J., Scott, D., Shaw, B., Sollenberger, J., Gell, C., Johansen, T., Oldham, N. J., Searle, M. S., & Layfield, R. (2016). Defective recognition of LC3B by mutant SQSTM1/p62 implicates impairment of autophagy as a pathogenic mechanism in ALS-FTLD. *Autophagy*, *12*(7), 1094-1104. https://doi.org/10.1080/15548627.2016.1170257

Graef, M. (2020). Recent advances in the understanding of autophagosome biogenesis. *F1000Res*, *9*. https://doi.org/10.12688/f1000research.22111.1

Greaves, C. V., & Rohrer, J. D. (2019). An update on genetic frontotemporal dementia. *J Neurol*, *266*(8), 2075-2086. https://doi.org/10.1007/s00415-019-09363-4

Hase, Y., Chen, A., Bates, L. L., Craggs, L. J. L., Yamamoto, Y., Gemmell, E., Oakley, A. E., Korolchuk, V. I., & Kalaria, R. N. (2018). Severe white matter astrocytopathy in CADASIL. *Brain Pathol*, *28*(6), 832-843. https://doi.org/10.1111/bpa.12621

Hatanpaa, K. J., Raisanen, J. M., Herndon, E., Burns, D. K., Foong, C., Habib, A. A., & White, C. L., 3rd. (2014). Hippocampal sclerosis in dementia, epilepsy, and ischemic injury: differential vulnerability of hippocampal subfields. *J Neuropathol Exp Neurol*, *73*(2), 136-142. https://doi.org/10.1097/OPX.0000000000000170

He, Z., Ismail, A., Kriazhev, L., Sadvakassova, G., & Bateman, A. (2002). Progranulin (PC-cell-derived growth factor/acrogranin) regulates invasion and cell survival. *Cancer Res*, *62*(19), 5590-5596. https://www.ncbi.nlm.nih.gov/pubmed/12359772

Hill, S. M., Wrobel, L., Ashkenazi, A., Fernandez-Estevez, M., Tan, K., Burli, R. W., & Rubinsztein, D. C. (2021). VCP/p97 regulates Beclin-1-dependent autophagy initiation. *Nat Chem Biol*, *17*(4), 448-455. https://doi.org/10.1038/s41589-020-00726-x

Hippocampus. (2011). http://medicine.academic.ru/3923/Hippocampus

Honda, D., Ishigaki, S., Iguchi, Y., Fujioka, Y., Udagawa, T., Masuda, A., Ohno, K., Katsuno, M., & Sobue, G. (2013). The ALS/FTLD-related RNA-binding proteins TDP-43 and FUS have common downstream RNA targets in cortical neurons. *FEBS Open Bio*, *4*, 1-10. https://doi.org/10.1016/j.fob.2013.11.001

Hou, X., Watzlawik, J. O., Fiesel, F. C., & Springer, W. (2020). Autophagy in Parkinson's Disease. *J Mol Biol*, *432*(8), 2651-2672. https://doi.org/10.1016/j.jmb.2020.01.037

Huang, C. C., Bose, J. K., Majumder, P., Lee, K. H., Huang, J. T., Huang, J. K., & Shen, C. K. (2014). Metabolism and mis-metabolism of the neuropathological signature protein TDP-43. *J Cell Sci*, *127*(Pt 14), 3024-3038. https://doi.org/10.1242/jcs.136150

Hutton, M., Lendon, C. L., Rizzu, P., Baker, M., Froelich, S., Houlden, H., Pickering-Brown, S., Chakraverty, S., Isaacs, A., Grover, A., Hackett, J., Adamson, J., Lincoln, S., Dickson, D., Davies, P., Petersen, R. C., Stevens, M., de Graaff, E., Wauters, E., . . . Heutink, P. (1998). Association of missense and 5'-splice-site mutations in tau with the inherited dementia FTDP-17. *Nature*, *393*(6686), 702-705. https://doi.org/10.1038/31508

Ishigaki, S., & Sobue, G. (2018). Importance of functional loss of FUS in FTLD/ALS. *Frontiers in molecular biosciences*, *5*, 44. https://doi.org/10.3389/fmolb.2018.00044

Ji, Y. J., Ugolino, J., Brady, N. R., Hamacher-Brady, A., & Wang, J. (2017). Systemic deregulation of autophagy upon loss of ALS- and FTD-linked C9orf72. *Autophagy*, *13*(7), 1254-1255. https://doi.org/10.1080/15548627.2017.1299312

Jinwal, U. K., O'Leary, J. C., 3rd, Borysov, S. I., Jones, J. R., Li, Q., Koren, J., 3rd, Abisambra, J. F., Vestal, G. D., Lawson, L. Y., Johnson, A. G., Blair, L. J., Jin, Y., Miyata, Y., Gestwicki, J. E., & Dickey, C. A. (2010). Hsc70 rapidly engages tau after microtubule destabilization. *J Biol Chem*, *285*(22), 16798-16805. https://doi.org/10.1074/jbc.M110.113753

Ju, J. S., Fuentealba, R. A., Miller, S. E., Jackson, E., Piwnica-Worms, D., Baloh, R. H., & Weihl, C. C. (2009). Valosin-containing protein (VCP) is required for autophagy and is disrupted in VCP disease. *J Cell Biol*, *187*(6), 875-888. https://doi.org/10.1083/jcb.200908115

Kabeya, Y., Mizushima, N., Yamamoto, A., Oshitani-Okamoto, S., Ohsumi, Y., & Yoshimori, T. (2004). LC3, GABARAP and GATE16 localize to autophagosomal membrane depending on form-II formation. *J Cell Sci*, *117*(Pt 13), 2805-2812. https://doi.org/10.1242/jcs.01131

Kaushik, S., & Cuervo, A. M. (2018). The coming of age of chaperone-mediated autophagy. *Nat Rev Mol Cell Biol*, *19*(6), 365-381. https://doi.org/10.1038/s41580-018-0001-6

Kawamura, N., Sun-Wada, G. H., Aoyama, M., Harada, A., Takasuga, S., Sasaki, T., & Wada, Y. (2012). Delivery of endosomes to lysosomes via microautophagy in the visceral endoderm of mouse embryos. *Nat Commun*, *3*, 1071. https://doi.org/10.1038/ncomms2069

Kertesz, A., Blair, M., McMonagle, P., & Munoz, D. G. (2007). The diagnosis and course of frontotemporal dementia. *Alzheimer Dis Assoc Disord*, *21*(2), 155-163. https://doi.org/10.1097/WAD.0b013e31806547eb

Kiffin, R., Christian, C., Knecht, E., & Cuervo, A. M. (2004). Activation of chaperone-mediated autophagy during oxidative stress. *Mol Biol Cell*, *15*(11), 4829-4840. https://doi.org/10.1091/mbc.e04-06-0477

Kim, J., Kundu, M., Viollet, B., & Guan, K. L. (2011). AMPK and mTOR regulate autophagy through direct phosphorylation of Ulk1. *Nat Cell Biol*, *13*(2), 132-141. https://doi.org/10.1038/ncb2152

Kimonis, V. E., Fulchiero, E., Vesa, J., & Watts, G. (2008). VCP disease associated with myopathy, Paget disease of bone and frontotemporal dementia: review of a unique disorder. *Biochim Biophys Acta*, *1782*(12), 744-748. https://doi.org/10.1016/j.bbadis.2008.09.003

Kirshner, H. S. (2014). Frontotemporal dementia and primary progressive aphasia, a review. *Neuropsychiatr Dis Treat*, *10*, 1045-1055. https://doi.org/10.2147/NDT.S38821

Komori, T., Arai, N., Oda, M., Nakayama, H., Mori, H., Yagishita, S., Takahashi, T., Amano, N., Murayama, S., Murakami, S., Shibata, N., Kobayashi, M., Sasaki, S., & Iwata, M.

(1998). Astrocytic plaques and tufts of abnormal fibers do not coexist in corticobasal degeneration and progressive supranuclear palsy. *Acta Neuropathologica*, *96*(4), 401-408. <Go to ISI>://WOS:000076123900012

Kopach, O., Esteras, N., Wray, S., Abramov, A. Y., & Rusakov, D. A. (2021). Genetically engineered MAPT 10+16 mutation causes pathophysiological excitability of human iPSC-derived neurons related to 4R tau-induced dementia. *Cell Death Dis*, *12*(8), 716. https://doi.org/10.1038/s41419-021-04007-w

Korac, J., Schaeffer, V., Kovacevic, I., Clement, A. M., Jungblut, B., Behl, C., Terzic, J., & Dikic, I. (2013). Ubiquitin-independent function of optineurin in autophagic clearance of protein aggregates. *J Cell Sci*, *126*(Pt 2), 580-592. https://doi.org/10.1242/jcs.114926

Kovacs, G. G. (2018). Chapter 25 - Tauopathies. In G. G. Kovacs & I. Alafuzoff (Eds.), *Handbook of Clinical Neurology* (Vol. 145, pp. 355-368). Elsevier. https://doi.org/https://doi.org/10.1016/B978-0-12-802395-2.00025-0

Kril, J. J., & Halliday, G. M. (2011). Pathological staging of frontotemporal lobar degeneration. *J Mol Neurosci*, *45*(3), 379-383. https://doi.org/10.1007/s12031-011-9528-0

Kuo, P. H., Doudeva, L. G., Wang, Y. T., Shen, C. K., & Yuan, H. S. (2009). Structural insights into TDP-43 in nucleic-acid binding and domain interactions. *Nucleic Acids Res*, *37*(6), 1799-1808. https://doi.org/10.1093/nar/gkp013

Kuusisto, E., Kauppinen, T., & Alafuzoff, I. (2008). Use of p62/SQSTM1 antibodies for neuropathological diagnosis. *Neuropathol Appl Neurobiol*, *34*(2), 169-180. https://doi.org/10.1111/j.1365-2990.2007.00884.x

Kuusisto, E., Salminen, A., & Alafuzoff, I. (2001). Ubiquitin-binding protein p62 is present in neuronal and glial inclusions in human tauopathies and synucleinopathies. *Neuroreport*, *12*(10), 2085-2090. http://www.ncbi.nlm.nih.gov/pubmed/11447312

Kwiatkowski, T. J., Bosco, D. A., Leclerc, A. L., Tamrazian, E., Vanderburg, C. R., Russ, C., Davis, A., Gilchrist, J., Kasarskis, E. J., Munsat, T., Valdmanis, P., Rouleau, G. A.,

Hosler, B. A., Cortelli, P., de Jong, P. J., Yoshinaga, Y., Haines, J. L., Pericak-Vance, M. A., Yan, J., . . . Brown, R. H. (2009). Mutations in the FUS/TLS gene on chromosome 16 cause familial amyotrophic lateral sclerosis. *Science*, *323*(5918), 1205-1208. https://doi.org/10.1126/science.1166066

Lace, G. L., Wharton, S. B., & Ince, P. G. (2007). A brief history of tau: the evolving view of the microtubule-associated protein tau in neurodegenerative diseases. *Clin Neuropathol*, *26*(2), 43-58. https://doi.org/10.5414/npp26043

Van Langenhove, T., Van Der Zee, J., Sleegers, K., Engelborghs, S., Vandenberghe, R., Gijselinck, I., ... & Van Broeckhoven, C. (2010). Genetic contribution of FUS to frontotemporal lobar degeneration. *Neurology*, *74*(5), 366-371. https://doi.org/10.1212/WNL.0b013e3181ccc732

Lashley, T., Rohrer, J. D., Mead, S., & Revesz, T. (2015). Review: an update on clinical, genetic and pathological aspects of frontotemporal lobar degenerations. *Neuropathol Appl Neurobiol*, *41*(7), 858-881. https://doi.org/10.1111/nan.12250

Lee, M. J., Lee, J. H., & Rubinsztein, D. C. (2013). Tau degradation: the ubiquitin-proteasome system versus the autophagy-lysosome system. *Prog Neurobiol*, *105*, 49-59. https://doi.org/10.1016/j.pneurobio.2013.03.001

Lee, E.B., Porta, S., Michael Baer, G. *et al.* Expansion of the classification of FTLD-TDP: distinct pathology associated with rapidly progressive frontotemporal degeneration. *Acta Neuropathol* **134**, 65–78 (2017). https://doi.org/10.1007/s00401-017-1679-9

Leibiger, C., Deisel, J., Aufschnaiter, A., Ambros, S., Tereshchenko, M., Verheijen, B. M., Buttner, S., & Braun, R. J. (2018). TDP-43 controls lysosomal pathways thereby determining its own clearance and cytotoxicity. *Hum Mol Genet*, *27*(9), 1593-1607. https://doi.org/10.1093/hmg/ddy066

Letourneau, P. C. (1996). The cytoskeleton in nerve growth cone motility and axonal pathfinding. *Perspect Dev Neurobiol*, *4*(2-3), 111-123. http://www.ncbi.nlm.nih.gov/pubmed/9168194

Leyk, J., Goldbaum, O., Noack, M., & Richter-Landsberg, C. (2015). Inhibition of HDAC6 modifies tau inclusion body formation and impairs autophagic clearance. *J Mol Neurosci*, *55*(4), 1031-1046. https://doi.org/10.1007/s12031-014-0460-y

Li, W. W., Li, J., & Bao, J. K. (2012). Microautophagy: lesser-known self-eating. *Cell Mol Life Sci*, *69*(7), 1125-1136. https://doi.org/10.1007/s00018-011-0865-5

Litvan, I., Agid, Y., Calne, D., Campbell, G., Dubois, B., Duvoisin, R. C., Goetz, C. G., Golbe, L. I., Grafman, J., Growdon, J. H., Hallett, M., Jankovic, J., Quinn, N. P., Tolosa, E., & Zee, D. S. (1996). Clinical research criteria for the diagnosis of progressive supranuclear palsy (Steele-Richardson-Olszewski syndrome): report of the NINDS-SPSP international workshop. *Neurology*, *47*(1), 1-9. https://doi.org/10.1212/wnl.47.1.1

Liu, J., & Li, L. (2019). Targeting Autophagy for the Treatment of Alzheimer's Disease: Challenges and Opportunities. *Front Mol Neurosci*, *12*, 203. https://doi.org/10.3389/fnmol.2019.00203

Ma, J. F., Huang, Y., Chen, S. D., & Halliday, G. (2010). Immunohistochemical evidence for macroautophagy in neurones and endothelial cells in Alzheimer's disease. *Neuropathol Appl Neurobiol*, *36*(4), 312-319. https://doi.org/10.1111/j.1365-2990.2010.01067.x

Mackenzie, I. R., Baborie, A., Pickering-Brown, S., Du Plessis, D., Jaros, E., Perry, R. H., Neary, D., Snowden, J. S., & Mann, D. M. (2006). Heterogeneity of ubiquitin pathology in frontotemporal lobar degeneration: classification and relation to clinical phenotype. *Acta Neuropathol*, *112*(5), 539-549. https://doi.org/10.1007/s00401-006-0138-9

Mackenzie, I. R., & Neumann, M. (2016). Molecular neuropathology of frontotemporal dementia: insights into disease mechanisms from postmortem studies. *Journal of Neurochemistry*, *138 Suppl 1*, 54-70. https://doi.org/10.1111/jnc.13588

Mackenzie, I. R., & Neumann, M. (2020). Subcortical TDP-43 pathology patterns validate cortical FTLD-TDP subtypes and demonstrate unique aspects of C9orf72 mutation cases. *Acta Neuropathol*, *139(1)*, 83-98. https://doi.org/10.1007/s00401-019-02070-4

Mackenzie, I. R., Neumann, M., Baborie, A., Sampathu, D. M., Du Plessis, D., Jaros, E., Perry, R. H., Trojanowski, J. Q., Mann, D. M., & Lee, V. M. (2011). A harmonized classification system for FTLD-TDP pathology. *Acta Neuropathol*, *122*(1), 111-113. https://doi.org/10.1007/s00401-011-0845-8

Mackenzie, I. R., Rademakers, R., & Neumann, M. (2010) TDP-43 and FUS in amyotrophic lateral sclerosis and frontotemporal dementia. *The Lancet Neurology, 9*(10), 995-1007. https://doi.org/10.1016/S1474-4422(10)70195-2

Mahoney, D. J., Kaczor, J. J., Bourgeois, J., Yasuda, N., & Tarnopolsky, M. A. (2006). Oxidative stress and antioxidant enzyme upregulation in SOD1-G93A mouse skeletal muscle. *Muscle Nerve*, *33*(6), 809-816. https://doi.org/10.1002/mus.20542

Masuda, S., Mizukami, S., Eguchi, A., Ichikawa, R., Nakamura, M., Nakamura, K., Okada, R., Tanaka, T., Shibutani, M., & Yoshida, T. (2019). Immunohistochemical expression of autophagosome markers LC3 and p62 in preneoplastic liver foci in high fat diet-fed rats. *J Toxicol Sci*, *44*(8), 565-574. https://doi.org/10.2131/jts.44.565

Mann, D. M., Rollinson, S., Robinson, A., Bennion Callister, J., Thompson, J. C., Snowden, J. S., Gendron, T., Petrucelli, L., Masuda-Suzukake, M., Hasegawa, M., Davidson, Y., & Pickering-Brown, S. (2013). Dipeptide repeat proteins are present in the p62 positive inclusions in patients with frontotemporal lobar degeneration and motor neurone disease associated with expansions in C9ORF72. Acta neuropathologica communications, 1, 68. https://doi.org/10.1186/2051-5960-1-68

Matej, R., Tesar, A., & Rusina, R. (2019). Alzheimer's disease and other neurodegenerative dementias in comorbidity: A clinical and neuropathological overview. *Clin Biochem*, *73*, 26-31. https://doi.org/10.1016/j.clinbiochem.2019.08.005

Menzies, F. M., Fleming, A., Caricasole, A., Bento, C. F., Andrews, S. P., Ashkenazi, A., Fullgrabe, J., Jackson, A., Jimenez Sanchez, M., Karabiyik, C., Licitra, F., Lopez Ramirez, A., Pavel, M., Puri, C., Renna, M., Ricketts, T., Schlotawa, L., Vicinanza, M., Won, H., . . . Rubinsztein, D. C. (2017). Autophagy and Neurodegeneration:

Pathogenic Mechanisms and Therapeutic Opportunities. *Neuron*, *93*(5), 1015-1034. https://doi.org/10.1016/j.neuron.2017.01.022

Menzies, F. M., Fleming, A., & Rubinsztein, D. C. (2015). Compromised autophagy and neurodegenerative diseases. *Nat Rev Neurosci*, *16*(6), 345-357. https://doi.org/10.1038/nrn3961

Mijaljica, D., Prescott, M., & Devenish, R. J. (2011). Microautophagy in mammalian cells: revisiting a 40-year-old conundrum. *Autophagy*, *7*(7), 673-682. http://www.ncbi.nlm.nih.gov/pubmed/21646866

Miller, D. W., Cookson, M. R., & Dickson, D. W. (2004). Glial cell inclusions and the pathogenesis of neurodegenerative diseases. *Neuron Glia Biol*, *1*(1), 13-21. https://doi.org/10.1017/s1740925x04000043

Misgeld, T., & Schwarz, T. L. (2017). Mitostasis in Neurons: Maintaining Mitochondria in an Extended Cellular Architecture. *Neuron*, *96*(3), 651-666. https://doi.org/10.1016/j.neuron.2017.09.055

Mol, M. O., Miedema, S. S. M., van Swieten, J. C., van Rooij, J. G. J., & Dopper, E. G. P. (2021). Molecular Pathways Involved in Frontotemporal Lobar Degeneration with TDP-43 Proteinopathy: What Can We Learn from Proteomics? *Int J Mol Sci*, *22*(19). https://doi.org/10.3390/ijms221910298

Moreno, F., Rabinovici, G. D., Karydas, A., Miller, Z., Hsu, S. C., Legati, A., Fong, J., Schonhaut, D., Esselmann, H., Watson, C., Stephens, M. L., Kramer, J., Wiltfang, J., Seeley, W. W., Miller, B. L., Coppola, G., & Grinberg, L. T. (2015). A novel mutation P112H in the TARDBP gene associated with frontotemporal lobar degeneration without motor neuron disease and abundant neuritic amyloid plaques. *Acta Neuropathol Commun*, *3*, 19. https://doi.org/10.1186/s40478-015-0190-6

Mulders, A. J., Fick, I. W., Bor, H., Verhey, F. R., Zuidema, S. U., & Koopmans, R. T. (2016). Prevalence and Correlates of Neuropsychiatric Symptoms in Nursing Home Patients With Young-Onset Dementia: The BEYOnD Study. *J Am Med Dir Assoc*, *17*(6), 495-500. https://doi.org/10.1016/j.jamda.2016.01.002

Murphy, K. E., Gysbers, A. M., Abbott, S. K., Tayebi, N., Kim, W. S., Sidransky, E., Cooper, A., Garner, B., & Halliday, G. M. (2014). Reduced glucocerebrosidase is associated with increased alpha-synuclein in sporadic Parkinson's disease. *Brain*, *137*, 834-848. https://doi.org/10.1093/brain/awt367

Nassif, M., Valenzuela, V., Rojas-Rivera, D., Vidal, R., Matus, S., Castillo, K., Fuentealba, Y., Kroemer, G., Levine, B., & Hetz, C. (2014). Pathogenic role of BECN1/Beclin 1 in the development of amyotrophic lateral sclerosis. *Autophagy*, *10*(7), 1256-1271. https://doi.org/10.4161/auto.28784

Nassif, M., Woehlbier, U., & Manque, P. A. (2017). The Enigmatic Role of C9ORF72 in Autophagy. *Front Neurosci*, *11*, 442. https://doi.org/10.3389/fnins.2017.00442

Nelson, P. T., Alafuzoff, I., Bigio, E. H., Bouras, C., Braak, H., Cairns, N. J., Castellani, R. J., Crain, B. J., Davies, P., Del Tredici, K., Duyckaerts, C., Frosch, M. P., Haroutunian, V., Hof, P. R., Hulette, C. M., Hyman, B. T., Iwatsubo, T., Jellinger, K. A., Jicha, G. A., . . . Beach, T. G. (2012). Correlation of Alzheimer disease neuropathologic changes with cognitive status: a review of the literature. *J Neuropathol Exp Neurol*, *71*(5), 362-381. https://doi.org/10.1097/NEN.0b013e31825018f7

Neubert, F. X., Mars, R. B., Thomas, A. G., Sallet, J., & Rushworth, M. F. (2014). Comparison of human ventral frontal cortex areas for cognitive control and language with areas in monkey frontal cortex. *Neuron*, *81*(3), 700-713. https://doi.org/10.1016/j.neuron.2013.11.012

Neumann, M., Rademakers, R., Roeber, S., Baker, M., Kretzschmar, H. A., & Mackenzie, I. R. (2009). A new subtype of frontotemporal lobar degeneration with FUS pathology. *Brain*, *132*(Pt 11), 2922-2931. https://doi.org/10.1093/brain/awp214

Niewiadomska, G., Niewiadomski, W., Steczkowska, M., & Gasiorowska, A. (2021). Tau Oligomers Neurotoxicity. *Life (Basel)*, *11*(1). https://doi.org/10.3390/life11010028

Nolan, M., Scott, C., Gamarallage, M. P., Lunn, D., Carpenter, K., McDonough, E., Meyer, D., Kaanumalle, S., Santamaria-Pang, A., Turner, M. R., Talbot, K., & Ansorge, O. (2020).

Quantitative patterns of motor cortex proteinopathy across ALS genotypes. *Acta Neuropathol Commun*, *8*(1), 98. https://doi.org/10.1186/s40478-020-00961-2

Novus. (2017). *LC3B Antibody*. https://www.novusbio.com/products/lc3b-antibody_nb100-2220#datasheet

Ntymenou, S., Tsantzali, I., Kalamatianos, T., Voumvourakis, K. I., Kapaki, E., Tsivgoulis, G., Stranjalis, G., & Paraskevas, G. P. (2021). Blood Biomarkers in Frontotemporal Dementia: Review and Meta-Analysis. *Brain Sci*, *11*(2). https://doi.org/10.3390/brainsci11020244

Nutma, E., Marzin, M. C., Cillessen, S. A., & Amor, S. (2021). Autophagy in white matter disorders of the CNS: mechanisms and therapeutic opportunities. *J Pathol*, *253*(2), 133-147. https://doi.org/10.1002/path.5576

Oh, S. H., Choi, Y. B., Kim, J. H., Weihl, C. C., & Ju, J. S. (2017). Quantification of autophagy flux using LC3 ELISA. *Anal Biochem*, *530*, 57-67. https://doi.org/10.1016/j.ab.2017.05.003

Oishi, K., Zilles, K., Amunts, K., Faria, A., Jiang, H., Li, X., Akhter, K., Hua, K., Woods, R., Toga, A. W., Pike, G. B., Rosa-Neto, P., Evans, A., Zhang, J., Huang, H., Miller, M. I., van Zijl, P. C., Mazziotta, J., & Mori, S. (2008). Human brain white matter atlas: identification and assignment of common anatomical structures in superficial white matter. *Neuroimage*, *43*(3), 447-457. https://doi.org/10.1016/j.neuroimage.2008.07.009

Orehek AJ, Iglesias-Rozas JR, Garrosa M (2018) Architectural Arrangement of Neurons as Part of the Functional Unit of the Central Nervous System. *Alzheimers Dis Dement 2*(1):56-69. DOI: 10.36959/734/374

Orenstein, S. J., Kuo, S. H., Tasset, I., Arias, E., Koga, H., Fernandez-Carasa, I., Cortes, E., Honig, L. S., Dauer, W., Consiglio, A., Raya, A., Sulzer, D., & Cuervo, A. M. (2013). Interplay of LRRK2 with chaperone-mediated autophagy. *Nat Neurosci*, *16*(4), 394-406. https://doi.org/10.1038/nn.3350

Padman, B. S., Nguyen, T. N., Uoselis, L., Skulsuppaisarn, M., Nguyen, L. K., & Lazarou, M. (2019). LC3/GABARAPs drive ubiquitin-independent recruitment of Optineurin and NDP52 to amplify mitophagy. *Nat Commun*, *10*(1), 408. https://doi.org/10.1038/s41467-019-08335-6

Pankiv, S., Clausen, T. H., Lamark, T., Brech, A., Bruun, J. A., Outzen, H., Overvatn, A., Bjorkoy, G., & Johansen, T. (2007). p62/SQSTM1 binds directly to Atg8/LC3 to facilitate degradation of ubiquitinated protein aggregates by autophagy. *J Biol Chem*, *282*(33), 24131-24145. https://doi.org/10.1074/jbc.M702824200

Peggion, C., Massimino, M. L., Bonadio, R. S., Lia, F., Lopreiato, R., Cagnin, S., Cali, T., & Bertoli, A. (2021). Regulation of Endoplasmic Reticulum-Mitochondria Tethering and Ca(2+) Fluxes by TDP-43 via GSK3beta. *Int J Mol Sci*, *22*(21). https://doi.org/10.3390/ijms222111853

Pickford, F., Masliah, E., Britschgi, M., Lucin, K., Narasimhan, R., Jaeger, P. A., Small, S., Spencer, B., Rockenstein, E., Levine, B., & Wyss-Coray, T. (2008). The autophagy-related protein beclin 1 shows reduced expression in early Alzheimer disease and regulates amyloid beta accumulation in mice. *J Clin Invest*, *118*(6), 2190-2199. https://doi.org/10.1172/JCI33585

Piepers, S., Veldink, J. H., de Jong, S. W., van der Tweel, I., van der Pol, W. L., Uijtendaal, E. V., Schelhaas, H. J., Scheffer, H., de Visser, M., de Jong, J. M., Wokke, J. H., Groeneveld, G. J., & van den Berg, L. H. (2009). Randomized sequential trial of valproic acid in amyotrophic lateral sclerosis. *Ann Neurol*, *66*(2), 227-234. https://doi.org/10.1002/ana.21620

Polinsky, R. J. (1998). Clinical pharmacology of rivastigmine: a new-generation acetylcholinesterase inhibitor for the treatment of Alzheimer's disease. *Clin Ther*, *20*(4), 634-647. https://doi.org/10.1016/s0149-2918(98)80127-6

Poorkaj, P., Bird, T. D., Wijsman, E., Nemens, E., Garruto, R. M., Anderson, L., Andreadis, A., Wiederholt, W. C., Raskind, M., & Schellenberg, G. D. (1998). Tau is a candidate gene

for chromosome 17 frontotemporal dementia. *Ann Neurol*, *43*(6), 815-825. https://doi.org/10.1002/ana.410430617

Qi, L., Zhang, X. D., Wu, J. C., Lin, F., Wang, J., DiFiglia, M., & Qin, Z. H. (2012). The role of chaperone-mediated autophagy in huntingtin degradation. *Molecular and Cellular Biology* https://doi.org/10.1007/s11010-022-04640-9

Rabinovici, G. D., & Miller, B. L. (2010). Frontotemporal lobar degeneration: epidemiology, pathophysiology, diagnosis and management. *CNS Drugs*, *24*(5), 375-398. https://doi.org/10.2165/11533100-000000000-00000

Ravikumar, B., Acevedo-Arozena, A., Imarisio, S., Berger, Z., Vacher, C., O'Kane, C. J., Brown, S. D. M., & Rubinsztein, D. C. (2005). Dynein mutations impair autophagic clearance of aggregate-prone proteins. *Nature Genetics*, *37*(7), 771-776. https://doi.org/10.1038/ng1591

Renton, A. E., Majounie, E., Waite, A., Simón-Sánchez, J., Rollinson, S., Gibbs, J. R., Schymick, J. C., Laaksovirta, H., van Swieten, J. C., Myllykangas, L., Kalimo, H., Paetau, A., Abramzon, Y., Remes, A. M., Kaganovich, A., Scholz, S. W., Duckworth, J., Ding, J., Harmer, D. W., . . . Consortium, I. (2011). A hexanucleotide repeat expansion in C9ORF72 is the cause of chromosome 9p21-linked ALS-FTD. *Neuron*, *72*(2), 257-268. https://doi.org/10.1016/j.neuron.2011.09.010

Rohan, Z., Rahimi, J., Weis, S., Kapas, I., Auff, E., Mitrovic, N., Liberski, P. P., Sikorska, B., Matej, R., & Kovacs, G. G. (2015). Screening for α-synuclein immunoreactive neuronal inclusions in the hippocampus allows identification of atypical MSA (FTLD-synuclein). *Acta Neuropathol*, *130*(2), 299-301. https://doi.org/10.1007/s00401-015-1455-7

Romanov, J., Walczak, M., Ibiricu, I., Schuchner, S., Ogris, E., Kraft, C., & Martens, S. (2012). Mechanism and functions of membrane binding by the Atg5-Atg12/Atg16 complex during autophagosome formation. *EMBO J*, *31*(22), 4304-4317. https://doi.org/10.1038/emboj.2012.278

Russell, R. C., Tian, Y., Yuan, H., Park, H. W., Chang, Y. Y., Kim, J., Kim, H., Neufeld, T. P., Dillin, A., & Guan, K. L. (2013). ULK1 induces autophagy by phosphorylating Beclin-1 and activating VPS34 lipid kinase. *Nat Cell Biol*, *15*(7), 741-750. https://doi.org/10.1038/ncb2757

Salvador, N., Aguado, C., Horst, M., & Knecht, E. (2000). Import of a cytosolic protein into lysosomes by chaperone-mediated autophagy depends on its folding state. *J Biol Chem*, *275*(35), 27447-27456. https://doi.org/10.1074/jbc.M001394200

Sampathu, D. M., Neumann, M., Kwong, L. K., Chou, T. T., Micsenyi, M., Truax, A., Bruce, J., Grossman, M., Trojanowski, J. Q., & Lee, V. M. (2006). Pathological heterogeneity of frontotemporal lobar degeneration with ubiquitin-positive inclusions delineated by ubiquitin immunohistochemistry and novel monoclonal antibodies. *Am J Pathol*, *169*(4), 1343-1352. https://doi.org/10.2353/ajpath.2006.060438

Sancesario, G. M., & Bernardini, S. (2015). How many biomarkers to discriminate neurodegenerative dementia? *Crit Rev Clin Lab Sci*, *52*(6), 314-326. https://doi.org/10.3109/10408363.2015.1051658

Schlafli, A. M., Berezowska, S., Adams, O., Langer, R., & Tschan, M. P. (2015). Reliable LC3 and p62 autophagy marker detection in formalin fixed paraffin embedded human tissue by immunohistochemistry. *Eur J Histochem*, *59*(2), 2481. https://doi.org/10.4081/ejh.2015.2481

Sebastian-Serrano, A., de Diego-Garcia, L., & Diaz-Hernandez, M. (2018). The Neurotoxic Role of Extracellular Tau Protein. *Int J Mol Sci*, *19*(4). https://doi.org/10.3390/ijms19040998

Seelaar, H., Rohrer, J. D., Pijnenburg, Y. A., Fox, N. C., & van Swieten, J. C. (2011). Clinical, genetic and pathological heterogeneity of frontotemporal dementia: a review. *J Neurol Neurosurg Psychiatry*, *82*(5), 476-486. https://doi.org/10.1136/jnnp.2010.212225

Seltman, R. E., & Matthews, B. R. (2012). Frontotemporal lobar degeneration: epidemiology, pathology, diagnosis and management. *CNS Drugs*, *26*(10), 841-870. https://doi.org/10.2165/11640070-000000000-00000

Sephton, C. F., Cenik, C., Kucukural, A., Dammer, E. B., Cenik, B., Han, Y., Dewey, C. M., Roth, F. P., Herz, J., Peng, J., Moore, M. J., & Yu, G. (2011). Identification of neuronal RNA targets of TDP-43-containing ribonucleoprotein complexes. *J Biol Chem*, *286*(2), 1204-1215. https://doi.org/10.1074/jbc.M110.190884

Sha, S., Hou, C., Viskontas, I. V., & Miller, B. L. (2006). Are frontotemporal lobar degeneration, progressive supranuclear palsy and corticobasal degeneration distinct diseases? *Nature clinical practice. Neurology*, *2*(12), 658-665. https://doi.org/10.1038/ncpneuro0357

Sharifi, M. N., Mowers, E. E., Drake, L. E., & Macleod, K. F. (2015). Measuring autophagy in stressed cells. *Methods Mol Biol*, *1292*, 129-150. https://doi.org/10.1007/978-1-4939-2522-3_10

Sheetz, M. P., Vale, R., Schnapp, B., Schroer, T., & Reese, T. (1987). Movements of vesicles on microtubules. *Ann N Y Acad Sci*, *493*, 409-416. http://www.ncbi.nlm.nih.gov/pubmed/3109300

Silva, M. C., & Haggarty, S. J. (2020). Tauopathies: Deciphering Disease Mechanisms to Develop Effective Therapies. *Int J Mol Sci*, *21*(23). https://doi.org/10.3390/ijms21238948

Silveri, M. C. (2007). Frontotemporal dementia to Alzheimer's disease. *Dialogues Clin Neurosci*, *9*(2), 153-160. https://www.ncbi.nlm.nih.gov/pubmed/17726914

Snowden, J., Neary, D., & Mann, D. (2007). Frontotemporal lobar degeneration: clinical and pathological relationships. *Acta Neuropathol*, *114*(1), 31-38. https://doi.org/10.1007/s00401-007-0236-3

Snowden, J. S., Hu, Q., Rollinson, S., Halliwell, N., Robinson, A., Davidson, Y. S., Momeni, P., Baborie, A., Griffiths, T. D., Jaros, E., Perry, R. H., Richardson, A., Pickering-Brown, S.

M., Neary, D., & Mann, D. M. (2011). The most common type of FTLD-FUS (aFTLD-U) is associated with a distinct clinical form of frontotemporal dementia but is not related to mutations in the FUS gene. *Acta Neuropathol*, *122*(1), 99-110. https://doi.org/10.1007/s00401-011-0816-0

Snowden, J. S., Neary, D., & Mann, D. M. (2002). Frontotemporal dementia. *Br J Psychiatry*, *180*, 140-143. https://doi.org/10.1192/bjp.180.2.140

Sou, Y. S., Tanida, I., Komatsu, M., Ueno, T., & Kominami, E. (2006). Phosphatidylserine in addition to phosphatidylethanolamine is an in vitro target of the mammalian Atg8 modifiers, LC3, GABARAP, and GATE-16. *J Biol Chem*, *281*(6), 3017-3024. https://doi.org/10.1074/jbc.M505888200

Spillantini, M. G., Murrell, J. R., Goedert, M., Farlow, M. R., Klug, A., & Ghetti, B. (1998). Mutation in the tau gene in familial multiple system tauopathy with presenile dementia. *Proc Natl Acad Sci U S A*, *95*(13), 7737-7741. https://www.ncbi.nlm.nih.gov/pubmed/9636220

Sposito, T., Preza, E., Mahoney, C. J., Seto-Salvia, N., Ryan, N. S., Morris, H. R., Arber, C., Devine, M. J., Houlden, H., Warner, T. T., Bushell, T. J., Zagnoni, M., Kunath, T., Livesey, F. J., Fox, N. C., Rossor, M. N., Hardy, J., & Wray, S. (2015). Developmental regulation of tau splicing is disrupted in stem cell-derived neurons from frontotemporal dementia patients with the 10 + 16 splice-site mutation in MAPT. *Hum Mol Genet*, *24*(18), 5260-5269. https://doi.org/10.1093/hmg/ddv246

Stan, D. M. (2018). *Investigating Alterations in Autophagy in Alzheimer's Disease using human brain tissue and skin-derived fibroblasts* University of Salford].

Strang, K. H., Golde, T. E., & Giasson, B. I. (2019). MAPT mutations, tauopathy, and mechanisms of neurodegeneration. *Lab Invest*, *99*(7), 912-928. https://doi.org/10.1038/s41374-019-0197-x

Tan, A. Y., Riley, T. R., Coady, T., Bussemaker, H. J., & Manley, J. L. (2012). TLS/FUS (translocated in liposarcoma/fused in sarcoma) regulates target gene transcription

via single-stranded DNA response elements. *Proc Natl Acad Sci U S A*, *109*(16), 6030-6035. https://doi.org/10.1073/pnas.1203028109

Tanaka, Y., Chambers, J. K., Matsuwaki, T., Yamanouchi, K., & Nishihara, M. (2014). Possible involvement of lysosomal dysfunction in pathological changes of the brain in aged progranulin-deficient mice. *Acta Neuropathol Commun*, *2*, 78. https://doi.org/10.1186/s40478-014-0078-x

Tanji, K., Zhang, H. X., Mori, F., Kakita, A., Takahashi, H., & Wakabayashi, K. (2012). p62/sequestosome 1 binds to TDP-43 in brains with frontotemporal lobar degeneration with TDP-43 inclusions. *J Neurosci Res*, *90*(10), 2034-2042. https://doi.org/10.1002/jnr.23081

Thal, D. R., Rub, U., Orantes, M., & Braak, H. (2002). Phases of A beta-deposition in the human brain and its relevance for the development of AD. *Neurology*, *58*(12), 1791-1800. http://www.ncbi.nlm.nih.gov/pubmed/12084879

Theofilas, P., Ehrenberg, A. J., Nguy, A., Thackrey, J. M., Dunlop, S., Mejia, M. B., Alho, A. T., Paraizo Leite, R. E., Rodriguez, R. D., Suemoto, C. K., Nascimento, C. F., Chin, M., Medina-Cleghorn, D., Cuervo, A. M., Arkin, M., Seeley, W. W., Miller, B. L., Nitrini, R., Pasqualucci, C. A., . . . Grinberg, L. T. (2018). Probing the correlation of neuronal loss, neurofibrillary tangles, and cell death markers across the Alzheimer's disease Braak stages: a quantitative study in humans. *Neurobiol Aging*, *61*, 1-12. https://doi.org/10.1016/j.neurobiolaging.2017.09.007

Thomas, S. J., & Grossberg, G. T. (2009). Memantine: a review of studies into its safety and efficacy in treating Alzheimer's disease and other dementias. *Clin Interv Aging*, *4*, 367-377. https://doi.org/10.2147/cia.s6666

Tian, G., Jin, X., Wang, Q., Ye, T., Li, G., & Liu, J. (2020). Recent advances in the study of progranulin and its role in sepsis. *Int Immunopharmacol*, *79*, 106090. https://doi.org/10.1016/j.intimp.2019.106090

Ting, Y.-L., Lim, L., Kandiah, N., & Lyn Ng, A. S. (2016). PREVALENCE OF FAMILY HISTORY OF DEMENTIA IN A SPECIALIST YOUNG-ONSET DEMENTIA CLINIC COHORT. *Alzheimer's*

& Dementia: The Journal of the Alzheimer's Association, *12*(7), P700. https://doi.org/10.1016/j.jalz.2016.06.1375

Tiryaki, E., & Horak, H. A. (2014). ALS and other motor neuron diseases. *Continuum (Minneap Minn)*, *20*(5 Peripheral Nervous System Disorders), 1185-1207. https://doi.org/10.1212/01.CON.0000455886.14298.a4

Tolnay, M., & Probst, A. (1999). REVIEW: tau protein pathology in Alzheimer's disease and related disorders. *Neuropathol Appl Neurobiol*, *25*(3), 171-187. https://doi.org/10.1046/j.1365-2990.1999.00182.x

Tome, S. O., Vandenberghe, R., Ospitalieri, S., Van Schoor, E., Tousseyn, T., Otto, M., von Arnim, C. A. F., & Thal, D. R. (2020). Distinct molecular patterns of TDP-43 pathology in Alzheimer's disease: relationship with clinical phenotypes. *Acta Neuropathol Commun*, *8*(1), 61. https://doi.org/10.1186/s40478-020-00934-5

Townley, R. A., Boeve, B. F., & Benarroch, E. E. (2018). Progranulin: Functions and neurologic correlations. *Neurology*, *90*(3), 118-125. https://doi.org/10.1212/WNL.0000000000004840

Trieu, C., Gossink, F., Stek, M. L., Scheltens, P., Pijnenburg, Y. A. L., & Dols, A. (2020). Effectiveness of Pharmacological Interventions for Symptoms of Behavioral Variant Frontotemporal Dementia: A Systematic Review. *Cogn Behav Neurol*, *33*(1), 1-15. https://doi.org/10.1097/WNN.0000000000000217

Tsai, R. M., & Boxer, A. L. (2016). Therapy and clinical trials in frontotemporal dementia: past, present, and future. *Journal of Neurochemistry*, *138 Suppl 1*, 211-221. https://doi.org/10.1111/jnc.13640

Tu, P. H., Gurney, M. E., Julien, J. P., Lee, V. M., & Trojanowski, J. Q. (1997). Oxidative stress, mutant SOD1, and neurofilament pathology in transgenic mouse models of human motor neuron disease. *Lab Invest*, *76*(4), 441-456. https://www.ncbi.nlm.nih.gov/pubmed/9111507

Turner, M. R., Al-Chalabi, A., Chio, A., Hardiman, O., Kiernan, M. C., Rohrer, J. D., Rowe, J., Seeley, W., & Talbot, K. (2017). Genetic screening in sporadic ALS and FTD. *J Neurol Neurosurg Psychiatry*. https://doi.org/10.1136/jnnp-2017-315995

Turner, M. R., Parton, M. J., Shaw, C. E., Leigh, P. N., & Al-Chalabi, A. (2003). Prolonged survival in motor neuron disease: a descriptive study of the King's database 1990-2002. *J Neurol Neurosurg Psychiatry*, *74*(7), 995-997. https://www.ncbi.nlm.nih.gov/pubmed/12810805

Uesaka, N., & Kano, M. (2018). Presynaptic Mechanisms Mediating Retrograde Semaphorin Signals for Climbing Fiber Synapse Elimination During Postnatal Cerebellar Development. *Cerebellum*, *17*(1), 17-22. https://doi.org/10.1007/s12311-017-0888-z

van Swieten, J., & Spillantini, M. G. (2007). Hereditary frontotemporal dementia caused by Tau gene mutations. *Brain Pathol*, *17*(1), 63-73. https://doi.org/10.1111/j.1750-3639.2007.00052.x

Vanacore, N., Bonifati, V., Colosimo, C., Fabbrini, G., De Michele, G., Marconi, R., Nicholl, D., Locuratolo, N., Romano, S., Talarico, G., Stocchi, F., Bonuccelli, U., Lamberti, P., Vieregge, P., Meco, G., & European Study Group on Atypical, P. (2001). Epidemiology of progressive supranuclear palsy. ESGAP Consortium. European Study Group on Atypical Parkinsonisms. *Neurol Sci*, *22*(1), 101-103. https://doi.org/10.1007/s100720170065

Vance, C., Rogelj, B., Hortobágyi, T., De Vos, K. J., Nishimura, A. L., Sreedharan, J., Hu, X., Smith, B., Ruddy, D., Wright, P., Ganesalingam, J., Williams, K. L., Tripathi, V., Al-Saraj, S., Al-Chalabi, A., Leigh, P. N., Blair, I. P., Nicholson, G., de Belleroche, J., . . . Shaw, C. E. (2009). Mutations in FUS, an RNA processing protein, cause familial amyotrophic lateral sclerosis type 6. *Science*, *323*(5918), 1208-1211. https://doi.org/10.1126/science.1165942

Vesa, J., Su, H., Watts, G. D., Krause, S., Walter, M. C., Martin, B., Smith, C., Wallace, D. C., & Kimonis, V. E. (2009). Valosin containing protein associated inclusion body

myopathy: abnormal vacuolization, autophagy and cell fusion in myoblasts. *Neuromuscul Disord*, *19*(11), 766-772. https://doi.org/10.1016/j.nmd.2009.08.003

Wang, I. F., Tsai, K. J., & Shen, C. K. (2013). Autophagy activation ameliorates neuronal pathogenesis of FTLD-U mice: a new light for treatment of TARDBP/TDP-43 proteinopathies. *Autophagy*, *9*(2), 239-240. https://doi.org/10.4161/auto.22526

Wang, J., Ho, W. Y., Lim, K., Feng, J., Tucker-Kellogg, G., Nave, K. A., & Ling, S. C. (2018). Cell-autonomous requirement of TDP-43, an ALS/FTD signature protein, for oligodendrocyte survival and myelination. *Proc Natl Acad Sci U S A*, *115*(46), E10941-E10950. https://doi.org/10.1073/pnas.1809821115

Wang, X., Ma, M., Teng, J., Che, X., Zhang, W., Feng, S., Zhou, S., Zhang, Y., Wu, E., & Ding, X. (2015). Valproate Attenuates 25-kDa C-Terminal Fragment of TDP-43-Induced Neuronal Toxicity via Suppressing Endoplasmic Reticulum Stress and Activating Autophagy. *Int J Biol Sci*, *11*(7), 752-761. https://doi.org/10.7150/ijbs.11880

Wang, X., Schwartz, J. C., & Cech, T. R. (2015). Nucleic acid-binding specificity of human FUS protein. *Nucleic Acids Res*, *43*(15), 7535-7543. https://doi.org/10.1093/nar/gkv679

Wang, Y., & Mandelkow, E. (2016). Tau in physiology and pathology. *Nat Rev Neurosci*, *17*(1), 5-21. https://doi.org/10.1038/nrn.2015.1

Wang, Y., Martinez-Vicente, M., Krüger, U., Kaushik, S., Wong, E., Mandelkow, E. M., Cuervo, A. M., & Mandelkow, E. (2009). Tau fragmentation, aggregation and clearance: the dual role of lysosomal processing. *Hum Mol Genet*, *18*(21), 4153-4170. https://doi.org/10.1093/hmg/ddp367

Warren, J. D., Rohrer, J. D., & Rossor, M. N. (2013). Clinical review. Frontotemporal dementia. *BMJ*, *347*, f4827. https://www.ncbi.nlm.nih.gov/pubmed/23920254

Watts, G. D., Wymer, J., Kovach, M. J., Mehta, S. G., Mumm, S., Darvish, D., Pestronk, A., Whyte, M. P., & Kimonis, V. E. (2004). Inclusion body myopathy associated with Paget disease of bone and frontotemporal dementia is caused by mutant valosin-containing protein. *Nat Genet*, *36*(4), 377-381. https://doi.org/10.1038/ng1332

Webster, C. P., Smith, E. F., Bauer, C. S., Moller, A., Hautbergue, G. M., Ferraiuolo, L., Myszczynska, M. A., Higginbottom, A., Walsh, M. J., Whitworth, A. J., Kaspar, B. K., Meyer, K., Shaw, P. J., Grierson, A. J., & De Vos, K. J. (2016). The C9orf72 protein interacts with Rab1a and the ULK1 complex to regulate initiation of autophagy. *EMBO J*. https://doi.org/10.15252/embj.201694401

Weihl, C. C., Dalal, S., Pestronk, A., & Hanson, P. I. (2006). Inclusion body myopathy-associated mutations in p97/VCP impair endoplasmic reticulum-associated degradation. *Hum Mol Genet*, *15*(2), 189-199. https://doi.org/10.1093/hmg/ddi426

Whitwell, J. L., Jack, C. R., Parisi, J. E., Senjem, M. L., Knopman, D. S., Boeve, B. F., Rademakers, R., Baker, M., Petersen, R. C., Dickson, D. W., & Josephs, K. A. (2010). Does TDP-43 type confer a distinct pattern of atrophy in frontotemporal lobar degeneration? *Neurology*, *75*(24), 2212-2220. https://doi.org/10.1212/WNL.0b013e31820203c2

WHO. (2021a). *Dementia*. World Health Organization. Retrieved 17/01/2022 from https://www.who.int/news-room/fact-sheets/detail/dementia

WHO. (2021b, 02/09/2021). World Health Organization. *Dementia*. Retrieved 02/01/2022 from https://www.who.int/en/news-room/fact-sheets/detail/dementia

Wilcock, G. K., Lilienfeld, S., & Gaens, E. (2000). Efficacy and safety of galantamine in patients with mild to moderate Alzheimer's disease: multicentre randomised controlled trial. Galantamine International-1 Study Group. *BMJ*, *321*(7274), 1445-1449. https://doi.org/10.1136/bmj.321.7274.1445

Williams, D. R. (2006). Tauopathies: classification and clinical update on neurodegenerative diseases associated with microtubule-associated protein tau. *Internal medicine journal*, *36*(10), 652-660.

Williams, U. E., Philip-Ephraim, E. E., & Oparah, S. K. (2014). Multidisciplinary Interventions in Motor Neuron Disease. *J Neurodegener Dis*, *2014*, 435164. https://doi.org/10.1155/2014/435164

Wilson, R. S., Yu, L., Trojanowski, J. Q., Chen, E. Y., Boyle, P. A., Bennett, D. A., & Schneider, J. A. (2013). TDP-43 pathology, cognitive decline, and dementia in old age. *JAMA Neurol*, *70*(11), 1418-1424. https://doi.org/10.1001/jamaneurol.2013.3961

Wittenberg, R., Hu, B., Jagger, C., Kingston, A., Knapp, M., Comas-Herrera, A., King, D., Rehill, A., & Banerjee, S. (2019). Projections of care for older people with dementia in England: 2015 to 2040. *Age and Ageing*, *49*(2), 264-269. https://doi.org/10.1093/ageing/afz154

Woollacott, I. O., & Rohrer, J. D. (2016). The clinical spectrum of sporadic and familial forms of frontotemporal dementia. *Journal of Neurochemistry*, *138 Suppl 1*, 6-31. https://doi.org/10.1111/jnc.13654

Wooten, M. W., Geetha, T., Babu, J. R., Seibenhener, M. L., Peng, J., Cox, N., Diaz-Meco, M. T., & Moscat, J. (2008). Essential role of sequestosome 1/p62 in regulating accumulation of Lys63-ubiquitinated proteins. *J Biol Chem*, *283*(11), 6783-6789. https://doi.org/10.1074/jbc.M709496200

Wu, Y., Shao, W., Todd, T. W., Tong, J., Yue, M., Koga, S., Castanedes-Casey, M., Librero, A. L., Lee, C. W., Mackenzie, I. R., Dickson, D. W., Zhang, Y. J., Petrucelli, L., & Prudencio, M. (2021). Microglial lysosome dysfunction contributes to white matter pathology and TDP-43 proteinopathy in GRN-associated FTD. *Cell Rep*, *36*(8), 109581. https://doi.org/10.1016/j.celrep.2021.109581

Xilouri, M., & Stefanis, L. (2015). Chaperone mediated autophagy to the rescue: A new-fangled target for the treatment of neurodegenerative diseases. *Mol Cell Neurosci*, *66*(Pt A), 29-36. https://doi.org/10.1016/j.mcn.2015.01.003

Xu, C. Y., Kang, W. Y., Chen, Y. M., Jiang, T. F., Zhang, J., Zhang, L. N., ... & Chen, S. D. (2017). DJ-1 inhibits α-synuclein aggregation by regulating chaperone-mediated autophagy. Frontiers in aging neuroscience, 9, 308. https://doi.org/10.3389/fnagi.2017.00308

Xu, X., Sun, Y., Cen, X., Shan, B., Zhao, Q., Xie, T., Wang, Z., Hou, T., Xue, Y., Zhang, M., Peng, D., Sun, Q., Yi, C., Najafov, A., & Xia, H. (2021). Metformin activates chaperone-mediated autophagy and improves disease pathologies in an Alzheimer disease

mouse model. *Protein Cell*, *12*(10), 769-787. https://doi.org/10.1007/s13238-021-00858-3

Yamanaka, K., Sasagawa, Y., & Ogura, T. (2012). Recent advances in p97/VCP/Cdc48 cellular functions. *Biochim Biophys Acta*, *1823*(1), 130-137. https://doi.org/10.1016/j.bbamcr.2011.07.001

Yang, C., Tan, W., Whittle, C., Qiu, L., Cao, L., Akbarian, S., & Xu, Z. (2010). The C-terminal TDP-43 fragments have a high aggregation propensity and harm neurons by a dominant-negative mechanism. *PLoS One*, *5*(12), e15878. https://doi.org/10.1371/journal.pone.0015878

Yin, Z., Pascual, C., & Klionsky, D. J. (2016). Autophagy: machinery and regulation. *Microb Cell*, *3*(12), 588-596. https://doi.org/10.15698/mic2016.12.546

Zhou, J., Broe, M., Huang, Y., Anderson, J. P., Gai, W. P., Milward, E. A., Porritt, M., Howells, D., Hughes, A. J., Wang, X., & Halliday, G. M. (2011). Changes in the solubility and phosphorylation of alpha-synuclein over the course of Parkinson's disease. *Acta Neuropathol*, *121*(6), 695-704. https://doi.org/10.1007/s00401-011-0815-1